CANNABINOID 2 RECEPTOR AND GPR55 AS THERAPEUTIC TARGETS IN EXPERIMENTAL SEPSIS

by

Olivia Hyewon Yang

Submitted in partial fulfillment of the requirements
for the degree of Master of Science

at

Dalhousie University
Halifax, Nova Scotia
July 2016

DEDICATION PAGE

I dedicate this thesis to my beloved parents,

Jaemok Yang and Heesuk Youn.

TABLE OF CONTENTS

LIST OF TABLES ..... **vii**

LIST OF FIGURES ..... **viii**

ABSTRACT ..... **x**

LIST OF ABBREVIATIONS USED ..... **xi**

ACKNOWLEDGEMENTS ..... **xv**

CHAPTER 1: INTRODUCTION **1**

1.1 General Introduction **1**

1.2 Sepsis **2**

1.2.1 Sepsis Definitions and Epidemiology 2

1.2.2 Pathophysiology of Sepsis 6

1.3 Microcirculation and Leukocyte Activation in Sepsis **10**

1.3.1 Function of Microcirculation in Sepsis 10

1.3.2 Leukocyte Activation and Recruitment 13

1.3.3 Intestinal Microcirculation 15

1.4 Current Treatments for Sepsis **17**

1.4.1 Current Therapeutic Approaches 17

1.5 The Endocannabinoid system **17**

1.5.1 Overview of the Endocannabinoid System 17

1.5.2 Cannabinoid Receptors 19

1.5.3 GPR55 23

1.5.4 Cannabinoid Receptors and GPR55 in Inflammation 26

1.6 Hypothesis and Objectives 29

CHAPTER 2: MATERIALS AND METHODS 31

2.1 Animals 31

2.2 Anesthesia 31

2.3 Endotoxemia Model 32

2.3.1 Surgical Procedures 32

2.3.2 Experimental Timeline 33

2.4 Pharmacological Agents 36

2.5 Experimental Groups 37

2.6 Intravital Microscopy 39

2.6.1 Fluorescence Staining 39

2.6.2 Laparotomy 39

2.6.3 Intravital Microscopy Setup 40

2.6.4 Microscopy 40

2.6.5 Leukocyte Activity 41

2.6.6 Functional Capillary Density 41

2.6.7 Video Analysis 42

2.7 Blood Collection 42

2.8 Plasma Cytokine and Chemokine Analysis 43

2.9 Neutrophil Transmigration 43

2.9.1 Mouse Neutrophil Isolation 43

2.9.2 Transwell Migration Assays 44

2.10 Statistical Analyses 45

CHAPTER 3: RESULTS 48

3.1 Endotoxemia in CB2KO Mice – CBR Modulation 48

3.1.1 Leukocyte Adherence 48

3.1.2 Leukocyte Rolling 52

3.1.3 Functional Capillary Density 52

3.1.4 Cytokines and Adhesion Molecules 57

3.2 Endotoxemia in WT Mice – GPR55 Modulation 61

3.2.1 Leukocyte Adherence 61

3.2.2 Leukocyte Rolling 64

3.2.3 Functional Capillary Density 64

3.2.4 Cytokines and Adhesion Molecules 69

3.3 Bone Marrow Neutrophil Transmigration 74

CHAPTER 4: DISCUSSION 78

4.1 Summary of Major Findings 78

4.2 Acute Endotoxemia Experiments 82

4.2.1 Intravital Microscopy (CB2R KO Mice) 82

4.2.2 Intravital Microscopy (Wild type mice) 85

4.2.3 Plasma Cytokine Measurements 87

4.3 Bone Marrow Neutrophil Transmigration Experiments 90

4.4 Final Thoughts: Limitations of the Experimental Models and Future Directions 92

4.5 Clinical Implications 95

4.6 Conclusion.....96

REFERENCES.....97

LIST OF TABLES

Table 1: Development of sepsis definition and clinical criteria.....5

Table 2: Experimental groups for the endotoxemia study. 38

Table 3: Experimental groups for neutrophil migration assay.....47

Table 4: Summary of CB2R and GPR55 activities on modulation of leukocyte-endothelial interaction.....81

LIST OF FIGURES

Figure 1: Immune status of septic patients over time as a consequence of the dysregulation of the immune response 9

Figure 2: Sepsis pathophysiology in microcirculatory unit, arterioles, capillaries and venules. 12

Figure 3: The steps of leukocyte migration. 16

Figure 4: Schematic overview of endocannabinoid, 2-AG, receptors, and degradation enzyme 21

Figure 5: Schematic diagram of the cannabinoid receptor signaling cascade 22

Figure 6: Schematic diagram of the GPR55 signaling cascade 25

Figure 7: Objective of CB2R and GPR55 modulation in sepsis 30

Figure 8: Experimental timeline for the endotoxemia protocol. 35

Figure 9: The neutrophil transmigration assay 46

Figure 10: Leukocyte adhesion in intestinal collecting venules after systemic administration of saline or LPS and cannabinoid treatments in CB2R KO mice 50

Figure 11: Leukocyte adhesion in intestinal post-capillary venules after systemic administration of saline or LPS and cannabinoid treatments in CB2R KO mice. 51

Figure 12: Leukocyte rolling in intestinal collecting venules after systemic administration of saline or LPS and cannabinoid treatments in CB2R KO mice. 53

Figure 13: Leukocyte rolling in intestinal post capillary venules after systemic administration of saline or LPS and cannabinoid treatments in CB2R KO mice 54

Figure 14: Capillary perfusion quantified through FCD within the muscle layers of the intestine after systemic administration of LPS/saline and cannabinoid treatments in CB2R KO mice 55

Figure 15: Capillary perfusion quantified through FCD within the mucosal villi of the intestinal lumen after systemic administration of saline or LPS and cannabinoid treatments in CB2R KO mice. 56

Figure 16: Levels of plasma cytokines in CB2R KO mice 58

Figure 17: Levels of plasma cytokines in CB2R KO mice 59

Figure 18: Levels of plasma adhesion molecules in CB2R KO mice 60

Figure 19: Leukocyte adhesion in intestinal collecting venules after systemic administration of saline or LPS and GPR55 agonist or antagonist in wild type mice 62

Figure 20: Leukocyte adhesion in post capillary venules after systemic administration of saline or LPS and GPR55 agonist or antagonist in wild type mice 63

Figure 21: Leukocyte rolling in intestinal collecting venules after systemic administration of saline or LPS and GPR55 agonist or antagonist in WT mice 65

Figure 22: Leukocyte rolling in post capillary venules after systemic administration of saline or LPS and GPR55 agonist or antagonist in wild type mice 66

Figure 23: Capillary perfusion quantified through FCD within the muscle layers of the intestine after systemic administration of saline or LPS and GPR55 agonist or antagonist in wild type mice.. 67

Figure 24: Capillary perfusion quantified through FCD within the mucosal villi of the intestinal lumen after systemic administration of saline or LPS and GPR55 agonist or antagonist in wild type mice. 68

Figure 25: Levels of plasma cytokines in wild type mice. 71

Figure 26: Levels of plasma cytokines in wild type mice 72

Figure 27: Levels of soluble adhesion molecules in wild type mice 73

Figure 28: fMLP concentration dependent transmigration of murine neutrophils 75

Figure 29: Transmigration of murine neutrophils with CB2R activation 76

Figure 30: Transmigration of murine neutrophils with GPR55 modulation 77

Figure 31: Schematic model of CB1R, CB2R and GPR55 signaling pathways and 2-AG degradation during inflammation. 80

ABSTRACT

Sepsis represents a dysregulated systemic acute inflammatory response to severe infection. Despite efforts to develop supportive sepsis therapies, none has been approved that address the immune dysregulation. The endogenous cannabinoid system becomes active during sepsis and may present a novel axis for controlling inflammation. In the present study, our aim was to determine the impact of cannabinoid 2 receptor and G protein-coupled receptor 55 (GPR55) modulation on the inflammatory response, using a murine sepsis model. Using intravital microscopy, leukocyte activity was evaluated within the intestinal microvasculature. We observed that sepsis-induced increased leukocyte adhesion was diminished by inhibition of endocannabinoid degradation by JZL184 or GPR55 antagonists. Leukocyte rolling was diminished during sepsis, and this was significantly reversed by inhibition of endocannabinoid degradation. However, we failed to observe a direct effect of cannabinoids on neutrophil migration *in vitro*. Modulation of the endocannabinoid response had consequences on the cytokines secreted into the blood during sepsis; in particular, GPR55 agonists heightened TNF and IL-1β levels. Thus, our data suggest an important role of endocannabinoid system including GPR55 in the host response in experimental sepsis, hinting there may be a novel therapeutic candidate within the endocannabinoid system for the treatment of sepsis-induced dysregulation of the inflammatory response.

LIST OF ABBREVIATIONS USED

Δ^9-THC	Δ^9-tetrahydrocannabinol
2-AG	2-arachidonoylglycerol
AA	arachidonic acid
AC	adenylate cyclase
ACCP	American College of Chest Physicians
ACEA	arachidonyl-2'-chloroethylamide
ACPA	arachidonyl-cyclopropylamide
AEA	N-arachidonoylethanolamine
AMP	adenosine monophosphate
ANOVA	analysis of variance
APC	antigen presenting cell
BSA	bovine serum albumin
CACF	Carleton Animal Care Facility
cAMP	cyclic adenosine monophosphate
CASP	colon ascendens stent peritonitis
CB1R	cannabinoid 1 receptor
CB2R	cannabinoid 2 receptor
CBD	cannabidiol
CBN	cannabinol
CLP	cecal ligation and puncture
DAG	diacylglycerol
DAGL	diacylglycerol lipase

DMSO	dimethyl sulfoxide
ECS	endocannabinoid system
EGDT	early goal directed therapy
ERK	extracellular signal regulated kinases
FAAH	fatty acid amide hydrolase
FCD	functional capillary density
FDA	Food And Drug Administration
FITC	fluorescein isothiocyanate
GPR55	G protein coupled receptor 55
GPCRs	G protein coupled receptors
i.p.	intraperitoneal
i.v.	intravenous
ICAM	intercellular adhesion molecule
IFN-γ	interferon-gamma
IL-1β	interleukin-1 beta
IL-6	interleukin-6
iNOS	inducible nitric oxide synthase
IVM	intravital microscopy
JAM	junctional adhesion molecules
JNK	c-Jun NH2-terminal kinase
LFA-1	lymphocyte function associated antigen-1
LPS	lipopolysaccharide
MAGL	monoacylglycerol lipase
MAP	mean arterial pressure

MAPK	mitogen activated protein kinase
MHC	major histocompatibility complex
NAPE-PLD	N-acyl phosphatidylethanolamine
NF-κB	nuclear factor-κB
NO	nitric oxide
NOD	nucleotide-binding oligomerization domain
OPS	orthogonal polarization spectral imaging
PAMP	pathogen associated molecular pattern
PEA	palmitoylethanolamide
PECAM	platelet endothelial cell adhesion molecule
PKA	protein kinase A
PLC	phospholipase C
PMN	polymorphonuclear neutrophil(s)
pO2	partial pressure of oxygen
PPARγ	peroxisome proliferator-activated receptor γ
PSGL-1	P-selectin glycoprotein ligand-1
qRT-PCR	quantitative reverse transcriptase polymerase chain reaction
RhoA	ras homologue gene family member A
ROCK	Rho-associated protein kinase
s.c.	subcutaneous
SCCM	Society of Critical Care Medicine
SIRS	systemic inflammatory response syndrome
SOFA	sepsis-related organ failure assessment
SSC	surviving sepsis campaign

TLR	toll like receptor
TNF	tumor necrosis factor
TRAM	TRIF related adapter protein
TRIF	TIR-domain-containing adapter-inducing interferon-β
VCAM	vascular cellular adhesion molecule
VLA-4	very late antigen-4

ACKNOWLEDGEMENTS

The completion of this thesis required immense support and guidance from many people and I was extremely privileged to have got this all along the course of my research. First and foremost, I would like to thank Dr. Christian Lehmann for his continuous support and guidance throughout my research. Without his inspiration, coaching and enthusiasm, I would not be able to complete this research. I would also like to thank Dr. Andrew Stadnyk for all of his knowledge and mentorship over the past two years. Also, I would like to thank my committee members Dr. Juan Zhou and Dr. Jean Marshall for the great support and insight throughout my degree.

I was very fortunate to have had the opportunity to do research and to be a part of the Lehmann lab. I would like to give special thanks to the fellow students of the Lehmann lab, Ian Burkovskiy, Tom Toguri, Joel Sardinha, Nick Fisher, Nipun Arora for the positive and learning environment. Many thanks to Nancy McGrath, Sufia Islam and all the current and past members of the Lehmann lab for the help and support in my project. I would like to thank Dr. Melanie Kelly and her lab members for their reagents, help and knowledge in cannabinoid pharmacology. I would also like to thank Hana James for her assistance with lab techniques and knowledge in immunology.

Last but not least, I would like to thank my family and friends for the support and love throughout my journey.

CHAPTER 1: INTRODUCTION

1.1 General Introduction

Sepsis is a complex and potentially lethal inflammatory disease involving a dysregulated immune system in response to infection (Bone et al., 1992). The mortality rate of sepsis per year is as high as mortalities from stroke or heart attack (Martin et al., 2003). While sepsis is one of the leading causes of mortality in intensive care units (ICU) worldwide, public awareness and understanding of the disease remains lacking. The main challenge in sepsis is the inability to re-balance the exaggerated or suppressed immune response to a systemic infection; there are no therapeutic agents in the current medicine arsenal that addresses the immune dysfunction. In addition, the treatments available for sepsis often involve prolonged inpatient stays in ICU and complex therapies, generating significant socio-economic burden on the healthcare system. Therefore, there remains a high demand for a drug or a therapy to better recognize and treat sepsis.

In this research, the endocannabinoid system (ECS), a regulator of essential physiological functions in our body, was interrogated as a potential axis for treatment of acute systemic inflammation in sepsis. Pharmacological approaches were used to understand the pathophysiology of sepsis and identify novel therapeutic targets in immune system modulation, which may aid the current therapeutic approaches and health care protocol. Therefore the goals of this research project were; 1) to determine the impact of cannabinoid 2 receptor and GPR55 modulation specifically on leukocyte activation within the intestinal microcirculation, 2) elucidate the mechanisms of CBR and GPR55 modulation during sepsis.

1.2 Sepsis

1.2.1 Sepsis Definitions and Epidemiology

The definition of sepsis was first classified and introduced in the American College of Chest Physicians (ACCP) and the Society of Critical Care Medicine (SCCM) consensus conference in 1992, as a suspected or presence of infection along with two or more systemic inflammatory response syndrome (SIRS) criteria which includes the following (Table 1) (Bone et al., 1992; Dellinger et al., 2013; Levy et al., 2003):

1) Fever (> 38°C) or hypothermia (< 36°C)

2) Heart rate ≥ 90/min

3) Hyperventilation with respiratory rate of ≥ 20 breaths/min or $PaCO_2$ 32 mmHg

4) Leukocytosis (WBC > 12,000 cells/μL) or leukopenia (WBC < 4,000 cells/μL) or > 10% immature forms

In the 1992 ACCP/SCCM Consensus, severe sepsis was also defined as sepsis with presence of sepsis-induced organ dysfunction or tissue hypoperfusion, and persisting hypotension despite fluid resuscitation was termed septic shock (Table 1) (Bone et al., 1992). However, the definition of sepsis using SIRS criteria has been ambiguous as the diagnostic symptoms are sensitive but not specific to a single disease.

Hence, sepsis was not only difficult to treat, but also difficult to diagnose due to the poor diagnostic specificity with these fore-mentioned definitions. Prompt recognition

and a diagnosis of sepsis are crucial for effective therapies to be applied, which determine patients' outcomes. Therefore, there has been a continuous effort and need to update and modify clinical criteria and definitions of sepsis syndromes for timely recognition of the disease in the clinics.

In 2015, the European Society of Intensive Care Medicine (ESICM) and the Society of Critical Care Medicine (SCCM) reassessed the existing clinical criteria and definitions, and published the new definition of sepsis (Sepsis-3) as "life-threatening organ dysfunction caused by a dysregulated host response to infection" (Singer et al., 2016). Therefore, the definition of severe sepsis became redundant and septic shock was also redefined as "a subset of sepsis in which underlying circulatory and cellular/metabolic abnormalities are profound enough to substantially increase mortality" (Table 1) (Singer et al., 2016). The new definitions focused on drawing clear distinction between sepsis and uncomplicated infection.

With new definitions, the baseline Sepsis-related Organ Failure Assessment (SOFA) score was taken into clinical criteria and diagnostic measures in replacement of the SIRS criteria. The SOFA score assesses abnormality in organ systems such as respiratory, liver, cardiovascular and central nervous system, with a higher score associated with increased probability of mortality (Table 1) (Singer et al., 2016). An acute increase of $\geq$ 2 SOFA points with suspected or documented infection is diagnostic of sepsis, and sepsis diagnosis plus vasopressor therapy needed to elevate mean arteriole pressure (MAP) $\geq$ 65 mmHg and lactate >2 mmol/L (18 mg/dL) despite adequate fluid resuscitation is used for the diagnosis of septic shock. For a simple bed-side screening, quick SOFA (qSOFA) criteria were proposed, which included the following parameters (Singer et al., 2016):

1) Respiratory rate ≥ 22/min

2) Altered mentation

3) Systolic blood pressure ≤100 mm Hg

The patients with suspected infection with at least two of qSOFA criteria were predicted to have poor outcome.

Despite the intense effort to characterize sepsis and implementation of medical support, sepsis remains the leading cause of death from infection in ICUs. Approximately 1,400 deaths occur from sepsis per day around the globe, due to the high mortality rate, ranging from 30%-50% and up to 80% for septic shock. In an observational study in critical care units of Canadian hospitals, the mortality rate of sepsis patients was recorded to be approximately 40% (Husak et al., 2010). According to the Canadian Institute for Health Information (CIHI) report in 2009, 30,587 Canadians were hospitalized with sepsis and 9,230 patients died in hospitals across Canada (excluding Quebec), which represented 10.9% of all deaths occurring in hospitals (CIHI, 2009; Husak et al., 2010). Unfortunately there continues to be an increase in the number of patients suffering from sepsis despite the advances in the therapeutic approaches (Angus et al., 2001).

Table 1: Development of sepsis definition and clinical criteria.

		Sepsis	**Septic Shock**
1991/2001 Consensus	Definition	Presence of both infection and a systemic inflammatory response	Sepsis induced hypotension persisting despite adequate fluid resuscitation
	Clinical Criteria	Suspected or confirmed infection with ≥ 2 SIRS criteria	Arterial hypotension (systolic blood pressure <90 mmHg, mean arterial pressure <70, or a systolic blood pressure decrease >40 mmHg in adults or <2 SD below normal for age)
2015 Consensus	Definition	Life-threatening organ dysfunction caused by a dysregulated host response to infection	A subset of sepsis in which underlying circulatory and cellular/metabolic abnormalities are profound enough to substantially increase mortality
	Clinical Criteria	Suspected or documented infection and an acute increase of ≥ 2 SOFA points (a proxy for organ dysfunction)	Sepsis and vasopressor therapy needed to elevate MAP ≥ 65 mmHg and lactate >2 mmol/L (18 mg/dL) despite adequate fluid resuscitation

Patients with weakened immune systems, infants and the elderly are at an even greater risk of developing sepsis. Also, patients with chronic illnesses, such as diabetes, AIDS, cancer and kidney or liver disease, are at increased risk, as are those who have experienced a severe burn or physical trauma. Thus there are multiple conditions which increase risk and the occurrence of sepsis after admission to hospital accounts for 23.6% of all sepsis patients (CIHI, 2009; Husak et al., 2010).

1.2.2 Pathophysiology of Sepsis

The infections in sepsis originate from multiple possible sites, including the lung (68%), the abdomen (22%), blood (20%) and urinary tract (14%) (Martin, 2012; Martin et al., 2003; Vincent et al., 2006). The pathogens which cause sepsis are mainly bacteria (90%) with some fungal and viral infections (Martin, 2012; Martin et al., 2003). Gram-negative bacteria have been the predominating causative agent of the sepsis infections in the past; however, the incidence of Gram-positive bacteria has been steadily rising, accounting for 52% of sepsis cases more recently, whereas Gram-negative bacteria accounted for 38% (Martin, 2012; Martin et al., 2003). The most common organisms were *Staphylococcus aureus* (30%), *Pseudomonas* species (14%), and *Escherichia coli* (13%) (Martin, 2012; Vincent et al., 2006).

Typically, inflammatory responses due to infections are localized. However, in sepsis, inflammation spreads throughout the body via the circulatory system. In addition, the causes of sepsis are not singular and therefore result in nonspecific, aberrant and complex immune response. For example, some of the immunopathological processes during sepsis are dysregulated coagulation, a systemic hyper- and hypo-inflammatory

response, metabolic alterations and cellular dysfunctions such as lymphocyte apoptosis, neutrophil hyperactivity and endothelial cell failure (Remick, 2007).

The scope of this research was focused on the inflammatory responses after the onset of acute sepsis. Conventionally, sepsis is thought to be a unbalanced pro-inflammatory response preceding or coinciding with a compensatory anti-inflammatory response followed by immune paralysis (Yao et al., 2015). At the early phases of sepsis, pro-inflammatory responses are mainly generated by activation of the innate immune system, which involves neutrophils, monocytes, macrophages, mast cells, granulocytes and natural killer cells (Remick, 2007; van der Poll and Opal, 2008; Yao et al., 2015). Microbes are recognized by immune cells through their pathogen-associated molecular patterns (PAMPs), such as lipopolysaccharide (LPS), the endotoxin of the Gram-negative bacteria. These foreign molecules interact with pattern recognition receptors (PRR) such as toll-like receptors (TLR) on host cells, leading to overproduction of inflammatory mediators. Among TLRs, bacterial endotoxins such as LPS are recognized by TLR4, which can signal though the myeloid differentiation factor 88 dependent pathway (MyD88) to induce activation of transcription factor NF-κB (Anas et al., 2010; van der Poll and Opal, 2008; Yao et al., 2015). This interaction between pathogens and innate immune cells trigger the production and release of pro-inflammatory cytokines such as TNF, IL-1β and IL-6, intended to protect the host from the infection (Figure 1) (Anas et al., 2010; Yao et al., 2015). Immune cells and endothelial cells are activated upon stimulation by these pro-inflammatory cytokines, which then lead to further release of inflammatory cytokines and chemokines and cause the release of pro-coagulatory molecules, complement, platelet-activating factor and nitric oxide. As a result of multiple pathways being activated, the endothelial barrier becomes activated and disrupted,

impacting the microcirculation and leading to the migration and extravasation of neutrophils and phagocytes to the site of infection, increased vascular permeability, and eventually tissue ischemia and organ dysfunction (Figure 1) (Anas et al., 2010; van der Poll and Opal, 2008; Yao et al., 2015). In order to balance the exaggerated pro-inflammatory response, a compensatory anti-inflammatory response typically comes into play with production of anti-inflammatory mediators such as IL-10 and IL-4 (Figure 1) (Hotchkiss et al., 2013). Ironically, patients are likely to develop lethal secondary infections during the immunosuppressive phase of sepsis.

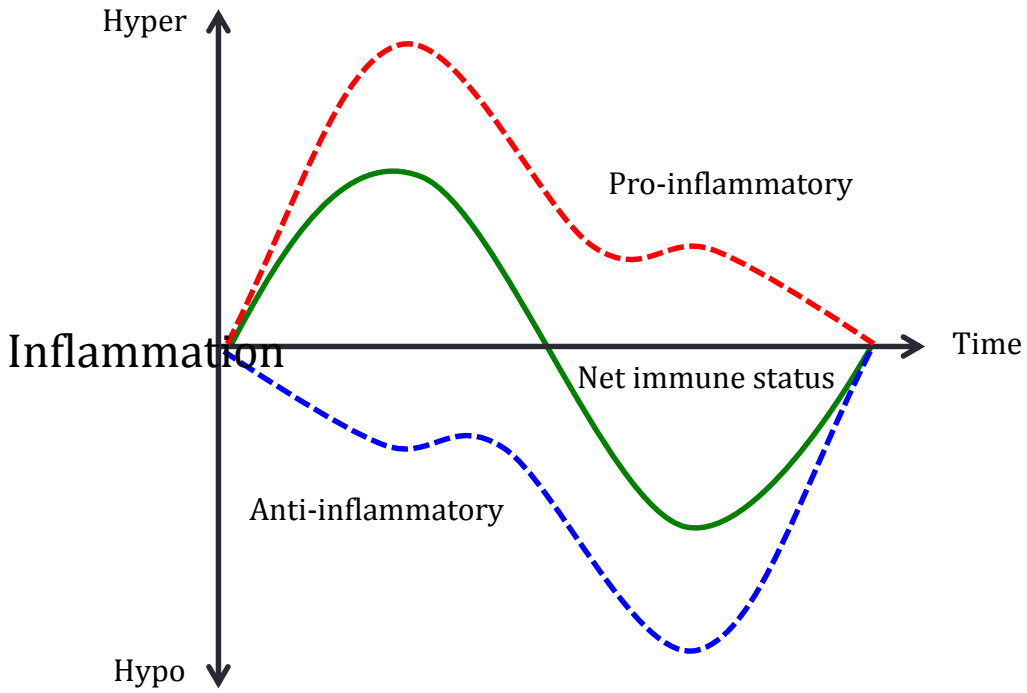

Figure 1: Immune status of septic patients over time as a consequence of the dysregulation of the immune response. The early phase of sepsis is often characterized by a hyper-inflammatory state, which is followed by a hypo-inflammatory state as the disease progresses.

1.3 Microcirculation and Leukocyte Activation in Sepsis

1.3.1 Function of Microcirculation in Sepsis

Impaired microcirculation is a key feature of sepsis and a major contributing factor to multiple organ dysfunction. The microcirculation is comprised of arterioles, capillaries and venules of less than 100 μm diameter, (Lush and Kvietys, 2000). Microcirculatory dysfunction involves altered exchange of oxygen, nutrients and removal of waste and carbon dioxide (Figure 2) (Spronk et al., 2004; Trzeciak et al., 2008).

The arterioles play an important role in vasoregulation during sepsis. Upon the induction of sepsis, arterioles are activated by vasodilators, particularly nitric oxide (NO), and become hypo-responsive to vasopressors within the microcirculation resulting in the misdistribution of blood flow, decreased peripheral resistance and eventually systemic hypotension (Figure 2) (Miranda et al., 2016; Spronk et al., 2004; Trzeciak et al., 2008). The capillaries are the primary sites of oxygen exchange and capillary endothelial cells are activated when exposed to pro-inflammatory mediators (e.g., IL-1β, IL-6, TNF) or oxidative stress during sepsis. Furthermore, the endothelial cells of the post-capillary venules are activated, they increase expression of adhesion molecules and decrease expression of thrombomodulin (Figure 2) (Colbert and Schmidt, 2016; Lush and Kvietys, 2000; Trzeciak et al., 2008). The endothelial cells then enter a forward-feeding cycle of amplification of the inflammatory response. The activation of endothelial cells mediates leukocyte activation, red blood cell deformability, aggregation and adherence which then result in decreased blood flow velocity, decreased density of perfused capillaries and tissue hypoxia (Figure 2) (Lush and Kvietys, 2000; Spronk et al., 2004; Trzeciak et al., 2008). The venules are also activated and respond with increased expression of surface

adhesion molecules. These changes in the endothelium and leukocytes facilitate the increase of microvascular permeability, edema, and disseminated intravascular coagulation, which eventually disturb the blood flow to tissues and organs resulting in tissue ischemia and organ damage (Spronk et al., 2004; Trzeciak et al., 2008).

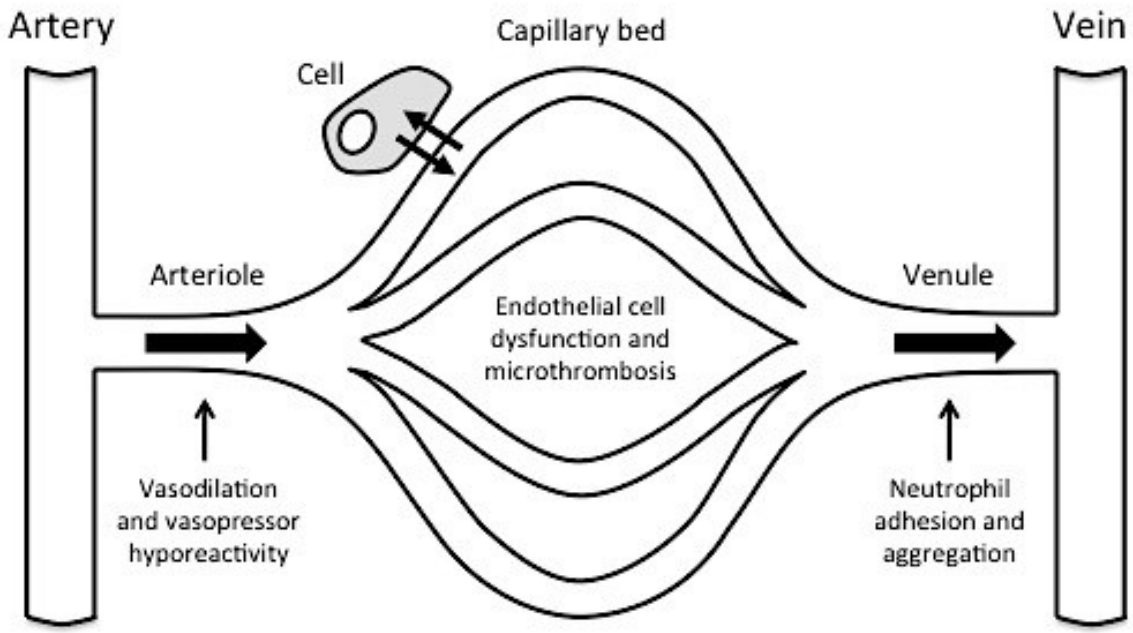

Figure 2: Sepsis pathophysiology in microcirculatory unit, arterioles, capillaries and venules. (Modified from Trzeciak et al., 2008)

1.3.2 Leukocyte Activation and Recruitment

Leukocytes such as neutrophils, monocytes, lymphocytes, eosinophils, basophils and dendritic cells, possess surface molecules for adhesion to endothelial cell and matrix glycoproteins, which enables their recruitment from the circulation to the site of infection in response to a chemotactic gradient. During sepsis, leukocyte-endothelial interactions and emigration of leukocytes are key pathophysiological features, possibility resulting in further activation and damage to non-infected tissues (Brown et al., 2006).

Leukocyte extravasation is a complex process involving interactions between multiple adhesion molecules, which is often divided into four fundamental steps: 1) rolling mediated by selectins; 2) activation by chemokines; 3) adhesion mediated by integrins binding to Ig-superfamily members; and 4) transendothelial migration (Figure 3) (Liu and Kubes, 2003; Petri et al., 2008). First, free flowing leukocytes tether to up-regulated selectins expressed on the activated endothelial cells, which slows down the velocity of leukocytes (Figure 3). The selectins are membrane glycoproteins with a lectin-like domain that binds specific carbohydrate groups (Kelly et al., 2007). L-selectin (CD62L) and P-selectin glycoprotein ligand-1 (PSGL-1) are expressed on the surface of circulating leukocytes. E-selectin (CD62E) and P-selectin (CD62P) are expressed on vascular endothelial cells during inflammation (Granger and Senchenkova, 2010; Zarbock and Ley, 2009). Repeated tethering by low affinity interaction between selectins and carbohydrates and detaching by shear force of the circulating blood results in reduced velocity of leukocytes, leading to rolling of the leukocytes along the vessels (Figure 3) (Granger and Senchenkova, 2010; Petri et al., 2008).

Firm adhesion of leukocytes and endothelial cells require another type of molecule called integrins. The integrins are heterodimeric proteins expressed on the cell surface consisting of an α chain and a β chain that are associated by a non-covalent bond. The integrins bind immunoglobulin-like adhesion molecules (ICAM-1, VCAM-1) that act as ligands. LFA-1 ($\alpha_L\beta_2$, CD11a/CD18) and MAC-1 ($\alpha_M\beta_2$, CD11b/CD18) are expressed on neutrophils upon activation by inflammatory mediators and allow firm adhesion of neutrophils on endothelium by binding to Ig-superfamily CAMs, intracellular adhesion molecule-1 (ICAM-1, CD51). Monocytes and lymphocytes express VLA-4 ($\alpha_4\beta_1$, CD11a/CD18) to bind endothelium with vascular cell adhesion molecule-1 (VCAM-1, CD106) (Granger and Senchenkova, 2010; Petri et al., 2008).

Once leukocytes are firmly adhered to the endothelium, the leukocytes undergo the final step of leukocyte extravasation, which is transendothelial migration. Transmigration requires endothelial junctional molecules such as Ig-superfamily platelet-endothelial-cell adhesion molecule-1 (PECAM-1, CD31) and junctional adhesion molecule (JAM-1, CD321). Homotypic binding of PECAM-1 (CD31) expressed on both leukocytes and the endothelial cells to initiate paracellular or transcellular migration of leukocytes (Figure 3) (Granger and Senchenkova, 2010; Petri et al., 2008). Leukocyte migration occurs between adjacent endothelial cells in paracellular migration, whereas in transcellular migration, leukocyte migrate through an individual endothelial cell by forming a transcellular pore (Wittchen, 2009).

1.3.3 Intestinal Microcirculation

The intestine is an important organ in sepsis pathophysiology. The intestinal microcirculation has an extensive microcirculatory network and also is a reservoir and source of pathogens. During sepsis, the intestinal epithelium that lines the gastrointestinal tract is frequently disrupted due to hypoperfusion, acidosis and subsequent ischemia (Schmidt et al., 1996; Stearns-Kurosawa et al., 2011; Tyagi et al., 2009). Breakdown of the gut barrier leads to escape of bacteria and their toxins into the systemic circulation creating a gut-derived state of sepsis and septic shock (Marshall et al., 1993). Furthermore, gut barrier disruption can lead to additional inflammatory mediators which exacerbate the dysregulated host immune system (Hatoum et al., 2006). Therefore, preserving intestinal microcirculation is crucial to prevent further release of bacteria contributing to multiple organ failure in systemic inflammation.

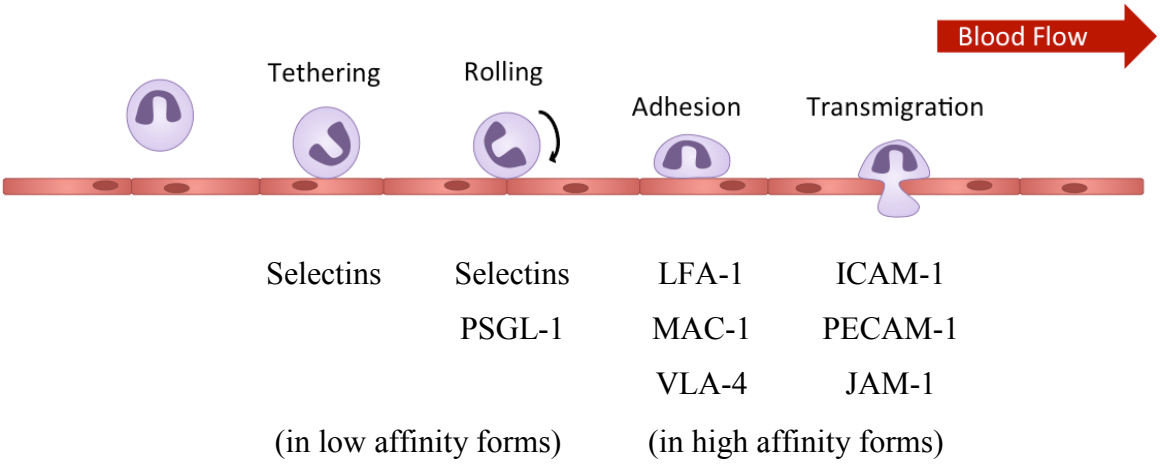

Figure 3: The steps of leukocyte migration. Leukocytes interact with endothelial cells by tethering and rolling mediated by selectins; adhesion mediated by integrins binding to Ig-family members; and transendothelial migration, to be recruited to the site of inflammation from the bloodstream.

1.4 Current Treatments for Sepsis

1.4.1 Current Therapeutic Approaches

Sepsis and septic shock are potentially lethal conditions that require immediate medical attention. Numerous procedures, such as an administration of broad-spectrum antimicrobial therapy, administration of vasopressors, source control, and fluid resuscitation are currently available as treatment regimen for sepsis. However, the mortality rates of sepsis patients still remain high despite the number of treatments and supportive care in ICUs. Moreover, even with the recent advancements in the understanding of sepsis pathophysiology both scientifically and clinically, a specific immune system targeted therapeutic strategy is still not available for treating sepsis. Although there has been several approaches for specific pro- and anti-inflammatory mediator-targeting sepsis treatments, such as TNF or IL-1 blockade, effective therapeutic agents are still lacking (Rice, 2006; Wheeler et al., 2009). Thus, the development of novel immune-modulatory molecules for sepsis treatment is critical.

1.5 The Endocannabinoid system

1.5.1 Overview of the Endocannabinoid System

For many centuries, *Cannabis sativa*, the marijuana plant, has been used medically and recreationally. The marijuana plant contains more than 80 active phytocannabinoids, which bind and activate specific receptors in the cell membrane to influence the central and peripheral nervous system (Howlett et al., 2002; Pertwee, 2006).

Cannabidiol and Δ9-tetrahydrocannabidiol (THC) are the most notable and widely investigated phytocannabinoids from *C. sativa* (Mechoulam, 2002). Although research is being conducted on the psychoactive properties of phytocannabinoids, their potential as therapeutic agents had been disregarded until the discovery of cannabinoid receptor 1 (CB1R), cannabinoid receptor 2 (CB2R) and the endocannabinoid system (ECS) in the early 1990s (Pertwee, 2006).

Endocannabinoids are endogenous lipid-signaling molecules, which bind specific G protein-coupled cannabinoid receptors, CB1R and CB2R. These molecules combined with the enzymes for biosynthesis as well as degradation constitute the endocannabinoid system. The two most widely studied endocannabinoids are N-arachidonyl ethanolamine (anandamide or AEA), classified as the first endocannabinoid in 1992, and 2-arachidonyl (2-AG) (Petrosino et al., 2009; Witkamp and Meijerink, 2014). As endogenous ligands of cannabinoid receptors, pharmacological actions of endocannabinoids resemble those of phytocannabinoids (Mechoulam, 2002; Pertwee, 2006).

Biosynthesis of endocannabinoids is upregulated on demand either through activity-dependent or receptor-stimulated cleavage of arachidonic acid (AA) in the cell membrane, which then activates specific enzymes such as N-acyl-phosphatidylethanol-amine-hydrolysing phospholipase D (NAPE-PLD), for AEA synthesis, and two isoforms of diacylglycerol lipases (DAGLα and DAGLβ) for 2-AG synthesis (Battista et al., 2012; Pertwee, 2015). The lipophilic nature of endocannabinoids prevents vesicle storage and lead to immediate release after production. In response to different physiological and pathological stimuli, local activation of cannabinoid receptors by these lipid transmitters can be observed after biosynthesis (Battista et al., 2012).

Endocannabinoid degradation is managed through enzymatic hydrolysis, which is mediated by specific intracellular enzymes to prevent excessive endocannabinoid signaling. The two main degradation enzymes are fatty acid amide hydrolase (FAAH) and monoacylglycerol lipase (MAGL) for AEA and 2-AG, respectively (Figure 4) (Cravatt et al., 1996; Karlsson et al., 1997). Inhibitors are available for the inhibition of endocannabinoid degradation. For the inhibition of MAGL degradation, specifically, the most well-known substance used is JZL184 (Figure 4) (Long et al., 2009; Seierstad and Breitenbucher, 2008).

1.5.2 Cannabinoid Receptors

The cannabinoid receptors belong to the seven-transmembrane spanning class A G protein-coupled receptor (GPCR) subfamily. GPCRs translate extracellular signals into intracellular responses with activation via intracellular G protein subunits, that triggers downstream signaling pathways (Rosenbaum et al., 2009). In the late 20th century, CB1R and CB2R were identified as the two high-affinity cannabinoid receptors that bind anandamide and 2-AG through molecular cloning (D'Addario et al., 2013; Matsuda et al., 1990; Sharir et al., 2012). CB1R and CB2R are homologous for 44% of their entire protein sequences, and 68% of their transmembrane domain (Galiègue et al., 1995). It is generally accepted that CB1R is mainly located in the central nervous system (CNS) and thus responsible for most of psychoactive effects. CB2R, primarily found in peripheral and immune cells, was reported to be involved in attenuation of inflammatory reactions and immune responses (Buckley, 2008; Hillard, 2015; Sardinha et al., 2014; Toguri et al., 2014; Tsou et al., 1998).

The discovery of cannabinoid receptors led to the development of selective synthetic CB1R and CB2R agonists and antagonists. Some of the well-known CB1-selective agonists include R-(+)-methanandamide, arachidonyl-2'-chloroethylamide (ACEA), arachidonyl-cyclopropylamide (ACPA) and HU210, and antagonists are AM251 and AM281. For CB2R-selective substances, JWH133, HU308 and AM1241 act as agonists, and SR144528 and AM630 act as antagonists (Pertwee, 2006). Compounds such as (–) 11-hydroxy- Δ8-THC- dimethylheptyl (HU-210), CP55940, and R-(+)-WIN55212 are capable of activating both CB1 and CB2 receptors (Figure 5) (Pertwee, 2006).

Both CB1 and CB2 receptors are coupled to $G\alpha_{i/o}$ heteromeric G proteins when activated by endocannabinoids, and thereby inhibit adenylyl cyclase, and activate mitogen-activated protein kinases (MAPKs). The MAPK cascade further results in sequential phosphorylation of various transcription factors downstream of JNK, ERK and p38, resulting in cellular processes such as cell differentiation, growth and survival. (Figure 5) (Battista et al., 2012)

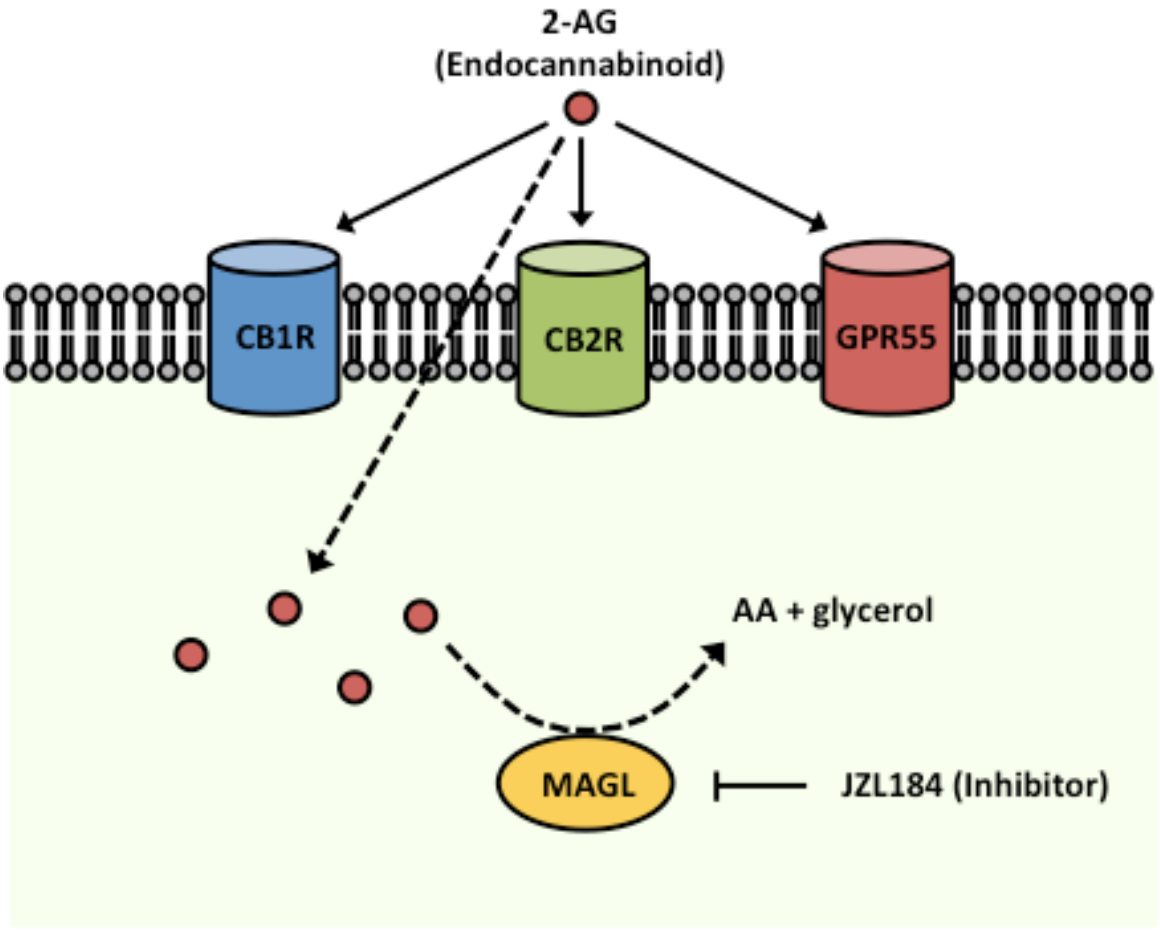

Figure 4: Schematic overview of endocannabinoid, 2-AG, receptors, and degradation enzyme. The cannabinoid receptors, CB1R and CB2R, and GPR55 respond to 2-AG. Intracellular MAGL breaks down 2-AG into arachidonic acid and glycerol, and this process is inhibited by the MAGL inhibitor, JZL184.

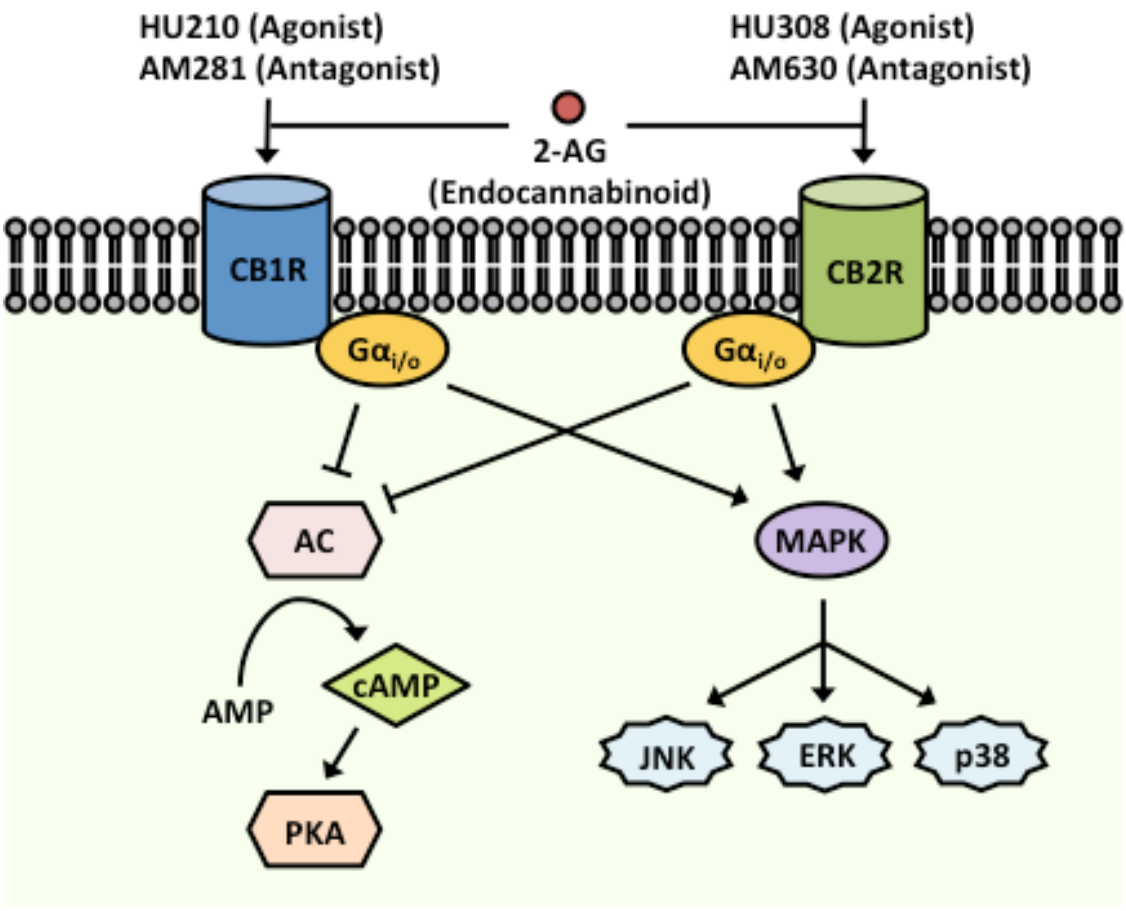

Figure 5: Schematic diagram of the cannabinoid receptor signaling cascade. Upon activation by 2-AG, CB1R and CB2R couple with $G\alpha_{i/o}$ and inhibit adenylyl cyclase and activate MAPK to phosphorylate JNK, ERK and p38 for gene expression.

1.5.3 GPR55

With the use of selective CB1R and CB2R ligands or receptor gene knock out (KO) mice, recent studies proposed the existence of one or more additional cannabinoid-responsive receptors distinct from CB1 and CB2 receptors (Begg et al., 2005). In 2007, it was suggested that there is a "third" cannabinoid receptor with GPR55 as the top candidate. It was indeed evident that the orphan G protein-coupled receptor 55 (GPR55) binds with some synthetic cannabinoids and endocannabinoid ligands; however, recent studies suggested that lysophosphatidylinositol is the main endogenous GPR55 ligand (Ross, 2011; Ryberg et al., 2007).

Human GPR55 (hGPR55) was isolated and cloned in 1999, with high expression in specific regions of the CNS such as the hippocampus, thalamus, hypothalamus, caudate, putamen, cerebellum, and pons. Expression of hGPR55 was also observed in peripheral tissues including adrenal glands, endothelial cells, and gastrointestinal tract (Ryberg et al., 2007; Sawzdargo et al., 1999). In more recent studies, high expression of GPR55 was also detected on lymphocytes and spleen and on cancer cells implying a correlation with the rate of cancer cell proliferation (Henstridge, 2012; Henstridge et al., 2011; Ross, 2011).

Despite the findings that GPR55 shares numerous cannabinoid ligands with CB1R and CB2R, a low amino acid identity is exhibited between GPR55 and CB1R (13.5%) and CB2R (14.4%). Nevertheless, based on amino acid homology, GPR55 is undoubtedly a member of class A GPCRs, which binds endocannabinoid 2-AG with high affinity (Sawzdargo et al., 1999).

The cannabinoid agonist, Δ9-THC, CB1R-selective antagonist/inverse agonist SR141716A (Rimonabant) and CB1R and CB2R agonist CP55,940 are several cannabinoids that interact with GPR55 despite its low homology with the classical cannabinoid receptors (CB1R and CB2R) (Rempel et al., 2013). Studies suggests that 1-lysophosphatidylinositol (LPI), O-1602 and AM251 have agonistic effects on GPR55 while CID16020046, Rimonabant, O-1918 and cannabidiol (CBD) have antagonistic effects (Kargl et al., 2013; Lin et al., 2011; Stančić et al., 2015). However, some studies suggest the opposite or divergent pharmacological effects through GPR55 compared to CB receptors posing a possibility for controversy or uncertainty (Kapur et al., 2009; Sharir and Abood, 2010).

Indeed, further studies are required for complete understanding of GPR55 and the endocannabinoid receptor signaling pathways. There are some differences between cannabinoid receptor and GPR55 signaling. CB1R and CB2R utilize Gαi/o heterotrimeric proteins and adenylate cyclase is known as the trigger for multiple different downstream cascades. On the other hand, GPR55 only couple to $G\alpha_{12,13}$ proteins, thereby activating ras homologue gene family member A (RhoA) and Rho-associated protein kinase (ROCK). Consequently, intracellular Ca^{2+} level is elevated as activation of RhoA and ROCK elicits the phospholipase C (PLC) pathway and small GTPase proteins rhoA, Rac and cdc42 are activated, which then leads to epidermal growth factor receptor kinase (ERK) phosphorylation for further changes in cellular functions (Figure 6) (Henstridge et al., 2009; Oka et al., 2009; Ryberg et al., 2007).

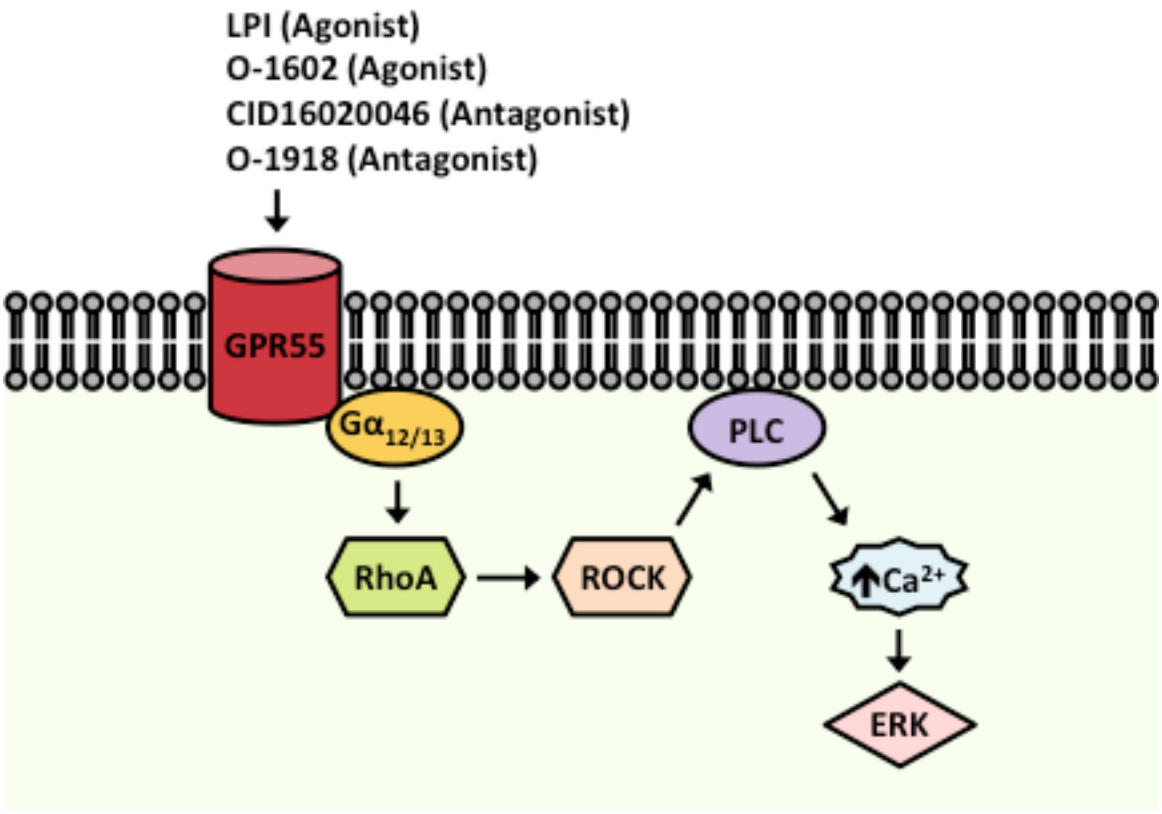

Figure 6: Schematic diagram of the GPR55 signaling cascade. Upon activation, GPR55 binds $G\alpha_{12,13}$ proteins thereby activating RhoA and ROCK. ROCK activates the phospholipase C (PLC) pathway to allow cytosolic concentration of Ca^{2+} to increase, which in turn leads to ERK phosphorylation and gene expression.

1.5.4 Cannabinoid Receptors and GPR55 in Inflammation

Despite the growing evidence of an up-regulation of the endocannabinoid system during local and systemic inflammation, the role of endocannabinoids and their receptors in the inflammatory and adaptive immune response are not fully elucidated (Varga et al., 1998). It has been reported that endocannabinoids, 2-AG and anandamide, are elevated in septic patients implicating the ECS in inflammation (Klein, 2005). Although incomplete, the role of CB1R and CB2R in inflammation is better described compared to GPR55 due to extensive research since their earlier discovery.

Many of characterized CB1R activities are localized in the CNS and vasculature, and less so in the immune system (Chevaleyre et al., 2006). CB1R activation on autonomic nerves and vascular endothelium further aggravates sepsis-associated hypotension, and also CB1R antagonism reduces leukocyte activation and improved capillary flow in the intestine and iris of the eye of septic mice (Al-Banna et al., 2013; Godlewski et al., 2004; Kianian et al., 2014). Nonetheless, there is much to be investigated regarding the underlying mechanism of CB1R action in inflammation.

Contrary to CB1R, CB2R are found mainly on immune cells and play a key role in inflammatory responses in both the periphery and the CNS (Pertwee, 2015). CB2R is generally thought to have an immunosuppressive consequence upon activation, which can be exploited to modulate inflammatory responses such as sepsis. There is evidence from *in vitro* studies that CB2R activation inhibits leukocyte proliferation and migration, and promotes immune cell apoptosis (Basu and Dittel, 2011). Furthermore, selective activation of CB2R with its agonist HU308 was shown to reduce leukocyte activation and their interactions with blood vessel walls in septic mice. Also, CB2R activation with

administration of endocannabinoid degradation enzyme inhibitors, JZL184 or URB597, resulted in a significant reduction in leukocyte-endothelial interactions and pro-inflammatory cytokines, TNF, IL-1β and IL-6, in plasma of septic mice (Lehmann et al., 2012; Sardinha et al., 2014; Toguri et al., 2014). Thus, CB2R is an attractive target in containing inflammation.

The distribution of GPR55 is extensive throughout the body and accumulating evidence has suggested its involvement in a wide range of processes both physiological and pathophysiological, including in the gut (Li et al., 2013; Lin et al., 2011; Schicho and Storr, 2012), inflammatory and neuropathic pain (Staton et al., 2008), and modulation of innate and adaptive immune system (Balenga et al., 2011; Cantarella et al., 2011; Chiurchiù et al., 2014).

Since the rodent gastrointestinal tract widely exhibits GPR55 expression, much research has been conducted to reveal the role of GPR55 in gastrointestinal disease models. In one example, LPS treated intestines increased expression of GPR55 *in vivo* (Lin et al., 2011), which suggests the involvement of GPR55 in intestinal inflammation. In addition, less severe colitis was observed in GPR55 knockout mice compared to CB1R- or CB2R- knockout mice, suggesting a pro-inflammatory role of GPR55 in dextran sulfate sodium induced experimental colitis (Schicho and Storr, 2012; Schicho et al., 2011). In another model of experimental colitis, neuroinflammation and chronic pain diminished in the dinitrobenzenesulfonic acid (DNBS) induced colitis with intracolonic administration of an endogenous anandamide-related lipid, palmitoylethanolamide (PEA) (Borrelli et al., 2015). In this study, PEA administration significantly increased mRNA expression of GPR55 compared to CB2R. Additionally, a mechanical hyperalgesia model using Freund's complete adjuvant suggests pro-inflammatory role of GPR55, which was

evident with neuropathic pain and hypersensitivity absence in GPR55 knockout mice (Staton et al., 2008). Collectively, evidences from the current literatures suggest a pro-inflammatory role of GPR55 in intestinal inflammation.

Although the role of GPR55 is still not entirely clear, GPR55 is particularly suggested to be a regulator of the innate immune system by modulating activities of neutrophils, monocytes and natural killer (NK) cells. For instance, involvement of GPR55 is suggested in neutrophil chemotaxis and recruitment via crosstalk with CB2R orchestrated by various chemoattractants in downstream signaling pathways (Balenga et al., 2011). Enhanced neutrophil migration efficiency and decreased degranulation and ROS formation in neutrophils is possible by inducing the interplay between GPR55 and CB2R during inflammation (Balenga et al., 2011). Moreover, GPR55 found on mast cells displayed anti-inflammatory properties by inhibiting mast cell-mediated release of nerve growth factor (NGF) (Cantarella et al., 2011). Lastly, compared to several innate and adaptive immune cell types from human PBMCs, high expression of GPR55 on monocytes and NK cells is reported (Chiurchiù et al., 2014). Increases in pro-inflammatory cytokines and cytolytic activity of NK cells and a decrease in endocytic activity of LPS-activated monocytes and NK cells is achieved through GPR55 activation (Chiurchiù et al., 2014). Overall, GPR55 modulation of innate immunity and inflammation is supported with this evidence, consequently, GPR55 may be considered as the novel candidate for treatment of inflammatory diseases.

1.6 Hypothesis and Objectives

Despite advances in care, sepsis remains a leading cause of mortality from infection. With growing evidence of the CB2R and GPR55 contributing to immune modulation in inflammatory diseases, the hypothesis raised is: manipulation of CB2R and GPR55 activity at the early phase of the sepsis cascade will improve microcirculation and reduce inflammation (Figure 7). In this study, the therapeutic potential of CB2R and GPR55 modulation was examined *in vivo* and *ex vivo* with the following objectives:

1) To determine the effect of increases in endocannabinoid ligands in the absence of CB2R and assess the physiological responses;
2) To assess the effect of GPR55 modulation on leukocyte-endothelial interactions and microcirculation;
3) To identify the mechanism by which CB2R and GPR55 modulate inflammatory mediators.

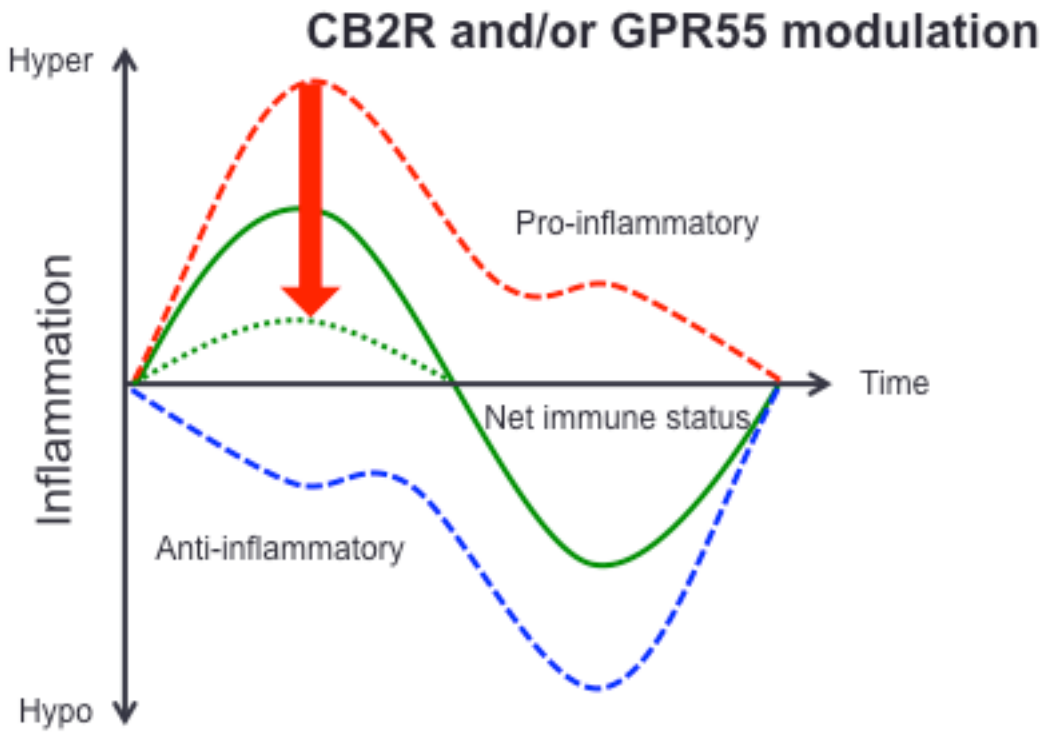

Figure 7: Objective of CB2R and GPR55 modulation in sepsis. The red downward arrow indicates investigations will be undertaken that are predicted to reduce the inflammation of sepsis.

CHAPTER 2: MATERIALS AND METHODS

2.1 Animals

Male C57BL/6 mice (6-8 weeks old; 20–30 g) were purchased from Charles River Laboratories International Inc. (Saint-Constant, QC, Canada) and used for all wild type (WT) endotoxemia and neutrophil transmigration experiments. Animals were allowed to acclimatize for one week and housed at the Carleton Animal Care Facility (CACF) of the Faculty of Medicine at Dalhousie University, Halifax, NS, Canada.

CB2R KO mice (C57BL/6 background; created by Deltagen, San Mateo, CA, USA) were purchased from Jackson Laboratories (Bar Harbor, ME, USA) and bred in house at the CACF. Male homozygous CB2R KO mice were used for experiments after 8 weeks of age. Animals were kept on a standard 12-hour light/dark cycle, with the room temperature maintained at 22°C and humidity 55%–60% prior to surgery. Animals were provided a standard diet of rodent chow and water *ad libitum*. This study was conducted in accordance with the guidelines and standards set forth by the Canadian Council on Animal Care and approved by the University Committee on Laboratory Animals at Dalhousie University, under protocol No. 15-051.

2.2 Anesthesia

Mice were weighed with a commercially available weighing scale prior to anesthesia. All animals received an intraperitoneal (i.p.) injection of sodium pentobarbital

(90 mg/kg, 54 mg/mL; Ceva Sante Animale, Montreal, QC, Canada) at a 50% dilution with 0.9% sodium chloride (Hospira, Montreal, QC, Canada) The depth of anesthesia was monitored by toe pinch, and maintained by additional intravenous (i.v.) injections of 10% pentobarbital as needed throughout the experiment. Animals were provided with oxygen if breathing was labored.

2.3 Endotoxemia Model

2.3.1 Surgical Procedures

After sufficient depth of anesthesia was reached, mice were placed on a heating pad in a supine position to maintain their body temperature at 37°C (98.6°F). A rectal thermometer was used to measure the body temperature, which was recorded every 15 minutes during the experiment. The left side of the neck region was shaved to gain access to the surgical area and disinfected with isopropyl alcohol swabs (Health Care, Toronto, ON, Canada). A small vertical incision was made on the skin using scissors (Fine Science Tools, North Vancouver, BC, Canada) and the surrounding connective tissues were dissected with blunt forceps. The jugular vein was visualized and dissected from surrounding connective tissue, fat and muscle under stereoscopic microscope using fine tip forceps (Fine Science Tools, North Vancouver, BC, Canada). Approximately 5-7 mm section of the left jugular vein was exposed for cannulation avoiding vessel damage. Fine tip forceps were gently placed underneath the vein to pass a folded piece of black braided silk thread (Ethicon, Somerville, NJ, USA), and the thread was cut at the folded end to obtain separate ends. A surgical knot was tied at the superior end of the vessel and a

loose knot was made at the inferior end of the vessel. The right end of the inferior knot was stretched with a hemostat clamp to fill the vessel with blood. Using micro-dissecting scissors (Fine Science Tools, North Vancouver, BC, Canada), a cross section nick was made close to the superior end of the vessel. A non-radiopaque polyethelene tubing (PE10, Clay Adams, Sparks, MD, USA) was inserted into the left jugular vein using fine-tipped micro-forceps (Fine Science Tools, North Vancouver, BC, Canada), and the inferior knot was adjusted to hold the tubing in place. The catheter tubing was inserted approximately 1 cm into the vessel and firmly secured by a triple knot over the vessel with the inserted catheter tubing. After checking the patency of the catheter by flushing with a small volume of normal saline, the surgical site was covered with a small piece of sterile saline soaked gauze. The catheter was used for intravenous (i.v.) administration of saline, LPS, treatment drugs, fluorochromes and anesthetics. During the experiment, extracting mucous and saliva buildup using a short cannula connected to 10 mL syringe prevented obstruction of the trachea.

2.3.2 Experimental Timeline

After the left jugular vein cannulation, endotoxemia was induced by i.v. administration of lipopolysaccharide from *Escherichia coli* (LPS; serotype O26:B6, Sigma-Aldrich, Oakville, ON, Canada). Lipopolysaccharide (LPS; 5 mg/kg, 1 mg/mL) was dissolved in sterile saline (0.9% Sodium chloride; Hospira, Montreal, QC, Canada) and administered i.v. slowly over 5 minutes to induce endotoxemia. Animals in the control group received an equal volume of normal saline i.v.. The treatment compounds were followed 15 minutes after the LPS challenge. Endotoxemia was carried out over 2

hours until intravital microscopy (IVM) with temperature measurements every 15 minutes (Figure 8). For IVM, fluorochromes were administered i.v. and laparotomy was performed 30 minutes and 15 minutes prior to IVM, respectively (details in section 2.6). Blood and tissue samples were collected for further analysis at the end of the experiment (details in section 2.7).

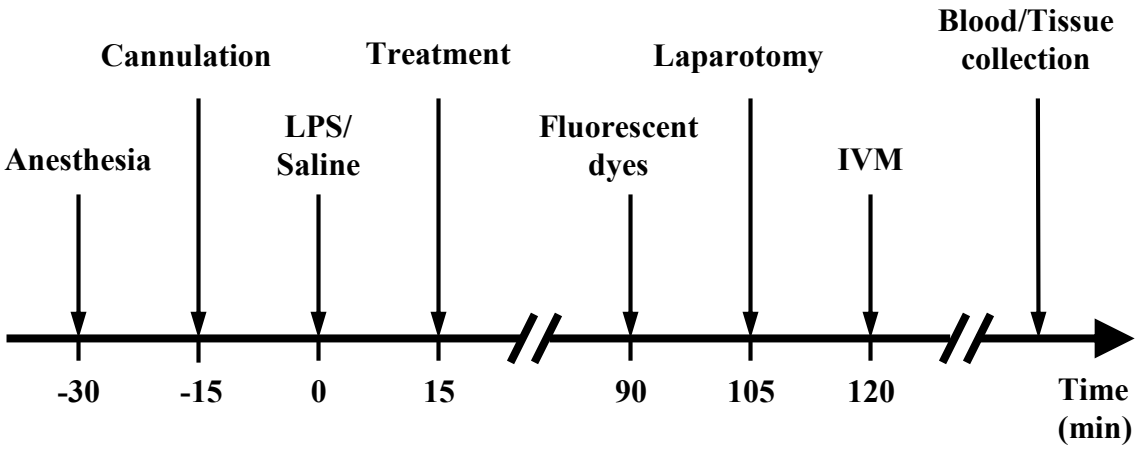

Figure 8: Experimental timeline for the endotoxemia protocol.

2.4 Pharmacological Agents

JZL184 (Tocris Bioscience, Ellisville, MO, USA) is a selective irreversible inhibitor of monoacylglycerol lipase (MAGL) with an IC_{50} value of 8.4 nM in mouse brain (Chang et al., 2012). JZL184 (16 mg/kg) was dissolved in 30% dimethyl sulfoxide (DMSO; Sigma Aldrich, Oakville, ON, Canada) vehicle solution. AM281 (Tocris Bioscience, Ellisville, MO, USA) is a potent and selective CB1R antagonist with K_i values of 12 and 4200 nM for CB1R and CB2R respectively (Lan et al., 1999). AM281 (2 mg/kg was dissolved in 10% DMSO vehicle solution.

Lysophosphatidylinositol (LPI, L-α-Lysophosphatidylinositol sodium salt from Glycine max (soybean); Sigma Aldrich, Oakville, ON, Canada) is a natural GPR55 agonist with an EC_{50} value of 200 nM (Sharir and Abood, 2010). LPI (5 mg/kg) was dissolved in sterile normal saline. O-1602 (Tocris Bioscience, Ellisville, MO, USA) is a potent GPR55 agonist with an EC_{50} value of 13, > 30000 and > 30000 nM for GPR55, CB1R and CB2R, respectively (Johns et al., 2007). O-1602 (5 mg/kg) was dissolved in 5% methyl acetate (Sigma Aldrich, Oakville, ON, Canada). CID16020046 (Tocris Bioscience, Ellisville, MO, USA) is a selective GPR55 antagonist with IC_{50} value of 210 nM in vitro (Kargl et al., 2013). CID16020046 (20 mg/kg) was dissolved in 20% DMSO and stock solutions were further diluted with normal saline to a final concentration of 10% DMSO. O-1918 (Tocris Bioscience, Ellisville, MO, USA) is a GPR55 antagonist (Offertáler et al., 2003). O-1918 (5 mg/kg) was dissolved in 5% methyl acetate (Sigma Aldrich, Oakville, ON, Canada).

2.5 Experimental Groups

Mice were randomly divided into 10 experimental groups with 5 to 7 animals per group (Table 2). Groups 1 to 4 consisted CB2R KO mice. Group 1 received normal saline in an equal volume as the volume of LPS as a healthy control group (CON). Group 2 was an untreated endotoxemia group (LPS; 5 mg/kg). Group 3 received LPS (5 mg/kg) and monoacylglycerol lipase (MAGL) inhibitor JZL184 (16 mg/kg) 15 minutes after LPS challenge. Group 4 received LPS (5 mg/kg), CB1R antagonist AM281 (2 mg/kg) and JZL184 (16 mg/kg) 7.5 minutes and 15 minutes after LPS challenge, respectively (Table 2).

Groups 5 to 10 were GPR55 modulation experiments in WT mice. Group 5 received normal saline at an equal volume of LPS as a healthy control group (CON). Group 6 was an untreated endotoxemia group (LPS; 5 mg/kg). Group 7 received LPS (5 mg/kg) and GPR55 agonist LPI (5 mg/kg). Group 8 received LPS (5 mg/kg) and GPR55 agonist O-1602 (5 mg/kg). Group 9 received LPS (5 mg/kg) and GPR55 antagonist CID16020046 (20 mg/kg). Group 10 received LPS (5 mg/kg) and GPR55 antagonist O-1918 (5 mg/kg). All treatment compounds were given 15 minutes post LPS administration (Table 2).

Table 2: Experimental groups for the endotoxemia study.

Groups	Mice	Intervention
Group 1: Control	CB2R KO	Saline
Group 2: Endotoxemia	CB2R KO	LPS (5 mg/kg)
Group 3: LPS + MAGL inhibitor	CB2R KO	LPS (5 mg/kg) + JZL184 (16 mg/kg)
Group 4: LPS + MAGL inhibitor + CB1R antagonist	CB2R KO	LPS (5 mg/kg) + JZL184 (16 mg/kg) + AM281 (2 mg/kg)
Group 5: Control	WT	Saline
Group 6: Endotoxemia	WT	LPS (5 mg/kg)
Group 7: LPS + GPR55 agonist	WT	LPS (5 mg/kg) + LPI (5 mg/kg)
Group 8: LPS + GPR55 agonist	WT	LPS (5 mg/kg) + O-1602 (5 mg/kg)
Group 9: LPS + GPR55 antagonist	WT	LPS (5 mg/kg) + CID16020046 (20 mg/kg)
Group 10: LPS + GPR55 antagonist	WT	LPS (5 mg/kg) + O-1918 (5 mg/kg)

2.6 Intravital Microscopy

Intravital microscopy (IVM) was performed in all groups 2 hours post endotoxemia induction. The duration of IVM procedure was approximately 30 to 40 minutes for each experiment. Procedures for animal preparation and IVM are outlined in the following sections.

2.6.1 Fluorescence Staining

Fluorescence staining was carried out 30 minutes prior to IVM to observe leukocyte-endothelial interactions within the intestinal microvasculature. Leukocyte staining was obtained by administering 0.05% rhodamine-6G (1.5 mL/kg, i.v.; Sigma Aldrich, Oakville, ON, Canada). To visualize the capillary flow by amplified flow of the plasma and observe capillary perfusion, 5% fluorescein isothiocyanate-bovine serum albumin (FITC-BSA, 1 mL/kg; Sigma Aldrich, Oakville, ON, Canada) was also administered 30 minutes prior to IVM. All fluorochromes were administered via left jugular vein catheter.

2.6.2 Laparotomy

Laparotomy was performed 15 minutes before IVM after ensuring the animal's anesthetic depth was sufficient. Using a scalpel, a superficial midline incision was made on the shaved animal's abdominal skin to expose the muscle layer. The muscular layer was lifted with fine-tipped forceps and cut along *linea alba* using fine tissue scissors to

expose the abdominal cavity. By lifting the muscular layer and cutting along *linea alba*, bleeding is minimized.

2.6.3 Intravital Microscopy Setup

Using saline soaked cotton tipped applicators, the caecum was located and a small portion of the terminal ileum was exteriorized onto a pre-heated hook (37°C) of a specially designed apparatus attached onto the heating pad (Lehmann et al., 2013; Pavlovic et al., 2006). The apparatus enabled continuous thermostat-controlled (37°C) saline to be perfused over the exposed intestine to reflect physiological conditions of both temperature and moisture. The saline was continuously pumped at a rate of 5 mL/hour and a glass slide was used to make a liquid contact with the section of intestine placed on the stage. The glass slide was placed over the intestine without compression to avoid blocking microcirculatory flow. Then, the heating pad containing the animal and the IVM apparatus was placed under microscope for observation.

2.6.4 Microscopy

IVM of the terminal ileum was performed using an epifluorescence microscope (Leica DMLM, Wetzlar, Germany) with a mercury-arc light source (LEG EBQ 100; Carl Zeiss, Jena, Germany). A water immersion lens (Leica N PLAN L 20X/0.40) was used to make a liquid contact between the lens and glass slide over the section of intestine for observation. Randomly chosen intestinal vessels were captured by a black and white DAGE CCD video camera (DAGE MTI Inc., Michigan city, IN, USA). Videos were recorded through video converter (DFG/USB2PRO, The Imaging Source, LLC, Charlotte,

NC, USA) and IC-capture software (The Imaging Source, LLC, Charlotte, NC, USA), and then stored on external hard drives for analysis. Six visual fields of each vascularity were video recorded for 30 seconds (described below).

2.6.5 Leukocyte Activity

The microscope was set to focus on the submucosal venules under the green excitation filter to investigate rhodamine 6G-labeled leukocyte activity. Six randomized visual fields containing non-branching, submucosal collecting venules (V1, diameter 50-100 μm) and postcapillary venules (V3, diameter <50 μm) over a length of 300 μm were observed and recorded for 30 seconds each.

2.6.6 Functional Capillary Density

The microscope was set to focus on the muscular layers and mucosal villi under the blue excitation filter to observe capillary perfusion with FITC. The longitudinal and circular muscle layers of the intestine were focused and six randomly selected fields of capillaries were recorded for 30 seconds.

To visualize capillary perfusion of the mucosal villi, the intestinal surface was cauterized longitudinally using a microcautery knife (Medtronic, FL, USA) and cut using a fine tissue scissors. The intestinal wall was cut open and the luminal content was flushed with warm normal saline. Then, the lumen of the intestine was gently cleaned and exposed using saline-soaked cotton tipped applicators. A glass slide was place over the exposed lumen to create liquid contact between the tissue and the glass slide. The

microscope was focused to the mucosal villi and six randomly selected fields of villi capillaries were recorded for 30 seconds.

2.6.7 Video Analysis

Evaluations of all video recordings were blinded and analyzed off-line using ImageJ software (NIH Image, USA). For each animal, the following parameters were analyzed: adherent leukocytes, rolling leukocytes, capillary perfusion of muscular layers and mucosal villi. Leukocytes adherent to the endothelia for 30 seconds were defined as adherent leukocytes while all non-adherent leukocytes passing through a designated point across the vessel with a speed of less than 50 μm/second were defined as rolling leukocytes. This data allowed us to quantify the number of adherent leukocytes in a predetermined area of vessel (cells/mm^2) and the number of rolling leukocytes (cells/minute). Functional capillary density (FCD) was used to quantify capillaries with observable erythrocyte perfusion. The lengths of perfused capillaries were measured in a defined area and the sum of the capillary lengths was used to calculate the FCD (μm/$μm^2$).

2.7 Blood Collection

Following IVM, cardiac puncture was performed and blood was collected using a 1 mL syringe with a 30-gauge needle pre-coated with 5 μL heparin (Pharmaceutical Partners of Canada Inc., Richmond Hill, ON, Canada). The blood sample was placed in a 1.5 mL microfuge tube and centrifuged at 10,000 x g for 10 minutes at room temperature.

The plasma was collected and aliquoted into 0.5 mL microtubes. The plasma samples were flash frozen in liquid nitrogen and stored at -80°C for subsequent use.

2.8 Plasma Cytokine and Chemokine Analysis

Cytokine levels in the plasma samples from all experimental groups were measured using a custom-made 12-plex Mouse Magnetic Luminex Screening Assay purchased from R&D Systems (Minneapolis, MN, USA). The cytokines and adhesion molecules measured were TNF, IL-1β, IL-2, IL-4, IL-6, IL-10, IL-12 p70, IL-13, IL-17A, IFN-γ, P-Selectin and ICAM-1 using the Luminex Technology Analyzer and BioPlex Manager software (Bio-Rad, Missisauga, ON, Canada). The detection of analytes was performed on 5 biological and 2 technical replicates of all experimental groups. According to the Procarta cytokine assay manual, the Luminex instruments were calibrated before each experiment and validated once every 30 days. The experiments were performed only when the calibration and validation were successful. The multiplex assay was carried out according to the manufacturer's specifications and the standard Affymetrix multiplex immunoassay protocol for detection of mouse molecules.

2.9 Neutrophil Transmigration

2.9.1 Mouse Neutrophil Isolation

Mouse bone marrow polymorphonuclear neutrophils (PMNs) were isolated from femurs and tibias of C57BL/6 mice (8 weeks old, male). Bone marrows were flushed

using a 26-gauge needle and 3 cc syringe filled with 1X HBSS (1 mM EDTA, 10 mM HEPES, 2% FBS). Bone marrow cells were centrifuged at 300 x g for 10 minutes at 4°C, and resuspended in 1X HBSS (1 mM EDTA, 10 mM HEPES, 2% FBS). PMNs were then isolated from single cell suspensions of bone marrow by negative selection by using EasySep™ Mouse Neutrophil Enrichment Kit and EasySep™ magnet (Stemcell Technologies, Vancouver, BC, Canada) following the manufacturer's instructions. Once neutrophils were isolated, the total number of cells and the purity were calculated for the transmigration assays. After the cells were washed, PMNs were resuspended in 1X HBSS (1 mM EDTA, 10 mM HEPES, 2% FBS) (Figure 9).

2.9.2 Transwell Migration Assays

Transmigration assays were performed using the transwell system (3.0 μm pores, clear polyester membrane for 24-well plates, Cat # 3472, Corning, Corning, NY, USA) inserted in 24-well plates. The transwell filters were pre-coated with 0.7 mL RPMI supplemented with 5% fetal bovine serum (FBS) for 4 hours at 37°C/5% CO_2 prior to use. Neutrophil migration was assessed in different concentrations of chemoattractant and treatment drugs (Table 3). In microfuge tubes, 200,000 neutrophils were pre-incubated with the vehicle or treatment drugs in 0.1 mL RPMI (1% FBS) for 30 minutes at 37°C/5% CO_2. The bottom chamber was filled with 0.6 mL RPMI (1% FBS) with or without the chemoattractant, N-formylmethionine-leucyl-phenylalanine (fMLP, 10 nM; Sigma Aldrich, Oakville, ON, Canada). Treatment drugs were added to the bottom chamber as well at an equal concentration with the top chamber. The pre-treated neutrophils were then loaded into the top chamber and incubated at 37°C/5% CO_2 for 60 minutes. The cells

in top and bottom chambers were subsequently collected into microfuge tubes and counted using a hemocytometer. The percentage of migrate cells was calculated by dividing the number of migrated cells over the total number of cells recovered from the transwell (Figure 9).

2.10 Statistical Analyses

Results were analyzed by using the software GraphPad Prism 6.0 (GraphPad Software, La Jolla, CA, USA). After Kolmogorov-Smirnov testing for normal distribution, all data were analyzed using a one-way ANOVA followed by Newman-Keuls multiple comparisons test for group wise comparisons. All data are expressed as mean ± standard deviation (SD). Significance was considered at $p < 0.05$.

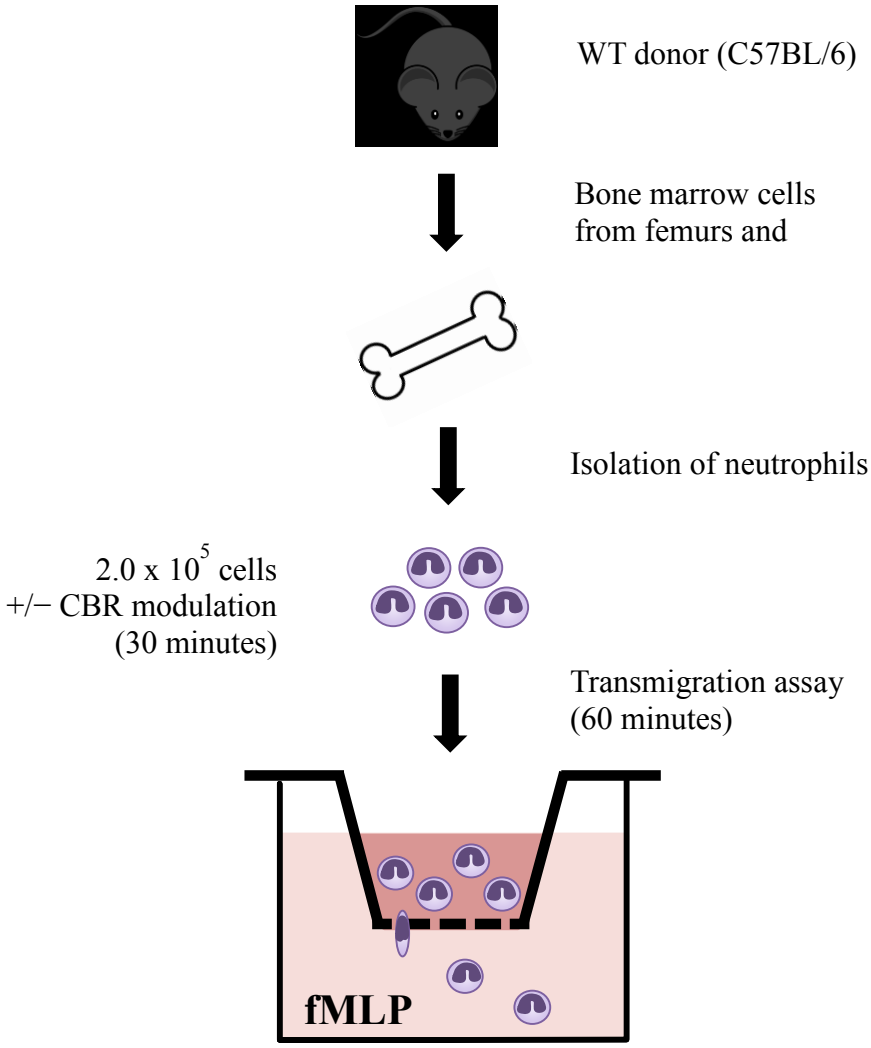

Figure 9: The neutrophil transmigration assay. Neutrophils were isolated from bone marrow of C57BL/6 mice. Purified neutrophils were then pre-incubated with or without treatment drugs for 30 minutes and added to the top chamber with the chemoattractant, fMLP, in the bottom chamber and the transwell left to incubate for 60 minutes.

Table 3: Experimental groups for neutrophil migration assay.

Groups	Chemoattractant	Treatment compound
Group 1: No treatment	-	Saline
Group 2: Chemoattractant control	10 nM fMLP	Saline
Group 3: fMLP + CB2R agonist (low dose)	10 nM fMLP	1 μM HU308
Group 4: fMLP + CB2R agonist (high dose)	10 nM fMLP	10 μM HU308
Group 5: fMLP + GPR55 agonist (low dose)	10 nM fMLP	1 μM LPI
Group 6: fMLP + GPR55 agonist (high dose)	10 nM fMLP	10 μM LPI
Group 7: fMLP + CB2R antagonist (low dose)	10 nM fMLP	1 μM CID16020046
Group 8: fMLP + CB2R antagonist (high dose)	10 nM fMLP	10 μM CID16020046

CHAPTER 3: RESULTS

3.1 Endotoxemia in CB2KO Mice – CBR Modulation

3.1.1 Leukocyte Adherence

Previous studies in our lab demonstrated that direct agonist-induced CB2R stimulation as well as enhanced CB2R activation through blocking the degradation enzyme, monoacylglycerol lipase (MAGL) with JZL184, resulted in suppression of leukocyte adhesion (Sardinha et al., 2014). To further investigate the role of CB2R in leukocyte activation during endotoxemia, CB2R KO mice were administered either JZL184 or the combination of JZL184 and a CB1R inhibitor, AM281. The outcome was analyzed by intravital microscopy. First, leukocyte adherence in the intestinal submucosal collecting venules (V1; > 50 μm vessel diameter) was measured in CB2R KO mice (Figure 10). Endotoxin challenge significantly increased the number of leukocytes adhering to the submucosal collecting venules compared to control animals ($p < 0.05$). Endotoxemic animals treated with JZL184 had significantly lower numbers of adherent leukocytes on V1 venules (Figure 10). JZL184 treatment combined with CB1R inhibition through AM281 administration also reduced leukocyte adherence in V1 venules compared to LPS group at a similar level with the JZL184 group (Figure 10). Considering an increase in endogenous cannabinoids significantly reverses adhesion in CB2R KO mice suggests the CB2R plays no role in adhesion during sepsis.

Similar results as seen in V1 were observed with leukocyte adherence in post-capillary venules (V3; < 50 μm vessel diameter). LPS administration significantly ($p < 0.05$) increased the number of adherent leukocytes compared to the control group (Figure 11). Treatment with JZL184 or AM281 with JZL184 post LPS challenge reduced the level of leukocyte adhesion to a similar level though lower than the LPS group (Figure 11).

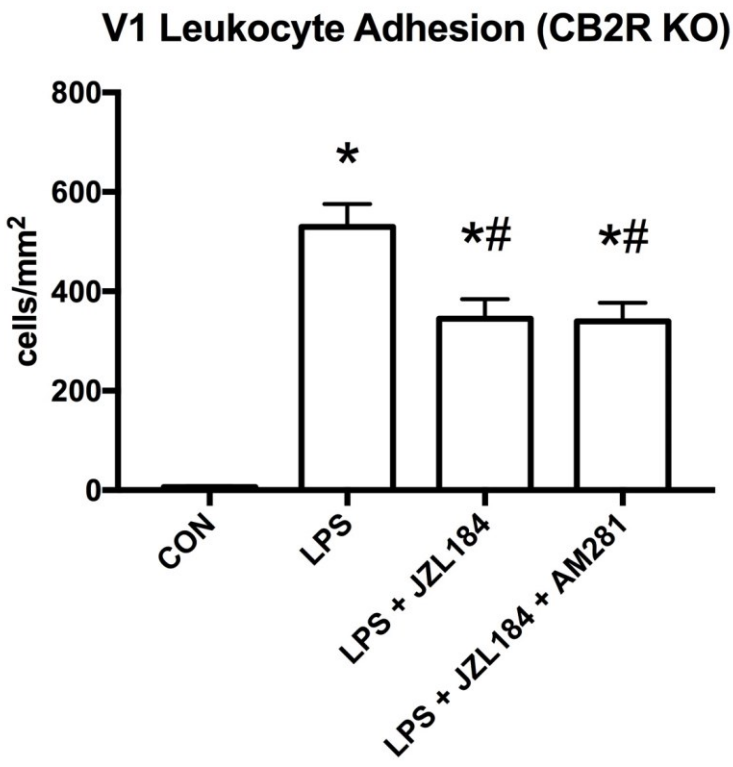

Figure 10: Leukocyte adhesion in intestinal collecting venules (V1; > 50 μm vessel diameter) after systemic administration of saline or LPS and cannabinoid treatments in CB2R KO mice. Bars represent the average number of adherent leukocytes in collecting venules per area (cells/mm^2). Data represented as mean ± SD (n = 5 per group). * $p < 0.05$ compared to the CON group. # $p < 0.05$ compared to the LPS group.

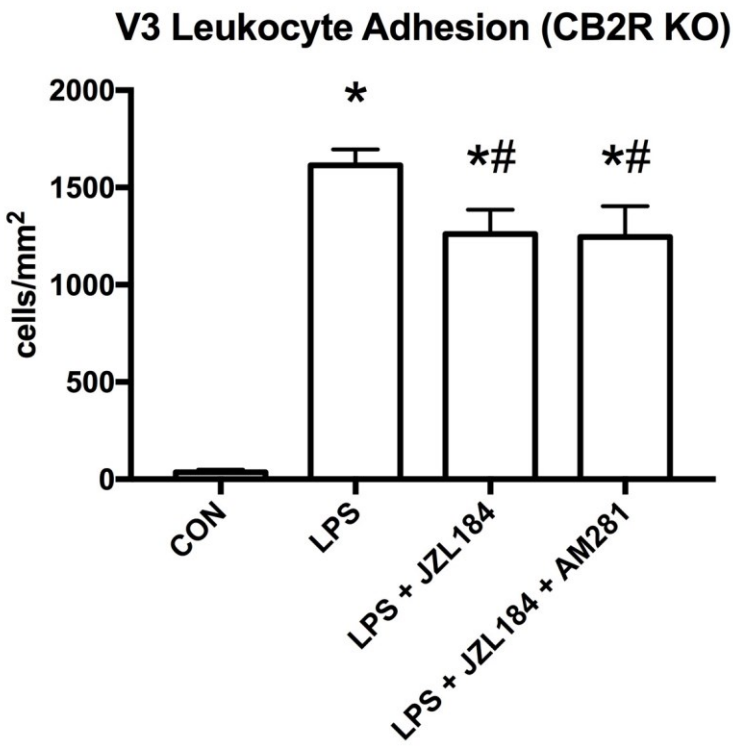

Figure 11: Leukocyte adhesion in intestinal post-capillary venules (V3; < 50 μm vessel diameter) after systemic administration of saline or LPS and cannabinoid treatments in CB2R KO mice. Bars represent the average number of adherent leukocytes in collecting venules per area (cells/mm^2). Data represented as mean ± SD (n = 5 per group). * $p < 0.05$ compared to the CON group. # $p < 0.05$ compared to the LPS group.

3.1.2 Leukocyte Rolling

The step preceding leukocyte adhesion, rolling, was also measured as another parameter of leukocyte activation and inflammation. The LPS challenge resulted in a significant reduction ($p < 0.05$) in the number of rolling leukocytes in intestinal post-capillary venules (V1) compared to control group. With administration of JZL184 or combined administration of JZL184 and AM281 after LPS challenge both significantly increased ($p < 0.05$) the number of rolling leukocytes in the collecting venules (V1) of intestine (Figure 12).

The number of leukocytes rolling in V3 venules was significantly decreased ($p < 0.05$) with endotoxemia compared to control group. Administration of JZL184 did not significantly increase ($p > 0.05$) leukocyte rolling compared to LPS. Furthermore, combination treatment with JZL184 and AM281 also did not result in a significant increase ($p > 0.05$) in V3 venules (Figure 13).

3.1.3Functional Capillary Density

A reduction in FCD is one of the sepsis-induced changes in the microcirculation. In the intestinal muscle layers of CB2R KO mice, FCD was slightly decreased (n.s.) after LPS administration (Figure 14). Treatment with JZL184 or JZL184 combined with AM281 after endotoxin challenge did not significantly change FCD compared to control or untreated LPS group (Figure 14).

Similar to FCD in the intestinal muscle, FCD in the mucosal villi was not impacted by endotoxemia and the drug treatments with JZL184 and AM281 (Figure 15).

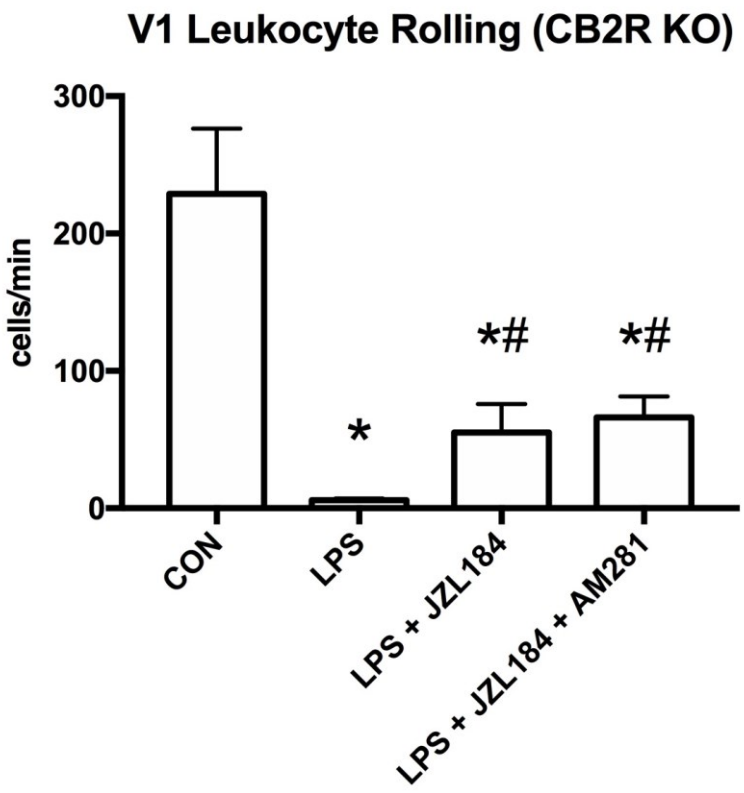

Figure 12: Leukocyte rolling in intestinal collecting venules (V1; > 50 μm vessel diameter) after systemic administration of saline or LPS and cannabinoid treatments in CB2R KO mice. Bar graphs represent the number of rolling leukocytes in collecting venules (cells/min). Data represented as mean ± SD (n = 5 per group). * $p < 0.05$ compared to the CON group. # $p < 0.05$ compared to the LPS group.

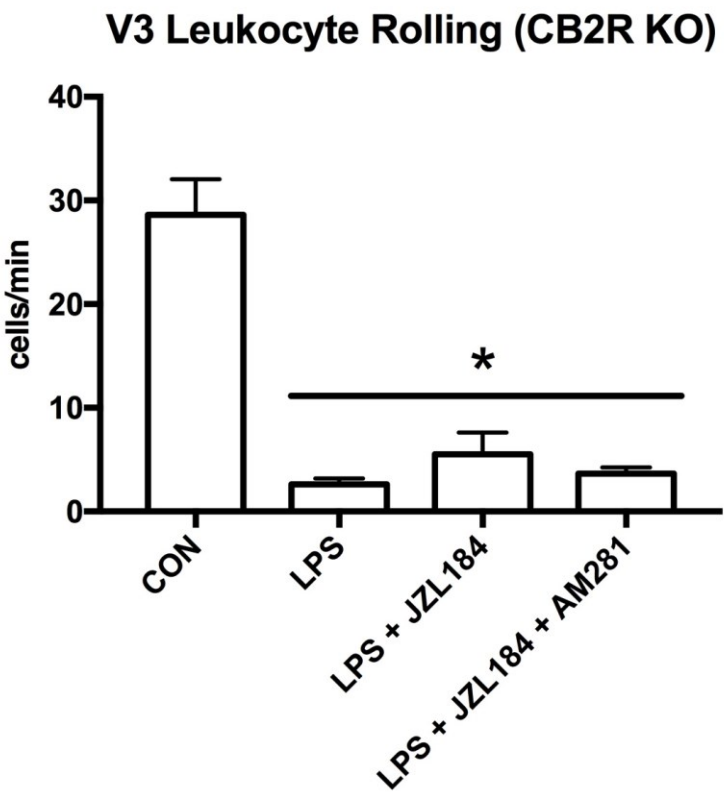

Figure 13: Leukocyte rolling in intestinal post capillary venules (V3; < 50 μm vessel diameter) after systemic administration of saline or LPS and cannabinoid treatments in CB2R KO mice. Bar graphs represent the number of rolling leukocytes in post capillary venules (cells/min). Data represented as mean ± SD (n = 5 per group). * $p < 0.05$ compared to the CON group.

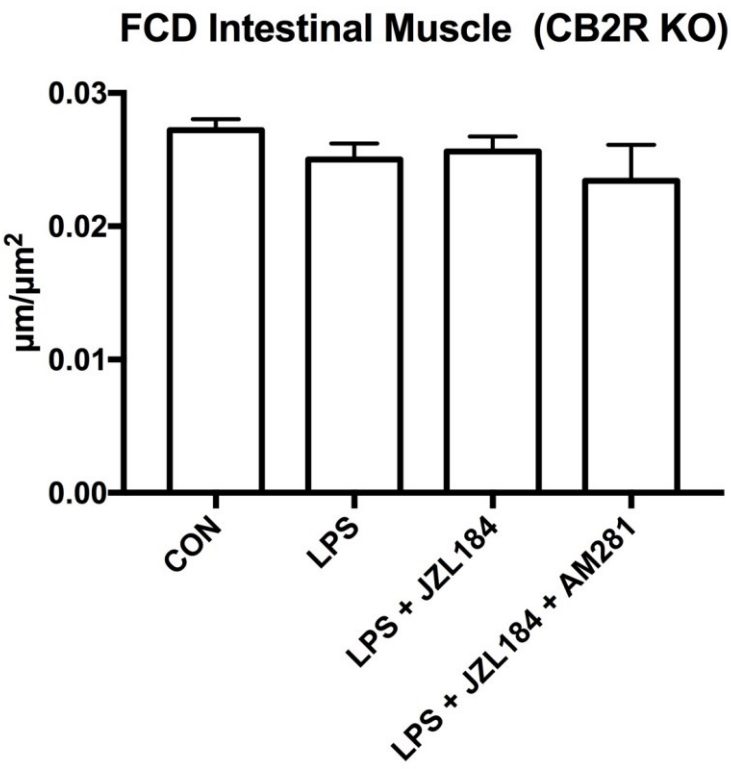

Figure 14: Capillary perfusion quantified through FCD within the muscle layers of the intestine after systemic administration of LPS/saline and cannabinoid treatments in CB2R KO mice. FCD quantified as total length of perfused capillaries within a predetermined rectangular area of the observed field ($\mu m/\mu m^2$). Data represented as mean ± SD (n = 5 per group).

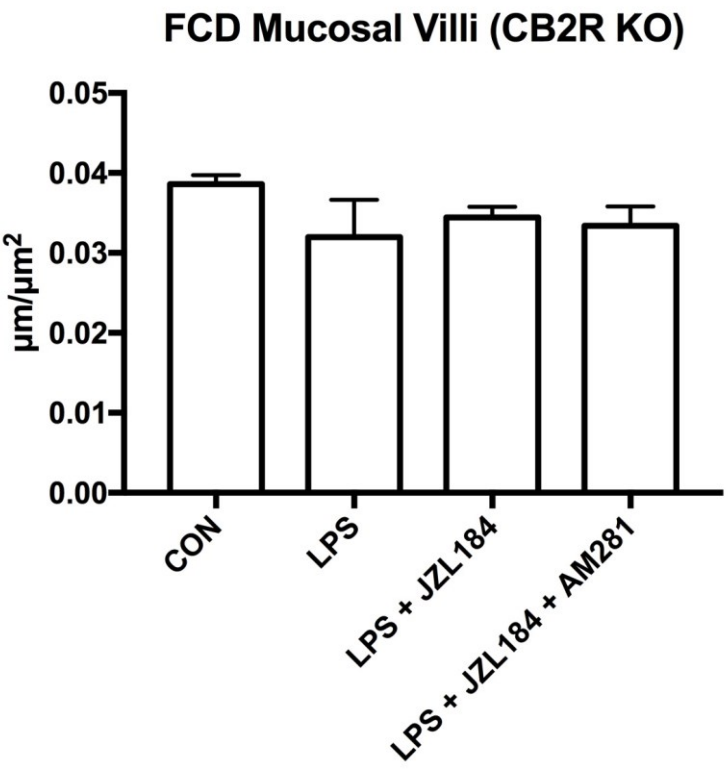

Figure 15: Capillary perfusion quantified through FCD within the mucosal villi of the intestinal lumen after systemic administration of saline or LPS and cannabinoid treatments in CB2R KO mice. FCD quantified as total length of perfused capillaries within a predetermined rectangular area of the observed field ($\mu m/\mu m^2$). Data represented as mean ± SD (n = 5 per group).

3.1.4 Cytokines and Adhesion Molecules

To investigate the effect of LPS and molecular mechanisms of the CBR modulation in leukocyte activation, circulating pro-inflammatory and anti-inflammatory cytokines were measured in the plasma samples. In the CB2R KO mice, LPS injection significantly increased ($p < 0.05$) the circulating levels of TNF, IL-6 and IL-10 (Figure 16). The levels of TNF and IL-6 were unaffected by treatments, JZL184 or JZL184 with AM281, whereas the level of IL-10 increased significantly ($p < 0.05$) with JZL184 treatment (Figure 16). The concentrations of IL-1β (Figure 16), IL-2, IL-4, IL-12 p70, IL-13, IL-17A, and IFN-γ were not significantly altered after induction of endotoxemia or administration of drug treatments (Figure 17).

The levels of soluble adhesion molecules, P-selectin and ICAM-1, were also measured. The P-selectin level was significantly decreased ($p < 0.05$) in the group with JZL184 treatment compared to LPS group (Figure 18). For the CON group, LPS group and JZL184 + AM281 group, plasma levels of P-selectin were comparable with no significant changes (Figure 18). The concentration of ICAM-1 had no significant differences in all groups (Figure 18).

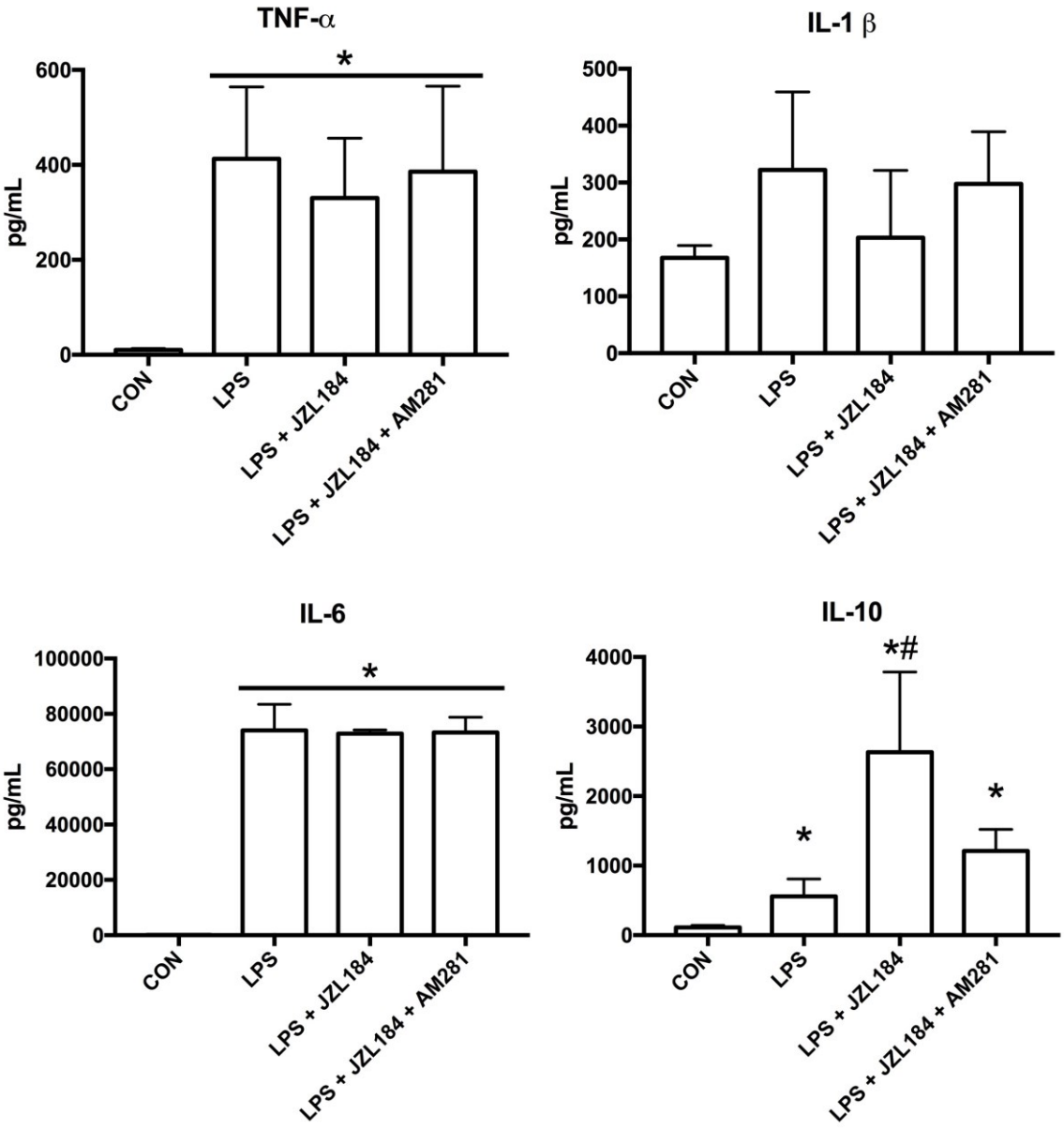

Figure 16: Levels of plasma cytokines in CB2R KO mice (pg/mL). Bar graphs represent the mean concentrations of TNF, IL-1β, IL-6 and IL-10. Results are represented as mean ± SD (n = 5 per group). * $p < 0.05$ compared to the CON group. # $p < 0.05$ compared to the LPS group.

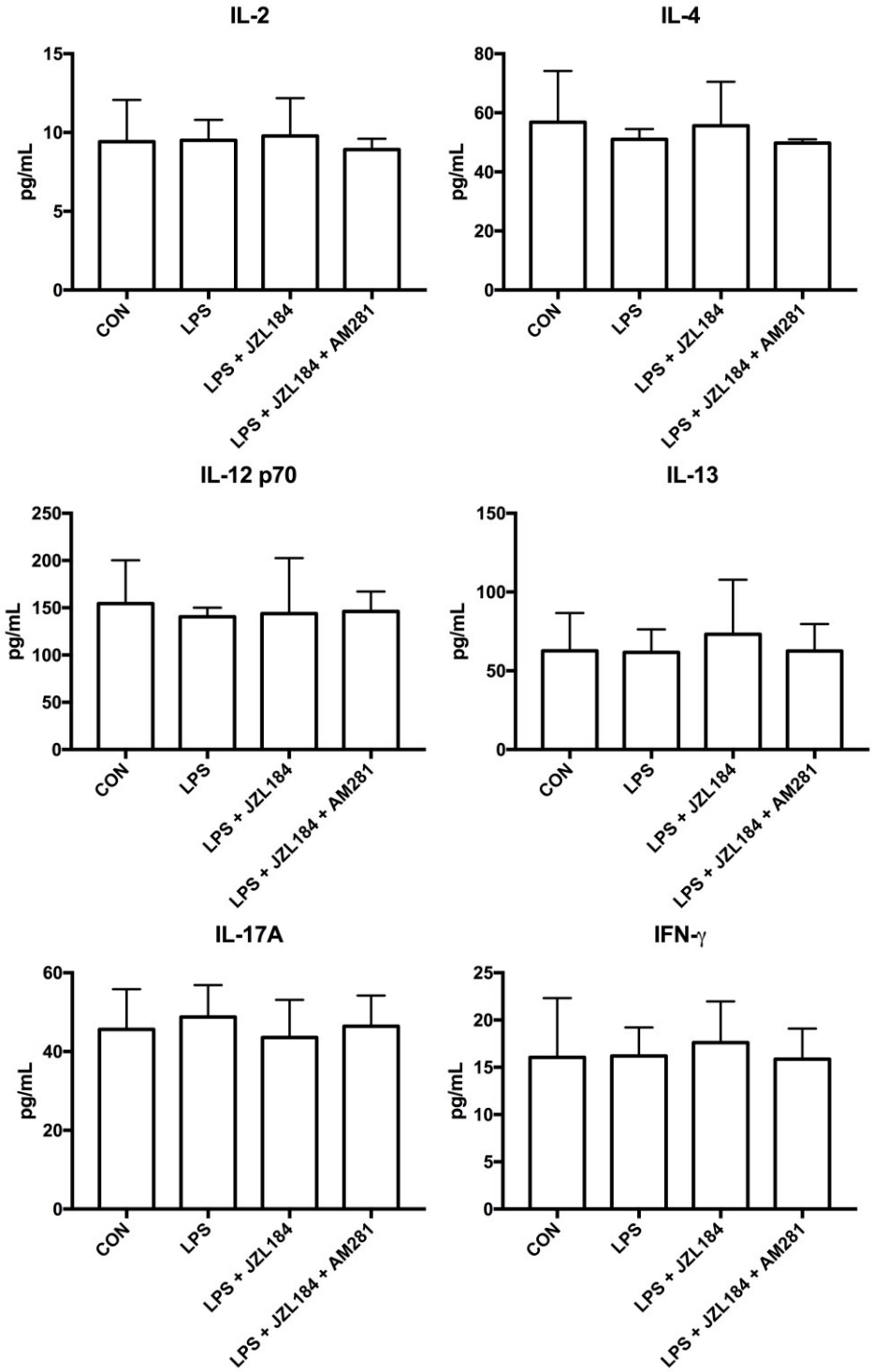

Figure 17: Levels of plasma cytokines in CB2R KO mice (pg/mL). Bar graphs represent the mean concentrations of IL-2, IL-4, IL-12 p70, IL-13, IL-17A and IFN-γ. Results are represented as mean ± SD (n = 5 per group).

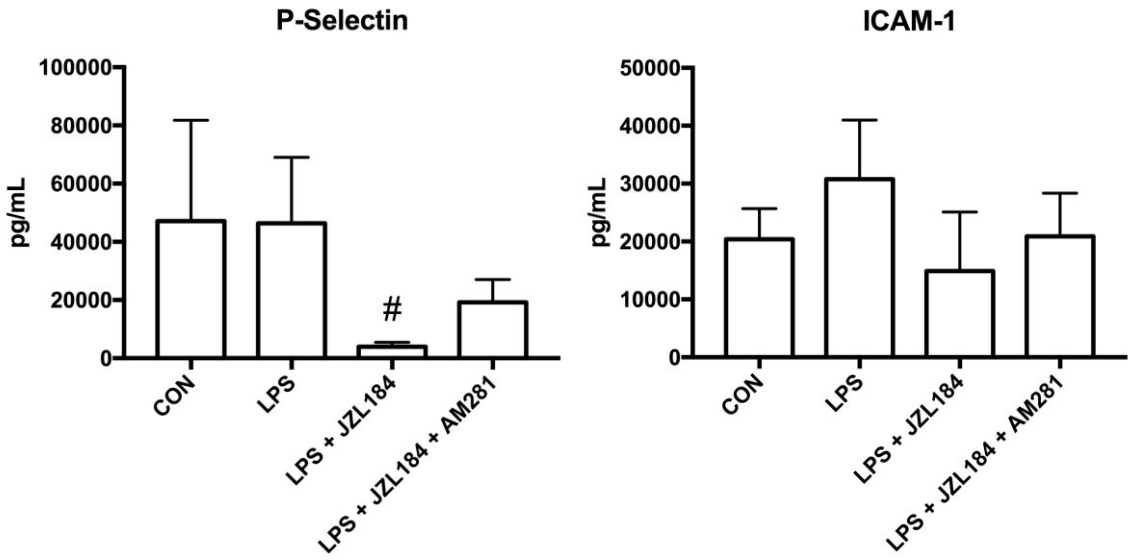

Figure 18: Levels of plasma adhesion molecules in CB2R KO mice (pg/mL). Bar graphs represent the mean concentrations of P-selectin and ICAM-1. Results are represented as mean ± SD (n = 5 per group). # $p < 0.05$ compared to the LPS group.

3.2 Endotoxemia in WT Mice – GPR55 Modulation

3.2.1 Leukocyte Adherence

Although several studies have reported on the immune-modulatory activity of GPR55 (Lin et al., 2011; Schicho et al., 2011), little is known about the role in sepsis. Intravital microscopy analysis was used to investigate the potential function of GPR55 on leukocyte activity during endotoxemia in wt mice. In control animals, the numbers of adherent leukocytes in intestinal collecting venules were minimal. As expected, LPS challenged animals showed significantly increased ($p < 0.05$) numbers of adherent leukocytes in V1 venules compared to control group (Figure 18). In contrast to the findings with CB2R, the levels of adherent leukocytes in V1 venules of animals treated with GPR55 activation by LPI and O-1602 were not anti-inflammatory, and instead did not differ from LPS group (Figure 18). Furthermore, the administration of GPR55 antagonists, CID16020046 or O-1918, showed significantly decreased ($p < 0.05$) numbers of adherent leukocytes compared to endotoxemic mice with no treatment (Figure 18).

Similar to the results in V1 venules, administration of LPS significantly increased ($p < 0.05$) leukocyte adhesion in V3 venules compared to controls (Figure 19). Treatments with GPR55 agonists, LPI and O-1602, resulted in a similar level of leukocyte adhesion as the LPS group (Figure 19). In the groups treated with GPR55 antagonists, CID16020046 and O-1918, were significantly decreased (Figure 19).

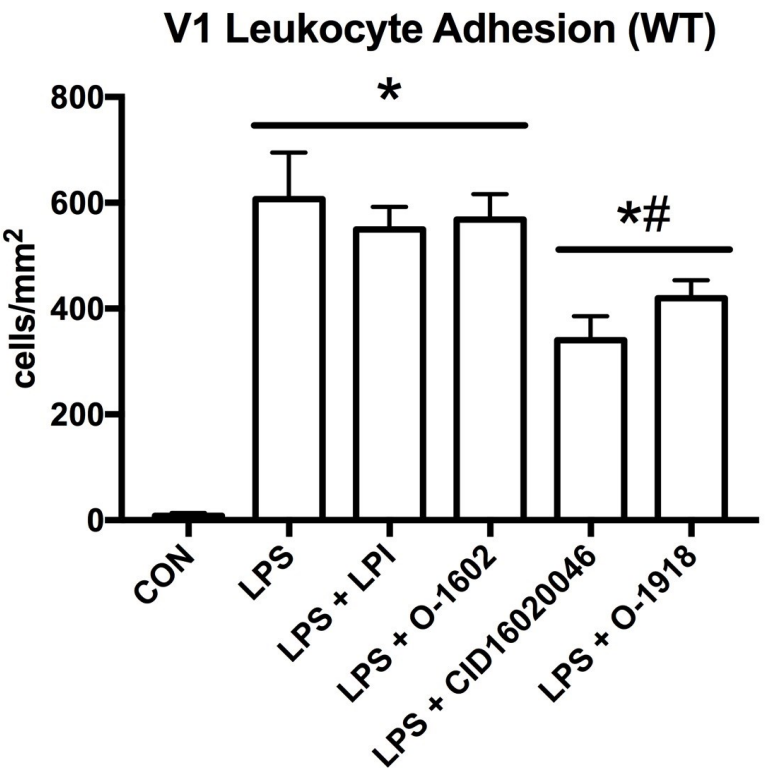

Figure 19: Leukocyte adhesion in intestinal collecting venules (V1; > 50 μm vessel diameter) after systemic administration of saline or LPS and GPR55 agonist or antagonist in wild type mice. Bar graphs represent the number of adherent leukocytes in collecting venules per area (cells/mm^2). Data represented as mean ± SD (n = 5-7 per group). * $p < 0.05$ compared to the CON group. # $p < 0.05$ compared to the LPS group.

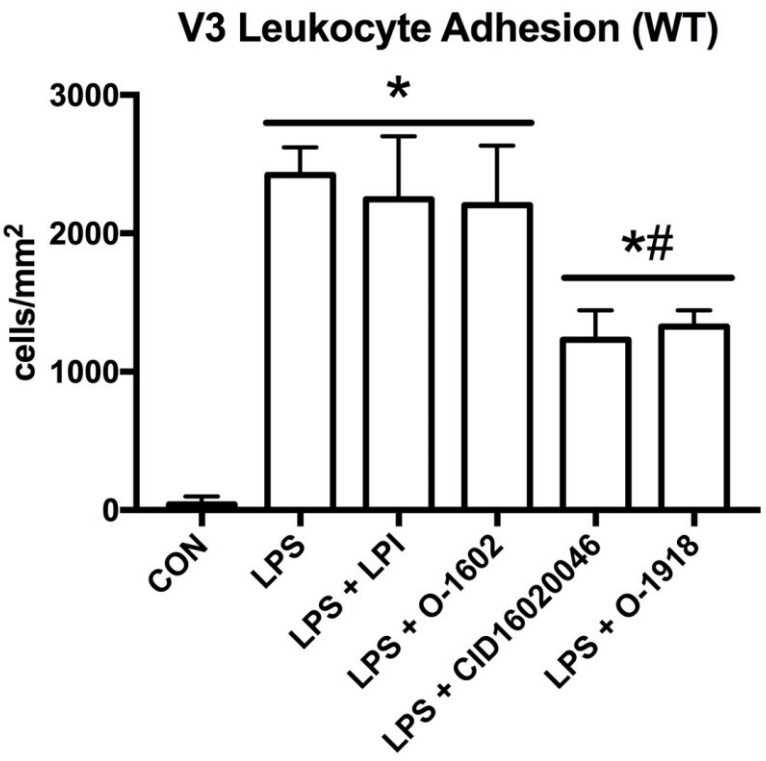

Figure 20: Leukocyte adhesion in post capillary venules (V3; < 50 μm vessel diameter) after systemic administration of saline or LPS and GPR55 agonist or antagonist in wild type mice. Bar graphs represent the number of adherent leukocytes in post capillary venules per area (cells/mm^2). Data represented as mean ± SD (n = 5-7 per group). * $p < 0.05$ compared to the CON group. # $p < 0.05$ compared to the LPS group.

3.2.2 Leukocyte Rolling

LPS-challenged animals showed a significant reduction ($p< 0.05$) in the number of rolling leukocytes in both V1 venules in comparison to control (Figure 20). The groups treated with CID16020046 and O-1918, but not LPI and O-1602 resulted in a significant increase ($p< 0.05$) in the number rolling leukocytes in V1 venules compared to LPS challenge with no treatment (Figure 20).

Similarly with V1 venules, the number of leukocytes rolling in V3 venules was significantly decreased ($p < 0.05$) with endotoxemia compared to the control group. Administration of LPI or O-1602 did not significantly alter ($p > 0.05$) leukocyte rolling compared to LPS. Furthermore, GPR55 antagonists, CID16020046 and O-1918 significantly enhanced ($p > 0.05$) leukocyte rolling in V3 venules (Figure 21).

3.2.3 Functional Capillary Density

In WT mice, LPS administration and all drug treatments significantly reduced ($p < 0.05$) muscular FCD in comparison to control (Figure 22). The group treated with GPR55 agonist, O-1602, showed a significant decrease ($p < 0.05$) of FCD in the intestinal muscle layer compared to LPS group (Figure 22).

Also, FCD in the mucosal villi were significantly decreased ($p < 0.05$) with endotoxemia and both GPR55 agonist and antagonist treatments compared to control (Figure 23). The group treated with O-1602 exhibited a significant reduction in mucosal villi FCD compared to LPS group (Figure 23).

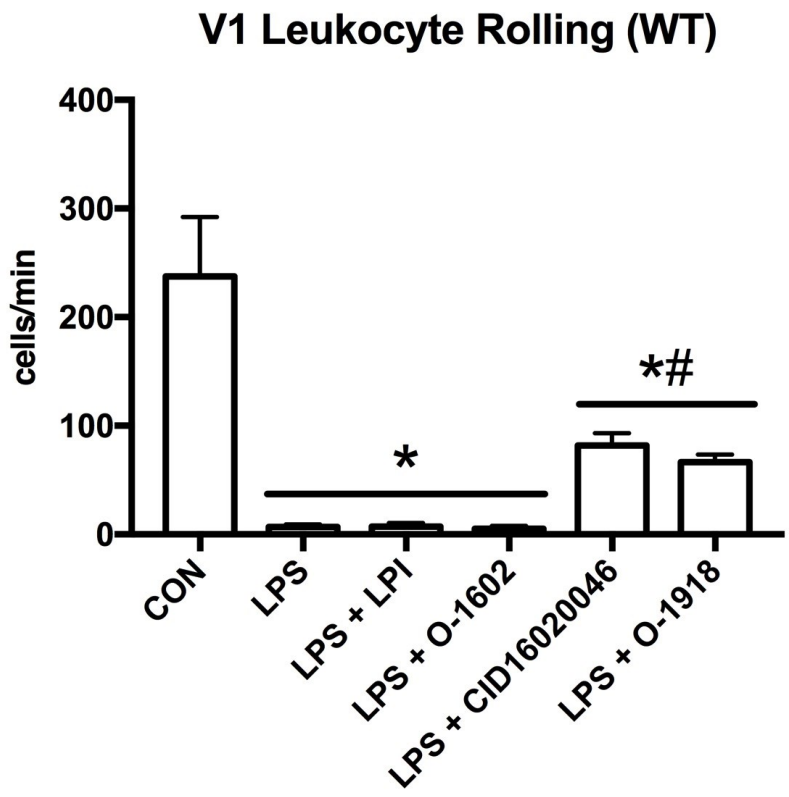

Figure 21: Leukocyte rolling in intestinal collecting venules (V1; > 50 μm vessel diameter) after systemic administration of saline or LPS and GPR55 agonist or antagonist in WT mice. Bar graphs represent the number of rolling leukocytes in collecting venules (cells/min). Data represented as mean ± SD (n = 5-7 per group). * $p < 0.05$ compared to the CON group. # $p < 0.05$ compared to the LPS group.

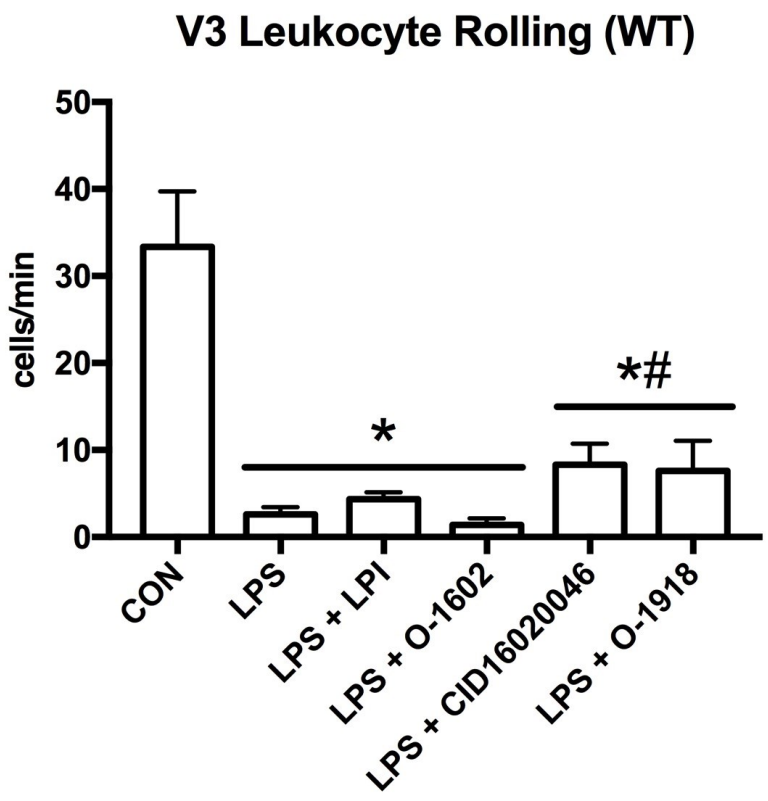

Figure 22: Leukocyte rolling in post capillary venules (V3; < 50 μm vessel diameter) after systemic administration of saline or LPS and GPR55 agonist or antagonist in wild type mice. Bar graphs represent the number of rolling leukocytes in collecting venules (cells/min). Data represented as mean ± SD (n = 5-7 per group). * $p < 0.05$ compared to the CON group. # $p < 0.05$ compared to the LPS group.

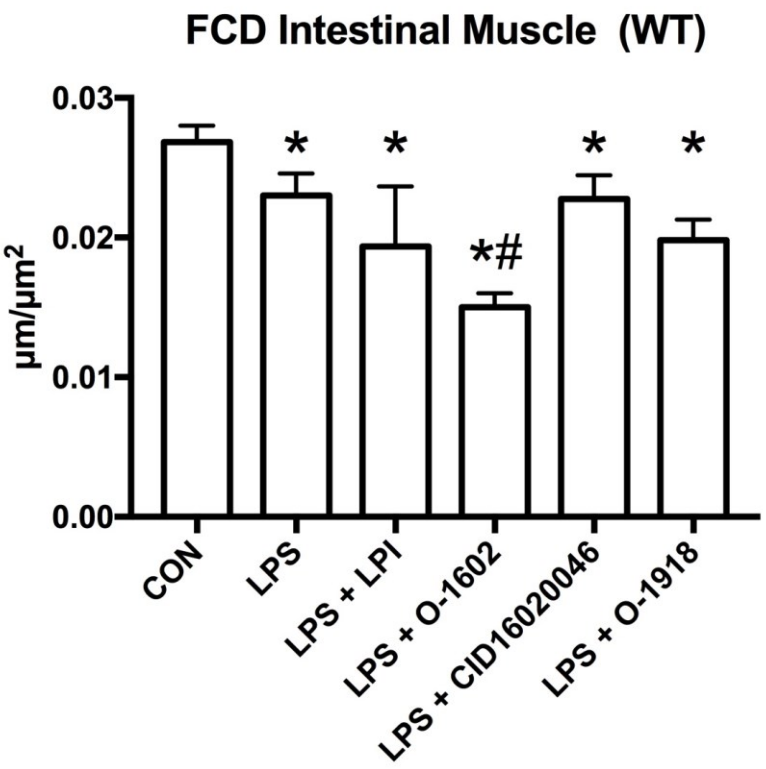

Figure 23: Capillary perfusion quantified through FCD within the muscle layers of the intestine after systemic administration of saline or LPS and GPR55 agonist or antagonist in wild type mice. FCD quantified as total length of perfused capillaries within a predetermined rectangular area of the observed field ($\mu m/\mu m^2$). Data represented as mean ± SD (n = 5-7 per group). * $p < 0.05$ compared to the CON group. # $p < 0.05$ compared to the LPS group.

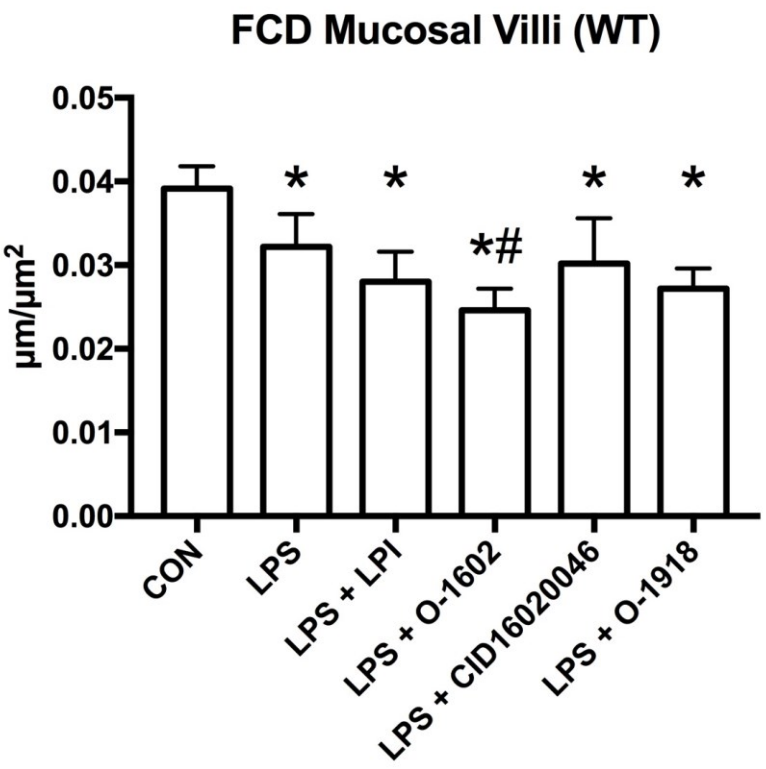

Figure 24: Capillary perfusion quantified through FCD within the mucosal villi of the intestinal lumen after systemic administration of saline or LPS and GPR55 agonist or antagonist in wild type mice. FCD quantified as total length of perfused capillaries within a predetermined rectangular area of the observed field ($\mu m/\mu m^2$). Data represented as mean ± SD (n = 5-7 per group). * $p < 0.05$ compared to the CON group. # $p < 0.05$ compared to the LPS group.

3.2.4 Cytokines and Adhesion Molecules

GPR55 modulation, especially blockade, impacts leukocyte activation and FCD. To provide additional indication for the inflammatory modulation and to examine the mechanism of the GPR55 modulation in leukocyte activation, plasma was collected and analyzed for cytokines in WT mice. Analysis of plasma cytokine levels indicated that the administration of LPS significantly increased ($p < 0.05$) the circulating levels of TNF, IL-6 and IL-10 in comparison to the control group (Figure 25). The level of TNF was significantly increased ($p < 0.05$) in all groups compared to the control group, and in GPR55 activation by LPI or O-1602 treatments compared to the LPS group (Figure 25). The concentration of IL-6 remained at a similar level with GPR55 agonist treatments, and decreased significantly ($p < 0.05$) with the antagonists, CID16020046 and O-1918 compared to LPS group (Figure 25). Furthermore, the level of IL-10 was significantly decreased ($p < 0.05$) with CID16020046 treatment compared to LPS group (Figure 25). The concentrations of IL-1β (Figure 25), IL-2, IL-4, IL-12 p70, IL-13, IL-17A, and IFN-γ were not significantly altered after induction of endotoxemia or administration of drug treatments (Figure 26).

The levels of plasma adhesion molecules, P-selectin and ICAM-1, were also measured. P-selectin level was significantly increased ($p < 0.05$) in the LPS group and with LPI or O-1602 treatments compared to the control group (Figure 27). Moreover, the levels of P-selectin were significantly increased ($p < 0.05$) with LPI or O-1602 treatments. However, the groups with GPR55 antagonists remained at a similar level with the control group (Figure 27). The concentration of ICAM-1 was significantly increased

($p < 0.05$) with O-1602 treatment compared to control, and showed no significant differences in all other groups (Figure 27).

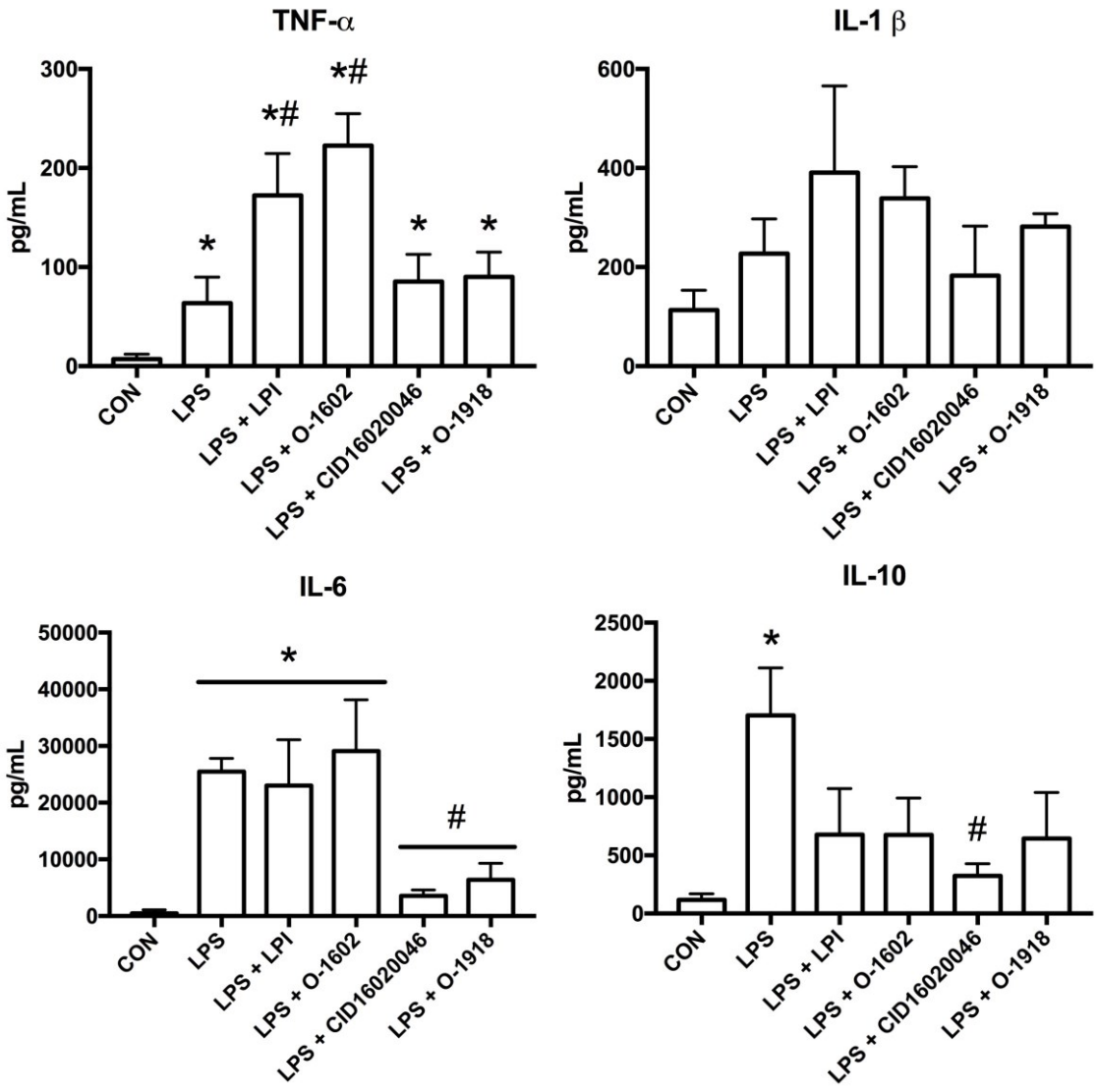

Figure 25: Levels of plasma cytokines in wild type mice (pg/mL). Bar graphs represent the mean concentrations of TNF, IL-1β, IL-6 and IL-10. Results are represented as mean ± SD (n = 5 per group). * $p < 0.05$ compared to the CON group. # $p < 0.05$ compared to the LPS group.

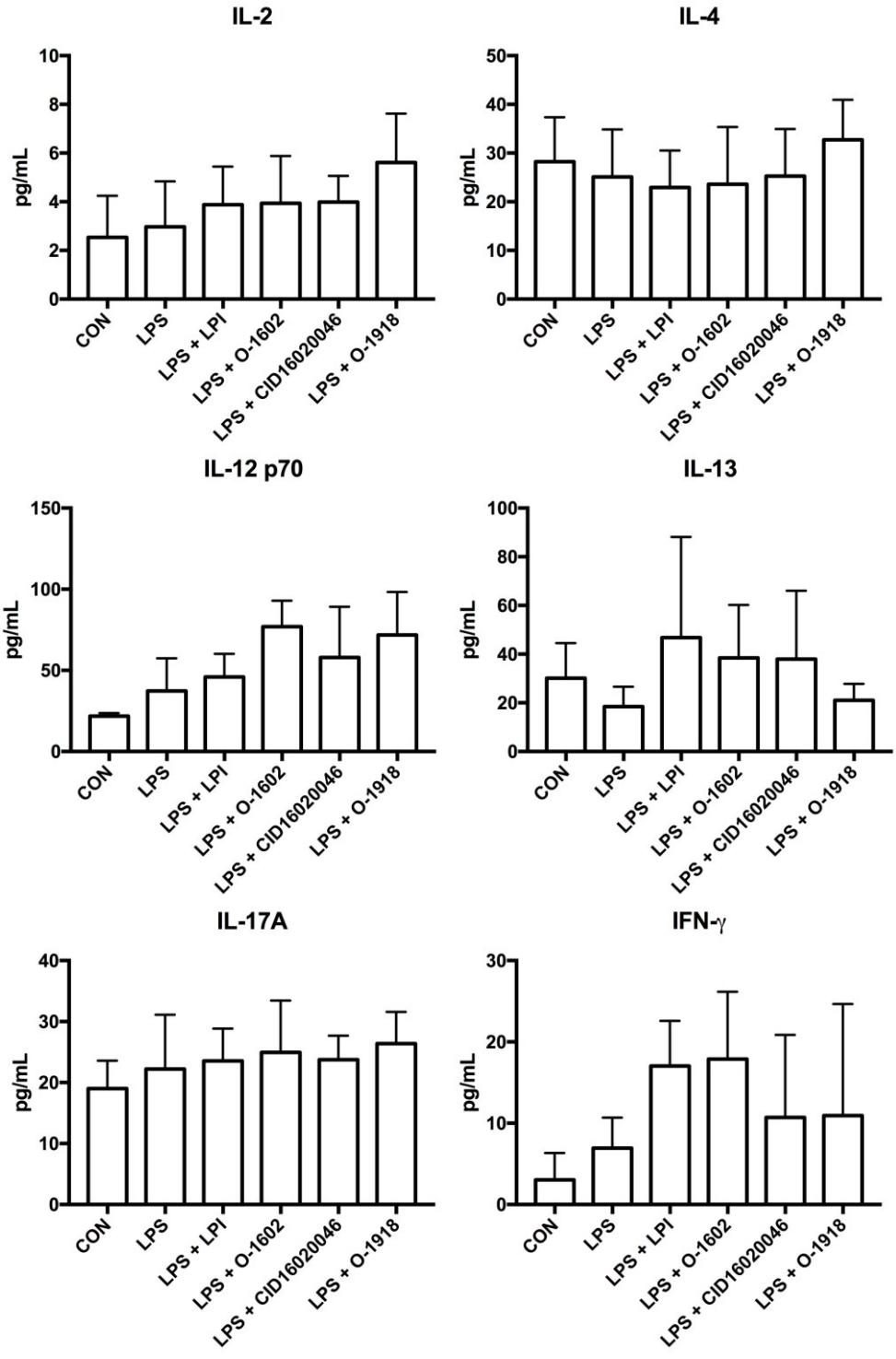

Figure 26: Levels of plasma cytokines in wild type mice (pg/mL). Bar graphs represent the mean concentrations of IL-2, IL-4, IL-12 p70, IL-13, IL-17A and IFN-γ. Results are represented as mean ± SD (n = 5 per group).

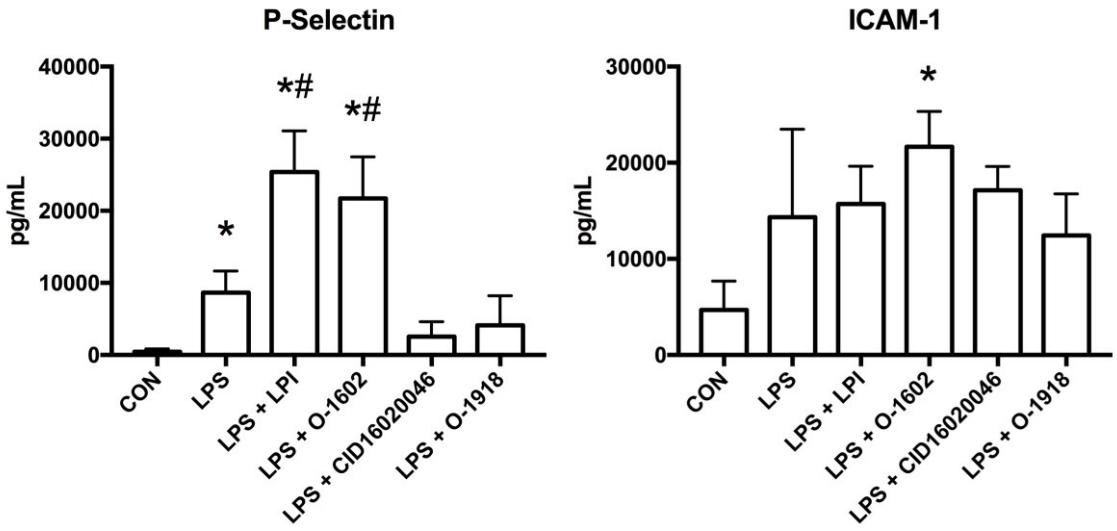

Figure 27: Levels of soluble adhesion molecules in wild type mice (pg/mL). Bar graphs represent the mean concentrations of P-selectin and ICAM-1. Results are represented as mean ± SD (n = 5 per group). * $p < 0.05$ compared to the CON group. # $p < 0.05$ compared to the LPS group.

3.3 Bone Marrow Neutrophil Transmigration

Neutrophils are considered as vital first-to-arrive players in the host defense against infection. Also, cell surface expression of both CB2R and GPR55 were detected in neutrophils (Henstridge et al., 2011; Pertwee, 2006), and endocannabinoids are thought to exert modulatory functions on leukocytes including neutrophils under the pro-inflammatory phase of sepsis (from the previous results). Therefore, in order to delineate whether there is a direct effect, and the stage of neutrophil activation cascade that is possibly affected by CB2R or GPR55 modulation, murine bone marrow derived neutrophils were examined in transmigration assays.

An *in vitro* transmigration assay was performed using the Transwell system, in which bone marrow neutrophils were placed on top of a 3 μm pore-size membrane and allowed to migrate toward fMLP in the bottom chamber, with or without CB2R or GPR55 modulation. The chemoattractant concentration in the bottom chamber was chosen based on the dose dependent migration curve, at a concentration of moderate migration to observe both increase and decrease in migration (Figure 28).

In the absence of a chemoattractant in the bottom of the transmigration chamber, approximately 5% of neutrophils (out of total recovered) transmigrated through filters (Figure 29). Neutrophil transmigration showed a marked increase from 5% to approximately 60% with fMLP in the bottom chamber (Figure 29). However, transmigration with CB2R activation, GPR55 activation or inhibition was not significantly changed when compared to the group that received fMLP alone (Figures 29 and 30).

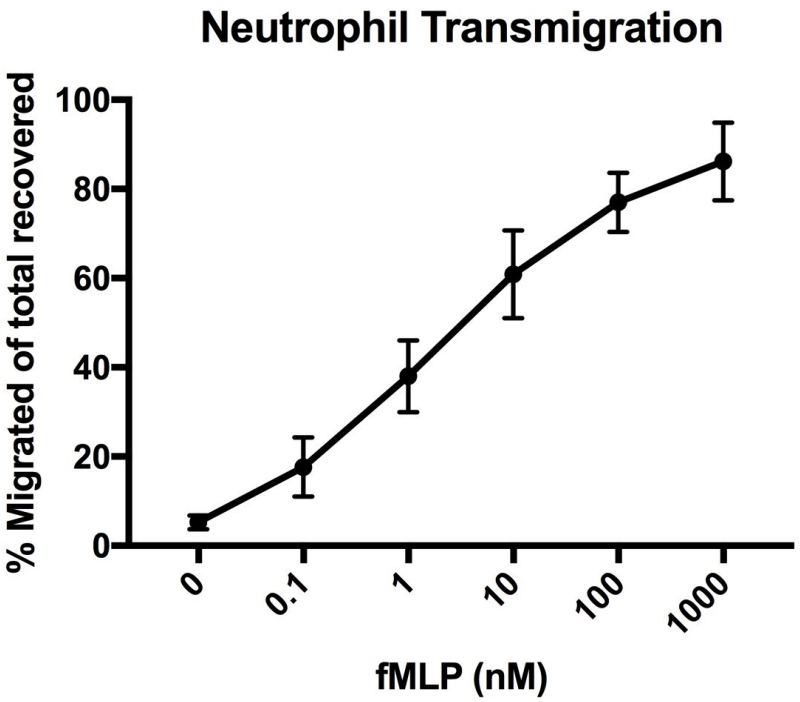

Figure 28: fMLP concentration dependent transmigration of murine neutrophils. Transmigration filters (3 μm pores) were coated with media supplemented with 5% FBS. Bone marrow-derived WT mouse neutrophils (2 x 10^5) were placed on top of the filters with diluent or different concentrations of fMLP. After an incubation period of 1 hour, the cells in top and bottom chambers were collected and reported as % migrated cells of total cells recovered. All samples were run in duplicate and the results are represented as mean ± SD from three independent experiments.

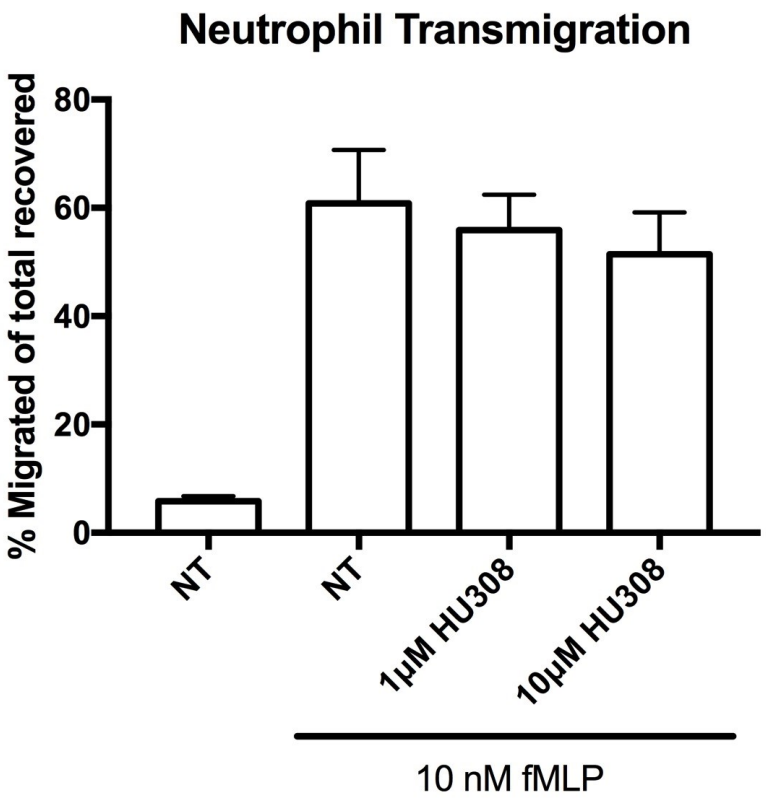

Figure 29: Transmigration of murine neutrophils with CB2R activation. Transmigration filters (3 μm pores) were coated with media supplemented with 5% FBS. WT bone marrow-derived mouse neutrophils (2 x 10^5) with or without CB2R agonist (HU308; 1μM or 10μM) were placed on top of the filters with saline or 10 nM fMLP. The agonist was also added to the bottom chamber. After an incubation period of 1 hour, the numbers of transmigrated cells in top and bottom chambers was determined. All samples were run in triplicate and the results are represented as mean ± SD from three independent experiments.

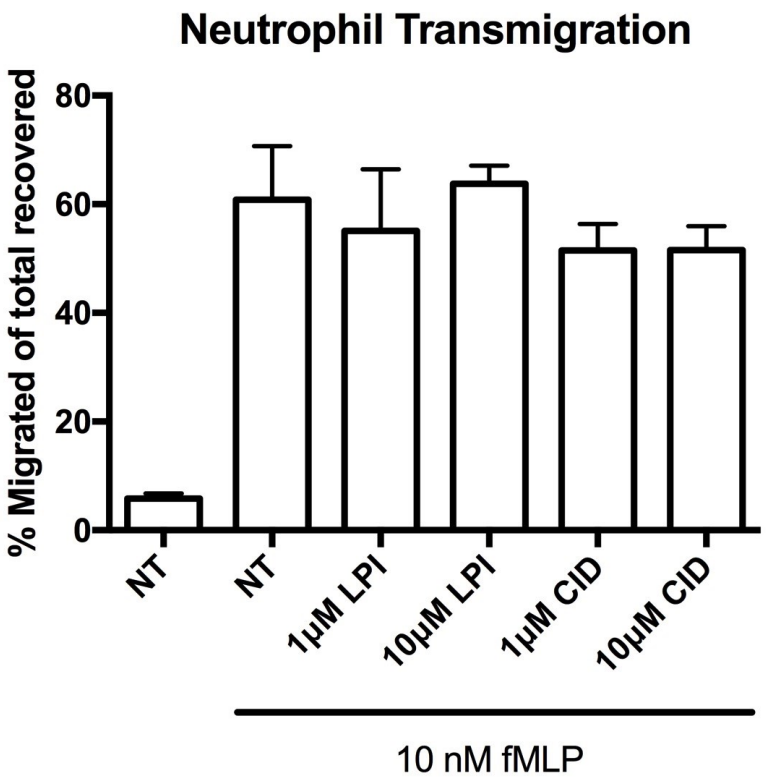

Figure 30: Transmigration of murine neutrophils with GPR55 modulation. Transmigration filters (3 μm pores) were coated with media supplemented with 5% FBS. Bone marrow-derived mouse neutrophils (2 x 10^5) with or without GPR55 agonist (LPI; 1μM or 10μM) or GPR55 antagonist (CID16020046; 1μM or 10μM) were placed on top of the filters with saline or 10 nM fMLP. After an incubation period of 1 hour, the numbers of transmigrated cells in top and bottom chambers was determined. All samples were run in triplicate and the results are represented as mean ± SD from three independent experiments.

CHAPTER 4: DISCUSSION

4.1 Summary of Major Findings

Although there have been a variety of drugs investigated for effectiveness in improving mortality in experimental sepsis, none has been effective in clinical trials. Still, given that the majority of infection-related deaths in intensive care units are due to sepsis, therapies targeting exaggerated inflammatory responses during sepsis are in high demand (Vincent et al., 2009). The endocannabinoid system is up-regulated during sepsis and its manipulation offers potential options to modulate the dysregulated immune response in sepsis (Lehmann et al., 2012; Li et al., 2010; Varga et al., 1998; Zhou et al., 2011).

Previous studies in our lab have shown that in the context of model sepsis, CB2R is anti-inflammatory upon activation (Lehmann et al., 2012; Sardinha et al., 2014; Toguri et al., 2014). Administration of endocannabinoid degradation enzyme inhibitor, JZL184, was used to amplify endogenous CB2R activation, which resulted in reduced pro-inflammatory responses during sepsis in WT mice. Therefore, JZL184 was suggested as a promising treatment for sepsis, which then required further studies to confirm its beneficial effects (Figure 31 and Table 4).

In the current study, the first objective was to confirm that the effect of JZL184 was indeed CB2R-mediated by using CB2R KO mice. CB2R KO mice were subjected to endotoxemia combined with administration of JZL184. Despite the finding in WT mice, there was a significant reduction in LPS-induced leukocyte-endothelial interaction in both collecting venules and post-capillary venules with JZL184 treatment in the absence of CB2R. JZL184 administration significantly increased IL-10 and decreased P-selectin in

plasma of septic CB2R KO mice. Administration of AM281, an antagonist to CB1R, which is also activated by 2-AG, did not abolish the effects of JZL184 treatment. This result indicates that CB1R is not responsible for JZL184-mediated anti-inflammatory effect in experimental sepsis, suggesting an alternative target of 2-AG that is both CB1R and CB2R-independent (Figure 31 and Table 4).

GPR55 is also activated by 2-AG and therefore another candidate for the JZL184-induced effects on leukocyte activation in experimental sepsis. Since there was no clear understanding of the role of GPR55 in the inflammatory response, the effect of GPR55 modulation was examined in our experimental sepsis model. Interestingly, GPR55 inhibition (CID16020046 or O-1918), but not activation (LPI or O-1602), significantly reduced leukocyte activation within the intestinal microcirculation in acute endotoxemia. Furthermore, administration of GPR55 antagonists reduced the circulating plasma level of IL-6. On the other hand, we report increased TNF and soluble P-selectin levels with GPR55 activation. Therefore, these findings indicate an anti-inflammatory effect of GPR55 inhibition in experimental sepsis (Figure 31 and Table 4).

Lastly, the subset of leukocytes, which are the first to arrive in considerable numbers to the site of inflammation, is neutrophils. Therefore, the consequence of CB2R and GPR55 modulation in transmigration of neutrophils were examined *in vitro*. The results demonstrated that within the doses examined, neither CB2R nor GPR55 modulation affected transmigration of bone marrow neutrophils toward the chemotactic peptide produced by bacteria, fMLP.

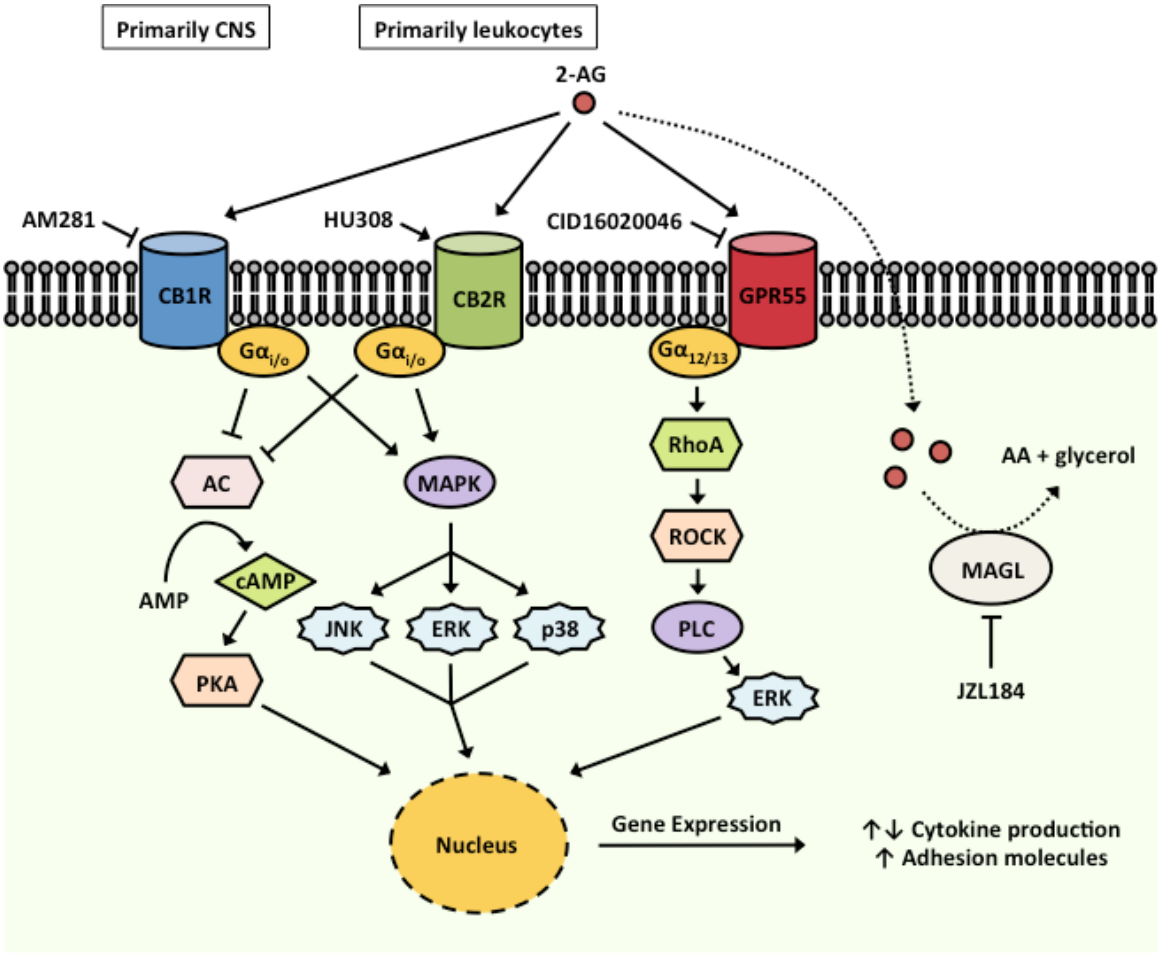

Figure 31: Schematic model of CB1R, CB2R and GPR55 signaling pathways and 2-AG degradation during inflammation.

Table 4: Summary of CB2R and GPR55 activities on modulation of leukocyte-endothelial interaction.

	Leukocyte-endothelial interactions	
	CB2R	GPR55
JZL184	↓	↓
Agonist	↓	↑
Antagonist	↑	↓

4.2 Acute Endotoxemia Experiments

Endotoxemia experiments utilizing LPS represent a prominent feature of sepsis without live infections. LPS, an oligomer of lipid and carbohydrate that constitutes the endotoxin of Gram-negative bacteria, substitutes for live bacteria. LPS-induced endotoxemia is a simple and reproducible model of sepsis (Remick and Ward, 2005). It represents a subset of inflammatory pathways activated exclusively by LPS, increasing production of pro-inflammatory cytokines, TNF, IL-1β and IL-6 (Cheng et al., 2015; Morris et al., 2015; Zhou et al., 2005).

4.2.1 Intravital Microscopy (CB2R KO Mice)

Leukocyte-endothelial interactions were observed using IVM to examine events in the intestinal microvasculature. This technique allowed us to gain live *in vivo* images of blood vessels and the leukocytes to assess various elements of inflammation. It has been reported using IVM that leukocytes are recruited to small venules during LPS-induced endotoxemia in rats and mice (Kianian et al., 2014; Lehmann et al., 2012; Sardinha et al., 2014; Zhou et al., 2011).

First, the anti-inflammatory effect of JZL184 in CB2R KO mice was further examined in order to confirm previous findings. In this study, LPS challenge significantly increased the number of leukocytes adhering to both V1 and V3 venules compared to the control group with saline injection (Figures 10 and 11). Increased leukocyte adhesion to the endothelial cells of the intestinal microcirculation has been well described in the literature (Matsuda and Hattori, 2007; Salomao et al., 2012). This increase in leukocyte adhesion upon activation by bacterial toxins has been determined to be an up-regulated

expression of adhesion molecules by endothelial cells and leukocytes (Cinel and Opal, 2009; Haraldsen et al., 1996). Administration of JZL184 was successful in attenuating the increase in leukocyte activation at the time of IVM (Figure 10 and 11). Endocannabinoid upregulation only prevented leukocyte activation at a moderate level instead of a complete reversal to a similar level of controls. However, a modest reduction of leukocyte activation is favored since an adequate level of pro-inflammatory response protects the patient from infection by promoting bacterial clearance while avoiding exaggerated cytokine production and subsequent damage to the host. JZL184 was also studied in inflammatory models such as inflammatory bowel disease, acute lung injury and hepatic ischemia/reperfusion injury resulting in decreased levels of leukocyte infiltration, pro-inflammatory mediators and tissue ischemia (Alhouayek et al., 2011; Cao et al., 2013; Costola-de-Souza et al., 2013). It has been shown that CB2R activation with specific cannabinoid ligands, JWH133 or O-1966 reduces leukocyte-endothelial interaction by suppressing the activity of adhesion molecules (Cinel and Opal, 2009; Ramirez et al., 2012). Furthermore, CB2R has higher affinity for 2-AG and was reported to have the immunomodulatory effect due to high expression levels. In our experiments, induction of endotoxemia with no CB2R present to exert an anti-inflammatory response and administration of treatment compounds were evaluated. Although CB1R was not reported to be deeply associated with the immune system (as much as CB2R), CB1R was suspected for eliciting the anti-inflammatory effects upon activation by JZL184 due to co-activation by 2-AG. If CB1R was indeed driving the anti-inflammatory response then administration of CB1R antagonist, AM281, presumably would reverse the decreased leukocyte activation. However, administration of AM281 prior to JZL184 treatment did

not change leukocyte adhesion significantly, suggesting an alternative receptor is acting that is CB1R and CB2R independent.

Conversely, the number of rolling leukocytes was decreased with intravenous administration of LPS compared to control group in V1 and V3 venules (Figures 12 and 13). This decrease in number of rolling leukocytes can be translated as an indication of the activated immune system. The disseminated inflammatory response elicited by LPS administration not only increases the circulating leukocytes, but also promotes activation and adhesion of the circulating leukocytes (Birnbaum et al., 2008; Hayes et al., 2004). Thus, excessive immune activation may result in a significant reduction in the number of rolling leukocytes and a robust increase in the number of adherent leukocytes, as seen in our results.

The decrease in FCD is another key feature of microcirculatory dysfunction during sepsis. It is crucial that oxygen and nutrient exchange occurs readily in the microcirculation to avoid tissue ischemia and organ damage. Therefore, functional capillary density was measured as a readout of physiologic impairment of the vasculature, both in muscular and mucosal layers of the small intestine. The FCD in controls and LPS-administered animals did not significantly differ; however, there was a decreasing trend (Figure 14 and 15). Also, the treatment groups with JZL184 or JZL184 with AM281 did not result in significant differences from controls or the LPS group, and we speculate that perhaps a longer time is required prior to observation for the drugs to show statistically significant effects.

With regard to the anti-inflammatory effect via 2-AG that are independent of CB1R and CB2R, there are suggestions that some cannabinoid agonists may be anti-inflammatory in the absence of cannabinoid receptors, from studies using genetic

knockout mice. This suggests that endocannabinoids can mediate their effects through CBR-independent mechanisms (Braun et al., 2011; Rockwell et al., 2006; Schicho et al., 2011). It has been reported that 2-AG can suppress activated leukocytes from releasing cytokines such as IL-2 by a cannabinoid receptor independent pathway through peroxisome proliferator-activated receptor γ. Moreover, pharmacologic and genetic blockade of CB1R and CB2R did not alter the anti-inflammatory effects of 2-AG, indicating that alternative pathways become activated (Rockwell et al., 2006).

4.2.2 Intravital Microscopy (Wild type mice)

Using the endotoxemia model in WT mice, we revealed that GPR55 inhibition alters leukocyte-endothelial interactions during systemic inflammation. Similar to endotoxemia in CB2R KO animals, WT mice produced significant increases in leukocyte adhesion concomitant with a decrease in leukocyte rolling in response to LPS. GPR55 activation did not significantly impact leukocyte activation compared to the LPS group in either V1 or V3 venules (Figures 19 and 20). Obviously the exaggerated leukocyte activation already reached its maximum by the chosen LPS dose (Figure 19 and 20). It could be further examined with lower doses of LPS, whether GPR55 activation is indeed pro-inflammatory and can modulate leukocyte activation. The most notable finding of the current research was that GPR55 antagonism is as effective as CB2R agonism in reducing leukocyte adhesion in endotoxemic mice (Figures 19, 20, 21 and 22). This action of GPR55 was mediated independent of CB1R and CB2R as confirmed by highly specific GPR55 antagonist, CID16020046.

The detrimental effect of GPR55 activation was observed as significantly lowered FCD in intestinal muscle and mucosa layers but not in leukocyte activity. However, it appears that GPR55 inhibition did not improve FCD (Figures 23 and 24). It is not completely understood how GPR55 modulation affects intestinal FCD. It is speculated that the decreased capillary perfusion in our endotoxemia experiments may be not only due to increased leukocyte activation but also related to decreased blood pressure and impaired red blood cell deformability (De Backer et al., 2014, 2011; Ince, 2005).

The exact pharmacology and mechanism by which GPR55 mediates an immune modulatory effect is still controversial in the literature. LPI is reported to activate GPR55 and GPR119 (Henstridge et al., 2010; Offertáler et al., 2003; Oka et al., 2007; Soga et al., 2005), and O-1602 activates both GPR55 and GPR18 (McHugh et al., 2012). Thus, the effect of LPI and O-1602 could be an additive effect by overlapping activation of non-GPR55 receptors and possibility through other off-target effects. It is especially difficult to identify the exact molecular mechanism of GPR55 modulation due to its biased pharmacology with ligand-specific and concentration-specific downstream signaling (Zeng et al., 2015). Both agonism and antagonism of GPR55 were reported from the use of different assays and cell systems (Pertwee et al., 2010). For instance, one study reported that GPR55 activation with O-1602 was protective against intestinal inflammation, and a second study reported that GPR55 inhibition with CIC16020046 was beneficial (Schicho et al., 2011; Stančić et al., 2015). Moreover, GPR55 can interact with the classical cannabinoid receptors via receptor coupling and heteroreceptor complex formation with CB1R and CB2R to elicit different signaling pathways and modulate CBR-regulated responses (Balenga et al., 2014; Henstridge et al., 2010; Kargl et al., 2012; Moreno et al., 2014; Yang et al., 2015). Additional studies are necessary in order to have

a clearer understanding of GPR55 pharmacology. Nevertheless, the results from the current study highlight the effectiveness of GPR55 inhibition and involvement in the anti-inflammatory response, and the therapeutic potential of GPR55 in inflammation and sepsis.

4.2.3 Plasma Cytokine Measurements

One hallmark of sepsis is an overwhelming production of pro-inflammatory cytokines such as TNF, IL-1β, and IL-6 (Cinel and Opal, 2009; Lerman et al., 2015; Yao et al., 2015). TNF is a key player in the progression of inflammation from multiple causes and induces the production of other pro-inflammatory cytokines. Excessive production of pro-inflammatory cytokines in acute endotoxemia has been previously reported, and TNF would peak within one to two hours-post LPS challenge (Angele and Chaudry, 2005; Lehmann et al., 1999). Therefore, treatments attenuating release of TNF have therapeutic potential (Clark, 2007; Lorente and Marshall, 2005). The results from the endotoxemia experiments in both CB2R KO and WT mice showed significant increases in circulating levels of TNF, IL-6 and IL-10 post LPS challenge, which represents characteristic concurrent pro- and anti-inflammatory response in sepsis (Figures 16, 18, 25 and 27).

From the literature and previous studies in our lab, a reduction in plasma levels of TNF and IL-6 by CB2R activation was observed during inflammation (Alhouayek et al., 2011; Cao et al., 2013). However, JZL184 treatment with or without AM281 in CB2R KO mice did not alter the levels of TNF and IL-6 compared to the LPS alone group, which presumably is due to the lack of CB2R (Figure 16). On the other hand, GPR55 activation with LPI and O-1602 significantly increased plasma levels of TNF, indicating

its pro-inflammatory role, whereas a significant reduction of IL-6 was observed with GPR55 antagonists (Figure 25). In the literature, activation of GPR55 is suspected to produce pro-inflammatory cytokines at the expense of anti-inflammatory cytokines (Lanuti et al., 2015). Inhibition of GPR55 has been also reported to result in lower increases of TNF and IL-6 during experimental models of intestinal inflammation, which is in agreement with our results (Stančić et al., 2015).

IL-1β is another important mediator of inflammation which is released by monocytes, macrophages, and intestinal epithelial cells, among other cell types (Haraldsen et al., 1996; Stadnyk, 2002; Toguri et al., 2014). Both CB2R KO and WT mice showed an increasing trend of IL-1β though levels did not reach statistical significance. With JZL184 treatment and GPR55 treatments, there was no significant change in IL-1β levels in our results (Figures 16 and 25). Similar to our findings, there are studies also showing inconsistent results in levels of IL-1β changes. In some studies, it was shown that activation of CB2R or inhibition of GPR 55 reduces the production of IL-1β (Cao et al., 2013; Stančić et al., 2015), while others report no impact on IL-1β levels (Di Filippo et al., 2004; Greineisen and Turner, 2010). It seems that changes in IL-1 are highly context dependent.

IL-10 is a potent anti-inflammatory cytokine released by cells such as monocytes, lymphocytes and endothelial cells, aiding in limiting and the resolution of inflammation (Oberholzer et al., 2002). IL-10 was shown to impede the release of pro-inflammatory cytokines and improve experimental outcome in sepsis models (Gérard et al., 1993; Howard et al., 1993). In this study, it was observed that using JZL184 resulted in increased IL-10 levels, presumably thereby having anti-inflammatory effects (Figure 16). On the other hand, using CID16020046 resulted in a significantly lower level of IL-10

while O-1918 showed minimal effects, suggesting that the anti-inflammatory effect of GPR55 antagonism is via an IL-10-independent mechanism (Figure 25).

P-selectin and ICAM-1 are adhesion molecules highly expressed by leukocytes and endothelial cells, which plays an important role in leukocyte recruitment and activation during inflammatory diseases such as sepsis (Liu and Kubes, 2003; Osuchowski et al., 2012). In the absence of CB2R, mice had high baseline levels of both P-selectin and ICAM-1 compared to WT animals (Figures 18 and 27). Since CB2R is anti-inflammatory, absence of the receptor might have contributed to a pro-inflammatory state, which was our observation. A significant reduction in P-selectin was observed only with JZL184 treatment in CB2R KO mice, suggesting another mechanism of 2-AG induced anti-inflammation in the absence of CB2R. It has been shown by others that GPR55 activation promotes migration and adhesion of cancer cells (Andradas et al., 2016; Kargl et al., 2016). For example, colon cancer cells showed a significant decrease in adhesion to endothelial cells after GPR55 inhibition with CID16020046 (Kargl et al., 2016). In agreement with other's published results, soluble P-selectin levels significantly increased with GPR55 agonists in comparison to endotoxemic animals with no treatment (Figure 27). Furthermore, administration of GPR55 antagonists showed a trend of reduction of P-selectin. The levels of ICAM-1 in both CB2R KO and WT mice were not significantly changed, albeit with an increasing trend with LPS administration (Figure 18 and 27). These results suggest that CB2R and GPR55 modulation is predominantly at the level of selectins. However, the levels of circulating (shed) adhesion molecules in the plasma are most likely not a direct proportion of the expression on leukocytes and endothelial cells. Furthermore, the pathological significance and the role of soluble adhesion molecules in leukocyte adhesion are not yet clarified. Thus, investigation on the

levels of adhesion molecules on endothelial cells is necessary in order to determine the relativity of the levels of soluble adhesion molecules to the expression on endothelium.

Overall, CB2R KO mice typically had higher cytokine levels compared to WT mice. However, we cannot exclude underlying compensatory mechanisms activated in CB2R KO mice. Moreover, the pro-inflammatory cytokines, such as TNF, IL-6 and IL-1β, are produced at the early phase of inflammation. It is possible that cytokine levels peaked early and are decreasing or have plateaued at the time of plasma collection, resulting in insignificant differences. Noteworthy, the receptors for these cytokines are all cleaved at the extracellular domain and circulate at concentrations that may antagonize the cytokine (Burkovskiy et al., 2013; Cortez-Cooper et al., 2013). Therefore, readout of the circulating concentrations of soluble receptor subunits for TNF, IL-6 and IL-1β could potentially serve as indicators of inflammation. Although the current findings were preliminary, cytokine profiling provided us with some insight into the impact of CB2R and GPR55 modulation on the acute inflammation in experimental sepsis.

4.3 Bone Marrow Neutrophil Transmigration Experiments

Polymorphonuclear neutrophils are the first-line defense of the innate leukocytes and are activated by microbes or microbial toxins. Neutrophils circulate within the blood, sensing inflammatory mediators along the endothelial linings for activation (Leoni et al., 2015; Sundd et al., 2013). In our experimental sepsis model using i.v. endotoxin, we were able to study the first stages of leukocyte-endothelial interactions (rolling, adhesion) *in vivo*. However, migration of leukocytes into the tissue is not usually observed in systemic

endotoxemia. Therefore, to study the impact of CB2R and GPR55 modulation on transmigration of neutrophils we performed *in vitro* experiments using the bacteria-derived chemoattractant fMLP.

When neutrophils are activated by chemoattractants such as fMLP, they undergo morphological changes from spherical to a polarized elongated shape, degranulate, upregulate the number and affinity of adhesion molecules in the cell membrane and migrate into the positive gradient of chemoattractant, presumably toward the site of infection. There is evidence for CB2R modulation of neutrophil chemotaxis: treatment with the selective CB2R agonist JWH-015 and 2-AG inhibited neutrophil migration toward fMLP (Kurihara et al., 2006; Miller and Stella, 2008). Neutrophils treated with these drugs showed morphological changes and motility but lacked front and rear polarity (Kurihara et al., 2006). In addition, CB2R activation by WIN55,212-2 inhibited TNF-induced neutrophil transmigration, confirming the anti-inflammatory effects of activation of CB2R (Nilsson et al., 2006). GPR55 has produced conflicting results with regard to effects on neutrophil migration. In one study, the GPR55 agonist O-1602 inhibited neutrophil recruitment, and in a second study, GPR55 activation by LPI augmented neutrophil migration synergistically with CB2R activation, while preventing neutrophil degranulation and ROS production (Balenga et al., 2011; Schicho et al., 2011), so more selective effects on the neutrophil state of activation.

In our assay, no effect on neutrophil transmigration across bare filters was observed in comparison to fMLP with either CB2R activation or GPR55 modulation (Figures 29 and 30). Certainly, these findings are based on a reductionist model of transmigration. Further refinement of the transmigration apparatus including neutrophil priming with LPS and migration across an endothelial monolayer would enhance the

applicability of the experimental results to the *in vivo* situation. This is especially true when neutrophil transendothelial migration is Mac-1 (CD11b/CD18) dependent while transmigration across acellular filters is independent of Mac-1 (Carrigan et al., 2007; Zhou et al., 2005). In one report, neutrophil transmigration was unaffected by leukocyte adhesion deficiency or the lack of Mac-1, which implies that neutrophil transmigration to chemoattractants is dependent on the affinity and not the increase in the expression of Mac-1 (Malawista et al., 2000). Therefore, additional studies focused on the effects of the endocannabinoid system of adhesion molecule properties remain to be done before excluding the potential of CB2R and GPR55 modulation as a means of reducing inflammation.

4.4 Final Thoughts: Limitations of the Experimental Models and Future Directions

This thesis is based on the work utilizing young (6-8 weeks old), male C57BL/6 mice. Mice are the most frequently used animal models in early-stage preclinical studies (Angus et al., 2001). However, there are a number of limitations with use of the mice in comparison with human physiology and the epidemiology of sepsis. First of all, severe sepsis cases are more frequent in females over 60-years-old. The physiology and immune response differs not only by sex, but also weakens with age. With the use of young male mice in our research, one can argue that it does not reflect the clinically relevant epidemiology as well as pathophysiology of human sepsis (Poli-de-Figueiredo et al., 2008). It is difficult to collect important data on vital parameters of the mice such as blood pressure and cardiac output due to their small size. Also compared to humans,

rodents are highly resistant to endotoxin, have smaller volume of blood and different hemodynamics (Dyson and Singer, 2009; Michie, 1998).

Despite the limitations of murine models of sepsis, there are a number of benefits associated with murine models. They are small and relatively inexpensive and therefore can be used in studies that require a large numbers of animals for statistical power. Also, the manipulation and genetics of mice are quite well exploited, and specific gene deficient or transgenic strains are readily available. Moreover, the variety of reagents available for immunologic studies of rodents are beyond that of any other animal models (Nemzek et al., 2008).

Secondly, the current study was limited to LPS-induced endotoxemia as a representation of acute sepsis. Endotoxemia is a popular method because of the convenience and reproducible results (Buras et al., 2005; Fink and Heard, 1990). Endotoxemia also carries fewer concerns with cost and animal welfare due to minimal invasiveness. However, LPS administration is limited to activation of a fragment of sepsis pathophysiology such as the TLR4 pathway. Also, administration of high doses of LPS to endotoxin-resistant animals has toxic effects that are not seen when low doses are administered to endotoxin-sensitive species, such as humans (Copeland et al., 2005; Piper et al., 1996). Furthermore, a characteristic of endotoxemia is the extremely rapid production of inflammatory cytokines and disease progression compared to human sepsis. Therefore, administration of LPS does not accurately replicate all of the features of human sepsis. Due to the aforementioned reasons, endotoxemia can be accompanied with a surgical, clinically relevant polymicrobial model of sepsis. One such model is Colon Ascendens Stent Peritonitis (CASP) or Cecal Ligation and Puncture. Effective treatments identified in the endotoxemia models can confirm their efficacy with live bacterial

infection. Thus, selected effective treatments such as CID16020046 and O-1918 should be tested in polymicrobial sepsis in the future studies.

The length of endotoxemia, the effect of drug vehicle, the dose and timing of drugs administered are important in the development of sepsis treatment. In previous studies, the vehicle excipients used to dissolve pharmacologic agents at the concentration used in the current study have been determined ineffective on leukocyte activity (Sardinha et al., 2014; Toguri et al., 2014). In this study, single doses of drugs were administered at 15 minutes post LPS challenge. Although the doses were selected based on pilot studies and literature, addition of experimental groups of lower or higher doses of the treatments, or combination of effective treatments could be explored to identify maximized immune modulation. Further studies should be done in the focus of investigating various time points of drug administration, preferably with survival data, in order to pinpoint the optimal treatment window for CB2R and GPR55 modulation in sepsis. Furthermore, some of the agonists and antagonists used have reported off-targets although at lower affinity. LPI is reported to also be an agonist for GPR119, and O-1602 is known to activate GPR18, though neither receptor is well characterized with regards to inflammation (McHugh et al., 2012; Soga et al., 2005). Also, the GPR55 antagonist, O-1918, is known to inhibit GPR18 (Offertáler et al., 2003). Therefore, the possibility remains that there are confounding direct and indirect effects on inflammation due to these drugs acting on other receptors.

Additionally, in order to further clarify the alternative pathways eliciting the anti-inflammatory effect in CB2R KO mice, CB1R and CB2R double KO mice can be used to confirm our data. Also, GPR55 KO mice can be subjected to sepsis survival studies to

determine whether GPR55 is a critical regulator of the inflammatory response to sepsis and to confirm their novelty and therapeutic potential.

Lastly, intravital microscopy is an effective method for visualizing leukocyte-endothelial interaction *in vivo*. However, the fluorescent labelling with Rhodamine-6G does not permit leukocyte-type specific observations, nor observations of platelets. There are alternate approaches to studying single leukocyte-type interactions and our results are strong enough to recommend undertaking that effort, particularly for studying neutrophils. For example, adoptive transfer of labeled cells is one method to study a subtype of leukocyte using IVM.

4.5 Clinical Implications

Specific and effective treatments for sepsis and septic shock are currently lacking, especially related to resolving whole body hyper- or hypo-inflammation with specific inflammatory mediators as targets. In recent clinical trials, therapies targeting pro-inflammatory cytokines such as TNF and IL-1 have failed to increase patient survival, and patient outcomes have only slightly improved. Considering prior evidence for anti-inflammatory effects of CB2R activation and GPR55 inhibition and now the evidence in the current research, the prospects are favorable for further investigation of CB2R activation and GPR55 inhibition as a treatment for patients diagnosed with sepsis in their pro-inflammatory phase. We have shown here that by inducing endotoxemia with LPS and then targeting CB2R and GPR55 using receptor specific drugs can be beneficial in inflamed intestinal microcirculation. Although various titrations of timing and doses of

treatment need to be examined, CB2R and GPR55 modulation was effective in at least dampening hyper-activation of leukocytes within 2 hours, which could be enough time for other treatments to have an effect and extend survival of the patient. Several treatments will likely be necessary in humans in the event of complex disease such as sepsis, and here, we have identified possible immunomodulatory treatments that can be applied in addition to current treatment regimen such as fluid resuscitation and antibiotics.

4.6 Conclusion

The present study investigated the effects of CB2R and GPR55 modulation with various pharmacological agents and genetically modified animals in an acute model of sepsis. The results obtained from this study showed that 2-AG up-regulation and GPR55 inhibition decreases leukocyte activation measured by interaction between leukocytes and endothelium in the intestinal microcirculation elicited by LPS administration. In the absence of CB2R, 2-AG up-regulation (by JZL184) exerted an anti-inflammatory effect associated with increased plasma levels of IL-10 and reduced P-selectin, whereas GPR55 antagonism showed an anti-inflammatory effect associated with reduced IL-6 in septic WT mice. We speculate that CB2R activation and GPR55 inhibition may significantly attenuate the hyper-inflammatory response of sepsis and therefore possibly improve patient outcomes, and even reduce mortality.

REFERENCES

Al-Banna, N.A., Toguri, J.T., Kelly, M.E.M., Lehmann, C., 2013. Leukocyte-endothelial interactions within the ocular microcirculation in inflammation and infection. Clin. Hemorheol. Microcirc. 55, 423–43. doi:10.3233/CH-131780

Alhouayek, M., Lambert, D.M., Delzenne, N.M., Cani, P.D., Muccioli, G.G., 2011. Increasing endogenous 2-arachidonoylglycerol levels counteracts colitis and related systemic inflammation. FASEB J. 25, 2711–21. doi:10.1096/fj.10-176602

Anas, A.A., Wiersinga, W.J., de Vos, A.F., van der Poll, T., 2010. Recent insights into the pathogenesis of bacterial sepsis. Neth. J. Med. 68, 147–52.

Andradas, C., Blasco-Benito, S., Castillo-Lluva, S., Dillenburg-Pilla, P., Diez-Alarcia, R., Juanes-García, A., García-Taboada, E., Hernando-Llorente, R., Soriano, J., Hamann, S., Wenners, A., Alkatout, I., Klapper, W., Rocken, C., Bauer, M., Arnold, N., Quintanilla, M., Megías, D., Vicente-Manzanares, M., Urigüen, L., Gutkind, J.S., Guzmán, M., Pérez-Gómez, E., Sánchez, C., 2016. Activation of the orphan receptor GPR55 by lysophosphatidylinositol promotes metastasis in triple-negative breast cancer. Oncotarget. doi:10.18632/oncotarget.10206

Angele, M.K., Chaudry, I.H., 2005. Surgical trauma and immunosuppression: pathophysiology and potential immunomodulatory approaches. Langenbeck's Arch. Surg. / Dtsch. Gesellschaft für Chir. 390, 333–41. doi:10.1007/s00423-005-0557-4

Angus, D.C., Linde-Zwirble, W.T., Lidicker, J., Clermont, G., Carcillo, J., Pinsky, M.R., 2001. Epidemiology of severe sepsis in the United States: analysis of incidence, outcome, and associated costs of care. Crit. Care Med. 29, 1303–10. doi:10.1097/00003246-200107000-00002

Balenga, N.A., Aflaki, E., Kargl, J., Platzer, W., Schröder, R., Blättermann, S., Kostenis, E., Brown, A.J., Heinemann, A., Waldhoer, M., 2011. GPR55 regulates cannabinoid 2 receptor-mediated responses in human neutrophils. Cell Res. 21, 1452–69. doi:10.1038/cr.2011.60

Balenga, N.A., Martínez-Pinilla, E., Kargl, J., Schröder, R., Peinhaupt, M., Platzer, W., Bálint, Z., Zamarbide, M., Dopeso-Reyes, I.G., Ricobaraza, a, Pérez-Ortiz, J.M., Kostenis, E., Waldhoer, M., Heinemann, a, Franco, R., 2014. Heteromerization of GPR55 and cannabinoid CB2 receptors modulates signalling. Br. J. Pharmacol. 1–20. doi:10.1111/bph.12850

Basu, S., Dittel, B.N., 2011. Unraveling the complexities of cannabinoid receptor 2 (CB2) immune regulation in health and disease. Immunol. Res. 51, 26–38. doi:10.1007/s12026-011-8210-5

Battista, N., Di Tommaso, M., Bari, M., Maccarrone, M., 2012. The endocannabinoid system: an overview. Front. Behav. Neurosci. 6, 9. doi:10.3389/fnbeh.2012.00009

Begg, M., Pacher, P., Bátkai, S., Osei-Hyiaman, D., Offertáler, L., Mo, F.M., Liu, J., Kunos, G., 2005. Evidence for novel cannabinoid receptors. Pharmacol. Ther. 106, 133–45. doi:10.1016/j.pharmthera.2004.11.005

Birnbaum, J., Klotz, E., Spies, C.D., Hein, O.V., Mallin, K., Kawka, R., Ziemer, S., Lehmann, C., 2008. The combinations C1 esterase inhibitor with coagulation factor XIII and N-acetylcysteine with tirilazad mesylate reduce the leukocyte adherence in an experimental endotoxemia in rats. Clin. Hemorheol. Microcirc. 40, 167–76.

Bone, R.C., Balk, R.A., Cerra, F.B., Dellinger, R.P., Fein, A.M., Knaus, W.A., Schein, R.M., Sibbald, W.J., 1992. Definitions for sepsis and organ failure and guidelines for the use of innovative therapies in sepsis. The ACCP/SCCM Consensus Conference Committee. American College of Chest Physicians/Society of Critical Care Medicine. Chest. 101, 1644–55.

Borrelli, F., Romano, B., Petrosino, S., Pagano, E., Capasso, R., Coppola, D., Battista, G., Orlando, P., Di Marzo, V., Izzo, A. a, 2015. Palmitoylethanolamide, a naturally occurring lipid, is an orally effective intestinal anti-inflammatory agent. Br. J. Pharmacol. 172, 142–58. doi:10.1111/bph.12907

Braun, A., Engel, T., Aguilar-Pimentel, J.A., Zimmer, A., Jakob, T., Behrendt, H., Mempel, M., 2011. Beneficial effects of cannabinoids (CB) in a murine model of allergen-induced airway inflammation: Role of CB1/CB2 receptors. Immunobiology 216, 466–76. doi:10.1016/j.imbio.2010.09.004

Brown, K.A., Brain, S.D., Pearson, J.D., Edgeworth, J.D., Lewis, S.M., Treacher, D.F., 2006. Neutrophils in development of multiple organ failure in sepsis. Lancet 368, 157–69. doi:10.1016/S0140-6736(06)69005-3

Buckley, N.E., 2008. The peripheral cannabinoid receptor knockout mice: an update. Br. J. Pharmacol. 153, 309–18. doi:10.1038/sj.bjp.0707527

Buras, J.A., Holzmann, B., Sitkovsky, M., 2005. Animal models of sepsis: setting the stage. Nat. Rev. Drug Discov. 4, 854–65. doi:10.1038/nrd1854

Burkovskiy, I., Sardinha, J., Zhou, J., Lehmann, C., 2013. Cytokine release in sepsis. Adv. Biosci. Biotechnol. 04, 860–5. doi:10.4236/abb.2013.49114

Canadian Institute for Health Information (CIHI), 2009. In Focus: A National Look at Sepsis. Ottawa, ON, Canada.

Cantarella, G., Scollo, M., Lempereur, L., Saccani-Jotti, G., Basile, F., Bernardini, R., 2011. Endocannabinoids inhibit release of nerve growth factor by inflammation-activated mast cells. Biochem. Pharmacol. 82, 380–88. doi:10.1016/j.bcp.2011.05.004

Cao, Z., Mulvihill, M., Mukhopadhyay, P., Xu, H., Erdélyi, K., Hao, E., Holovac, E., Haskó, G., Cravatt, B., Nomura, D., Pacher, P., 2013. Monoacylglycerol lipase controls endocannabinoid and eicosanoid signaling and hepatic injury in mice. Gastroenterology 144, 808–17. doi:10.1053/j.gastro.2012.12.028

Carrigan, S.O., Pink, D.B.S., Stadnyk, A.W., 2007. Neutrophil transepithelial migration in response to the chemoattractant fMLP but not C5a is phospholipase D-dependent and related to the use of CD11b/CD18. J. Leukoc. Biol. 82, 1575–84. doi:10.1189/jlb.0806528

Chang, J.W., Niphakis, M.J., Lum, K.M., Cognetta, A.B., Wang, C., Matthews, M.L., Niessen, S., Buczynski, M.W., Parsons, L.H., Cravatt, B.F., 2012. Highly selective inhibitors of monoacylglycerol lipase bearing a reactive group that is bioisosteric with endocannabinoid substrates. Chem. Biol. 19, 579–88. doi:10.1016/j.chembiol.2012.03.009

Cheng, B., Hoeft, A.H., Book, M., Shu, Q., Pastores, S.M., 2015. Sepsis: Pathogenesis, Biomarkers, and Treatment. Biomed. Res. Int. 2015, 846935. doi: 10.1155/2015/846935

Chevaleyre, V., Takahashi, K.A., Castillo, P.E., 2006. Endocannabinoid-mediated synaptic plasticity in the CNS. Annu. Rev. Neurosci. 29, 37–76. doi:10.1146/annurev.neuro.29.051605.112834

Chiurchiù, V., Lanuti, M., De Bardi, M., Battistini, L., Maccarrone, M., 2014. The differential characterization of GPR55 receptor in human peripheral blood reveals a distinctive expression in monocytes and NK cells and a proinflammatory role in these innate cells. Int. Immunol. 27, 153-60. doi:10.1093/intimm/dxu097

Cinel, I., Opal, S.M., 2009. Molecular biology of inflammation and sepsis: a primer. Crit. Care. Med. 37, 291–304. doi:10.1097/CCM.0b013e31819267fb

Clark, I.A., 2007. How TNF was recognized as a key mechanism of disease. Cytokine Growth Factor Rev. 18, 335-43. doi:10.1016/j.cytogfr.2007.04.002

Colbert, J.F., Schmidt, E.P., 2016. Endothelial and Microcirculatory Function and Dysfunction in Sepsis. Clin. Chest Med. 37, 263–75. doi:10.1016/j.ccm.2016.01.009

Copeland, S., Warren, H.S., Lowry, S.F., Calvano, S.E., Remick, D., Inflammation and the Host Response to Injury Investigators, 2005. Acute inflammatory response to endotoxin in mice and humans. Clin. Diagn. Lab. Immunol. 12, 60–7. doi:10.1128/CDLI.12.1.60-67.2005

Cortez-Cooper, M., Meaders, E., Stallings, J., Haddow, S., Kraj, B., Sloan, G., McCully, K.K., Cannon, J.G., 2013. Soluble TNF and IL-6 receptors: indicators of vascular health in women without cardiovascular disease. Vasc. Med. 18, 282–9. doi:10.1177/1358863X13508336

Costola-de-Souza, C., Ribeiro, A., Ferraz-de-Paula, V., Calefi, A.S., Aloia, T.P.A., Gimenes-Júnior, J.A., de Almeida, V.I., Pinheiro, M.L., Palermo-Neto, J., 2013. Monoacylglycerol lipase (MAGL) inhibition attenuates acute lung injury in mice. PLoS One 8, e77706. doi:10.1371/journal.pone.0077706

Cravatt, B.F., Giang, D.K., Mayfield, S.P., Boger, D.L., Lerner, R. a, Gilula, N.B., 1996. Molecular characterization of an enzyme that degrades neuromodulatory fatty-acid amides. Nature 384, 83–7. doi:10.1038/384083a0

D'Addario, C., Di Francesco, A., Pucci, M., Finazzi Agrò, A., Maccarrone, M., 2013. Epigenetic mechanisms and endocannabinoid signalling. FEBS J. 280, 1905–17. doi:10.1111/febs.12125

De Backer, D., Donadello, K., Taccone, F.S., Ospina-Tascon, G., Salgado, D., Vincent, J.-L., 2011. Microcirculatory alterations: potential mechanisms and implications for therapy. Ann. Intensive Care. 1, 27. doi:10.1186/2110-5820-1-27

De Backer, D., Orbegozo Cortes, D., Donadello, K., Vincent, J.-L., 2014. Pathophysiology of microcirculatory dysfunction and the pathogenesis of septic shock. Virulence 5, 73–9. doi:10.4161/viru.26482

Dellinger, R.P., Levy, M.M., Rhodes, A., Annane, D., Gerlach, H., Opal, S.M., Sevransky, J.E., Sprung, C.L., Douglas, I.S., Jaeschke, R., Osborn, T.M., Nunnally, M.E., Townsend, S.R., Reinhart, K., Kleinpell, R.M., Angus, D.C., Deutschman, C.S., Machado, F.R., Rubenfeld, G.D., Webb, S.A., Beale, R.J., Vincent, J.-L., Moreno, R., Surviving Sepsis Campaign Guidelines Committee including the Pediatric Subgroup, 2013. Surviving sepsis campaign: international guidelines for management of severe sepsis and septic shock: 2012. Crit. Care Med. 41, 580–637. doi:10.1097/CCM.0b013e31827e83af

Di Filippo, C., Rossi, F., Rossi, S., D'Amico, M., 2004. Cannabinoid CB2 receptor activation reduces mouse myocardial ischemia-reperfusion injury: involvement of cytokine/chemokines and PMN. J. Leukoc. Biol. 75, 453–9. doi:10.1189/jlb.0703303

Dyson, A., Singer, M., 2009. Animal models of sepsis: Why does preclinical efficacy fail to translate to the clinical setting? Crit. Care Med. 37, S30–7. doi:10.1097/CCM.0b013e3181922bd3

Fink, M.P., Heard, S.O., 1990. Laboratory models of sepsis and septic shock. J. Surg. Res. 49, 186–196. doi:10.1016/0022-4804(90)90260-9

Galiègue, S., Mary, S., Marchand, J., Dussossoy, D., Carrière, D., Carayon, P., Bouaboula, M., Shire, D., Le Fur, G., Casellas, P., 1995. Expression of central and peripheral cannabinoid receptors in human immune tissues and leukocyte subpopulations. Eur. J. Biochem. 232, 54–61.

Gérard, C., Bruyns, C., Marchant, A., Abramowicz, D., Vandenabeele, P., Delvaux, A., Fiers, W., Goldman, M., Velu, T., 1993. Interleukin 10 reduces the release of tumor necrosis factor and prevents lethality in experimental endotoxemia. J. Exp. Med. 177, 547–50.

Godlewski, G., Malinowska, B., Schlicker, E., 2004. Presynaptic cannabinoid CB(1) receptors are involved in the inhibition of the neurogenic vasopressor response during septic shock in pithed rats. Br. J. Pharmacol. 142, 701–8. doi:10.1038/sj.bjp.0705839

Granger, D.N., Senchenkova, E., 2010. Inflammation and the Microcirculation. Morgan & Claypool Life Sciences. San Rafael, CA, USA.

Greineisen, W.E., Turner, H., 2010. Immunoactive effects of cannabinoids: considerations for the therapeutic use of cannabinoid receptor agonists and antagonists. Int. Immunopharmacol. 10, 547–55. doi:10.1016/j.intimp.2010.02.012

Haraldsen, G., Kvale, D., Lien, B., Farstad, I.N., Brandtzaeg, P., 1996. Cytokine-regulated expression of E-selectin, intercellular adhesion molecule-1 (ICAM-1), and vascular cell adhesion molecule-1 (VCAM-1) in human microvascular endothelial cells. J. Immunol. 156, 2558–65.

Hatoum, O.A., Heidemann, J., Binion, D.G., 2006. The intestinal microvasculature as a therapeutic target in inflammatory bowel disease. Ann. N. Y. Acad. Sci. 1072, 78–97. doi:10.1196/annals.1326.003

Hayes, J.K., Havaleshko, D.M., Plachinta, R. V, Rich, G.F., 2004. Isoflurane pretreatment supports hemodynamics and leukocyte rolling velocities in rat mesentery during lipopolysaccharide-induced inflammation. Anesth. Analg. 98, 999–1006.

Henstridge, C.M., 2012. Off-target cannabinoid effects mediated by GPR55. Pharmacology 89, 179–87. doi:10.1159/000336872

Henstridge, C.M., Balenga, N. a B., Ford, L. a, Ross, R. a, Waldhoer, M., Irving, A.J., 2009. The GPR55 ligand L-alpha-lysophosphatidylinositol promotes RhoA-dependent Ca^{2+} signaling and NFAT activation. FASEB J. 23, 183–93. doi:10.1096/fj.08-108670

Henstridge, C.M., Balenga, N. a B., Kargl, J., Andradas, C., Brown, A.J., Irving, A., Sanchez, C., Waldhoer, M., 2011. Minireview: recent developments in the physiology and pathology of the lysophosphatidylinositol-sensitive receptor GPR55. Mol. Endocrinol. 25, 1835–48. doi:10.1210/me.2011-1197

Henstridge, C.M., Balenga, N.A., Schröder, R., Kargl, J.K., Platzer, W., Martini, L., Arthur, S., Penman, J., Whistler, J.L., Kostenis, E., Waldhoer, M., Irving, A.J., 2010. GPR55 ligands promote receptor coupling to multiple signalling pathways. Br. J. Pharmacol. 160, 604–14. doi:10.1111/j.1476-5381.2009.00625.x

Hillard, C.J., 2015. The Endocannabinoid Signaling System in the CNS: A Primer. Int. Rev. Neurobiol. 125, 1–47. doi:10.1016/bs.irn.2015.10.001

Hotchkiss, R.S., Monneret, G., Payen, D., 2013. Sepsis-induced immunosuppression: from cellular dysfunctions to immunotherapy. Nat. Rev. Immunol. 13, 862–74. doi:10.1038/nri3552

Howard, M., Muchamuel, T., Andrade, S., Menon, S., 1993. Interleukin 10 protects mice from lethal endotoxemia. J. Exp. Med. 177, 1205–8.

Howlett, A.C., Barth, F., Bonner, T.I., Cabral, G., Casellas, P., Devane, W.A., Felder, C.C., Herkenham, M., Mackie, K., Martin, B.R., Mechoulam, R., Pertwee, R.G., 2002. International Union of Pharmacology. XXVII. Classification of cannabinoid receptors. Pharmacol. Rev. 54, 161–202.

Husak, L., Marcuzzi, A., Herring, J., Wen, E., Yin, L., Capan, D.D., Cernat, G., 2010. National analysis of sepsis hospitalizations and factors contributing to sepsis in-hospital mortality in Canada. Healthc. Q. 13 Spec No, 35–41.

Ince, C., 2005. The microcirculation is the motor of sepsis. Crit. Care 9 Suppl 4, S13–9. doi:10.1186/cc3753

Johns, D.G., Behm, D.J., Walker, D.J., Ao, Z., Shapland, E.M., Daniels, D. a, Riddick, M., Dowell, S., Staton, P.C., Green, P., Shabon, U., Bao, W., Aiyar, N., Yue, T.-L., Brown, a J., Morrison, a D., Douglas, S. a, 2007. The novel endocannabinoid receptor GPR55 is activated by atypical cannabinoids but does not mediate their vasodilator effects. Br. J. Pharmacol. 152, 825–31. doi:10.1038/sj.bjp.0707419

Kapur, A., Zhao, P., Sharir, H., Bai, Y., Caron, M.G., Barak, L.S., Abood, M.E., 2009. Atypical responsiveness of the orphan receptor GPR55 to cannabinoid ligands. J. Biol. Chem. 284, 29817–27. doi:10.1074/jbc.M109.050187

Kargl, J., Andersen, L., Hasenöhrl, C., Feuersinger, D., Stančić, A., Fauland, A., Magnes, C., El-Heliebi, A., Lax, S., Uranitsch, S., Haybaeck, J., Heinemann, A., Schicho, R., 2016. GPR55 promotes migration and adhesion of colon cancer cells indicating a role in metastasis. Br. J. Pharmacol. 173, 142–54. doi:10.1111/bph.13345

Kargl, J., Balenga, N., Parzmair, G.P., Brown, A.J., Heinemann, A., Waldhoer, M., 2012. The cannabinoid receptor CB1 modulates the signaling properties of the lysophosphatidylinositol receptor GPR55. J. Biol. Chem. 287, 44234–48. doi:10.1074/jbc.M112.364109

Kargl, J., Brown, A.J., Andersen, L., Dorn, G., Schicho, R., Waldhoer, M., Heinemann, A., 2013. A selective antagonist reveals a potential role of G protein-coupled receptor 55 in platelet and endothelial cell function. J. Pharmacol. Exp. Ther. 346, 54–66. doi:10.1124/jpet.113.204180

Karlsson, M., Contreras, J. a., Hellman, U., Tornqvist, H., Holm, C., 1997. cDNA cloning, tissue distribution, and identification of the catalytic triad of monoglyceride lipase. Evolutionary relationship to esterases, lysophospholipases, and haloperoxidases. J. Biol. Chem. 272, 27218–23. doi:10.1074/jbc.272.43.27218

Kelly, M., Hwang, J.M., Kubes, P., 2007. Modulating leukocyte recruitment in inflammation. J. Allergy Clin. Immunol. 120, 3–10. doi:10.1016/j.jaci.2007.05.017

Kianian, M., Kelly, M.E.M., Zhou, J., Hung, O., Cerny, V., Rowden, G., Lehmann, C., 2014. Cannabinoid receptor 1 inhibition improves the intestinal microcirculation in experimental endotoxemia. Clin. Hemorheol. Microcirc. 58, 333–42. doi:10.3233/CH-131668

Klein, T.W., 2005. Cannabinoid-based drugs as anti-inflammatory therapeutics. Nat. Rev. Immunol. 5, 400–11. doi:10.1038/nri1602

Kurihara, R., Tohyama, Y., Matsusaka, S., Naruse, H., Kinoshita, E., Tsujioka, T., Katsumata, Y., Yamamura, H., 2006. Effects of peripheral cannabinoid receptor ligands on motility and polarization in neutrophil-like HL60 cells and human neutrophils. J. Biol. Chem. 281, 12908–18. doi:10.1074/jbc.M510871200

Lan, R., Gatley, J., Lu, Q., Fan, P., Fernando, S.R., Volkow, N.D., Pertwee, R., Makriyannis, A., 1999. Design and synthesis of the CB1 selective cannabinoid antagonist AM281: a potential human SPECT ligand. AAPS PharmSci. 1, 39-45.

Lanuti, M., Talamonti, E., Maccarrone, M., Chiurchiù, V., 2015. Activation of GPR55 Receptors Exacerbates oxLDL-Induced Lipid Accumulation and Inflammatory Responses, while Reducing Cholesterol Efflux from Human Macrophages. PLoS One. 10, e0126839. doi:10.1371/journal.pone.0126839

Lehmann, C., Egerer, K., Georgiew, A., Weber, M., Grune, T., Kox, W.J., 1999. Inhibition of tumor necrosis factor-alpha release in rat experimental endotoxemia by treatment with the 21-aminosteroid U-74389G. Crit. Care Med. 27, 1164–7.

Lehmann, C., Götz, F., Schuster, L., Zhou, J., 2013. Improved setup for intestinal intravital microscopy in mice - the “floating table”. Anestesiol. 79, 102–3.

Lehmann, C., Kianian, M., Zhou, J., Küster, I., Kuschnereit, R., Whynot, S., Hung, O., Shukla, R., Johnston, B., Cerny, V., Pavlovic, D., Spassov, A., Kelly, M.E., 2012. Cannabinoid receptor 2 activation reduces intestinal leukocyte recruitment and systemic inflammatory mediator release in acute experimental sepsis. Crit. Care. 16, R47. doi:10.1186/cc11248

Leoni, G., Gripentrog, J., Lord, C., Riesselman, M., Sumagin, R., Parkos, C.A., Nusrat, A., Jesaitis, A.J., 2015. Human neutrophil formyl peptide receptor phosphorylation and the mucosal inflammatory response. J. Leukoc. Biol. 97, 87–101. doi:10.1189/jlb.4A0314-153R

Lerman, Y. V, Lim, K., Hyun, Y., Falkner, K.L., Yang, H., Pietropaoli, A.P., Sonnenberg, A., Sarangi, P.P., Kim, M., 2015. Sepsis lethality via exacerbated tissue infiltration and TLR-induced cytokine production by neutrophils is integrin α3β1-dependent. Blood 124, 3515–24. doi:10.1182/blood-2014-01-552943

Levy, M.M., Fink, M.P., Marshall, J.C., Abraham, E., Angus, D., Cook, D., Cohen, J., Opal, S.M., Vincent, J.L., Ramsay, G., 2003. 2001 SCCM/ESICM/ACCP/ATS/SIS International Sepsis Definitions Conference. Crit Care Med. 31, 1250–6. doi:10.1097/01.CCM.0000050454.01978.3B

Li, K., Fichna, J., Schicho, R., Saur, D., Bashashati, M., Mackie, K., Li, Y., Zimmer, A., Göke, B., Sharkey, K. a, Storr, M., 2013. A role for O-1602 and G protein-coupled receptor GPR55 in the control of colonic motility in mice. Neuropharmacology. 71, 255–63. doi:10.1016/j.neuropharm.2013.03.029

Li, Y.-Y., Li, Y.-N., Ni, J.-B., Chen, C.-J., Lv, S., Chai, S.-Y., Wu, R.-H., Yüce, B., Storr, M., 2010. Involvement of cannabinoid-1 and cannabinoid-2 receptors in septic ileus. Neurogastroenterol. Motil. 22, 350–e88. doi:10.1111/j.1365-2982.2009.01419.x

Lin, X.H., Yuece, B., Li, Y.Y., Feng, Y.J., Feng, J.Y., Yu, L.Y., Li, K., Li, Y.N., Storr, M., 2011. A novel CB receptor GPR55 and its ligands are involved in regulation of gut movement in rodents. Neurogastroenterol. Motil. 23, 862-e342. doi:10.1111/j.1365-2982.2011.01742.x

Liu, L., Kubes, P., 2003. Molecular mechanisms of leukocyte recruitment: organ-specific mechanisms of action. Thromb. Haemost. 89, 213–20. doi:10.1267/THRO03020213

Long, J.Z., Li, W., Booker, L., Burston, J.J., Kinsey, S.G., Schlosburg, J.E., Pavón, F.J., Serrano, A.M., Selley, D.E., Parsons, L.H., Lichtman, A.H., Cravatt, B.F., 2009. Selective blockade of 2-arachidonoylglycerol hydrolysis produces cannabinoid behavioral effects. Nat. Chem. Biol. 5, 37–44. doi:10.1038/nchembio.129

Lorente, J.A., Marshall, J.C., 2005. Neutralization of tumor necrosis factor in preclinical models of sepsis. Shock 24 Suppl 1, 107–19.

Lush, C.W., Kvietys, P.R., 2000. Microvascular dysfunction in sepsis. Microcirculation 7, 83–101.

Malawista, S.E., de Boisfleury Chevance, A., Boxer, L.A., 2000. Random locomotion and chemotaxis of human blood polymorphonuclear leukocytes from a patient with leukocyte adhesion deficiency-1: normal displacement in close quarters via chimneying. Cell Motil. Cytoskeleton 46, 183–9. doi:10.1002/1097-0169(200007)46:3<183::AID-CM3>3.0.CO;2-2

Marshall, J.C., Christou, N. V, Meakins, J.L., 1993. The gastrointestinal tract. The "undrained abscess" of multiple organ failure. Ann. Surg. 218, 111–9.

Martin, G.S., 2012. Sepsis, severe sepsis and septic shock: changes in incidence, pathogens and outcomes. Expert Rev. Anti. Infect. Ther. 10, 701–6. doi:10.1586/eri.12.50

Martin, G.S., Mannino, D.M., Eaton, S., Moss, M., 2003. The epidemiology of sepsis in the United States from 1979 through 2000. N. Engl. J. Med. 348, 1546–54. doi:10.1056/NEJMoa022139

Matsuda, L.A., Lolait, S.J., Brownstein, M.J., Young, A.C., Bonner, T.I., 1990. Structure of a cannabinoid receptor and functional expression of the cloned cDNA. Nature 346, 561–4. doi:10.1038/346561a0

Matsuda, N., Hattori, Y., 2007. Vascular biology in sepsis: pathophysiological and therapeutic significance of vascular dysfunction. J. Smooth Muscle Res. 43, 117–37.

McHugh, D., Page, J., Dunn, E., Bradshaw, H.B., 2012. Δ(9) -Tetrahydrocannabinol and N-arachidonyl glycine are full agonists at GPR18 receptors and induce migration in human endometrial HEC-1B cells. Br. J. Pharmacol. 165, 2414–24. doi:10.1111/j.1476-5381.2011.01497.x

Mechoulam, R., 2002. Discovery of endocannabinoids and some random thoughts on their possible roles in neuroprotection and aggression. Prostaglandins. Leukot. Essent. Fatty Acids 66, 93–9. doi:10.1054/plef.2001.0340

Michie, H.R., 1998. The value of animal models in the development of new drugs for the treatment of the sepsis syndrome. J. Antimicrob. Chemother. 41 Suppl A, 47–9.

Miller, A.M., Stella, N., 2008. CB2 receptor-mediated migration of immune cells: it can go either way. Br. J. Pharmacol. 153, 299–308. doi:10.1038/sj.bjp.0707523

Miranda, M.L. de, Balarini, M. de M., Caixeta, D.M. da L., Bouskela, E., 2016. Microcirculatory dysfunction in sepsis: pathophysiology, clinical monitoring, and potential therapies. Am. J. Physiol. Heart Circ. Physiol. 311, H24-35. doi:10.1152/ajpheart.00034.2016

Moreno, E., Andradas, C., Medrano, M., Caffarel, M.M., Pérez-Gómez, E., Blasco-Benito, S., Gómez-Cañas, M., Pazos, M.R., Irving, A.J., Lluís, C., Canela, E.I., Fernández-Ruiz, J., Guzmán, M., McCormick, P.J., Sánchez, C., 2014. Targeting CB2-GPR55 receptor heteromers modulates cancer cell signaling. J. Biol. Chem. 289, 21960–72. doi:10.1074/jbc.M114.561761

Morris, M.C., Gilliam, E.A., Li, L., 2015. Innate immune programing by endotoxin and its pathological consequences. Front. Immunol. 6, 1–8. doi:10.3389/fimmu.2014.00680

Nemzek, J.A., Hugunin, K.M.S., Opp, M.R., 2008. Modeling sepsis in the laboratory: merging sound science with animal well-being. Comp. Med. 58, 120–8.

Nilsson, O., Fowler, C.J., Jacobsson, S.O.P., 2006. The cannabinoid agonist WIN 55,212-2 inhibits TNF-α-induced neutrophil transmigration across ECV304 cells. Eur. J. Pharmacol. 547, 165–73. doi:10.1016/j.ejphar.2006.07.016

Oberholzer, A., Oberholzer, C., Moldawer, L.L., 2002. Interleukin-10: a complex role in the pathogenesis of sepsis syndromes and its potential as an anti-inflammatory drug. Crit. Care Med. 30, S58–63.

Offertáler, L., Mo, F.-M., Bátkai, S., Liu, J., Begg, M., Razdan, R.K., Martin, B.R., Bukoski, R.D., Kunos, G., 2003. Selective ligands and cellular effectors of a G protein-coupled endothelial cannabinoid receptor. Mol. Pharmacol. 63, 699–705.

Oka, S., Nakajima, K., Yamashita, A., Kishimoto, S., Sugiura, T., 2007. Identification of GPR55 as a lysophosphatidylinositol receptor. Biochem. Biophys. Res. Commun. 362, 928–34. doi:10.1016/j.bbrc.2007.08.078

Oka, S., Toshida, T., Maruyama, K., Nakajima, K., Yamashita, A., Sugiura, T., 2009. 2-Arachidonoyl-sn-glycero-3-phosphoinositol: A possible natural ligand for GPR55. J. Biochem. 145, 13–20. doi:10.1093/jb/mvn136

Osuchowski, M.F., Craciun, F., Weixelbaumer, K.M., Duffy, E.R., Remick, D.G., 2012. Sepsis chronically in MARS: systemic cytokine responses are always mixed regardless of the outcome, magnitude, or phase of sepsis. J. Immunol. 189, 4648–56. doi:10.4049/jimmunol.1201806

Pavlovic, D., Frieling, H., Lauer, K.-S., Bac, V.H., Richter, J., Wendt, M., Lehmann, C., Usichenko, T., Meissner, K., Gruendling, M., 2006. Thermostatic tissue platform for intravital microscopy: “the hanging drop” model. J. Microsc. 224, 203–10. doi:10.1111/j.1365-2818.2006.01665.x

Pertwee, R.G., 2015. Endocannabinoids and their pharmacological actions. Handb. Exp. Pharmacol. 231, 1–37. doi:10.1007/978-3-319-20825-1_1

Pertwee, R.G., 2006. The pharmacology of cannabinoid receptors and their ligands: an overview. Int. J. Obes. (Lond). 30 Suppl 1, S13–8. doi:10.1038/sj.ijo.0803272

Pertwee, R.G., Howlett, A.C., Abood, M.E., Alexander, S.P.H., Di Marzo, V., Elphick, M.R., Greasley, P.J., Hansen, H.S., Kunos, G., Mackie, K., Mechoulam, R., Ross, R.A., 2010. International Union of Basic and Clinical Pharmacology. LXXIX. Cannabinoid receptors and their ligands: beyond CB1 and CB2. Pharmacol. Rev. 62, 588–631. doi:10.1124/pr.110.003004

Petri, B., Phillipson, M., Kubes, P., 2008. The physiology of leukocyte recruitment: an in vivo perspective. J. Immunol. 180, 6439–46.

Petrosino, S., Ligresti, A., Di Marzo, V., 2009. Endocannabinoid chemical biology: a tool for the development of novel therapies. Curr. Opin. Chem. Biol. 13, 309–20. doi:S1367-5931(09)00061-1 [pii]10.1016/j.cbpa.2009.04.616

Piper, R.D., Cook, D.J., Bone, R.C., Sibbald, W.J., 1996. Introducing critical appraisal to studies of animal models investigating novel therapies in sepsis. Crit. Care Med. 24, 2059–70.

Poli-de-Figueiredo, L.F., Garrido, A.G., Nakagawa, N., Sannomiya, P., 2008. Experimental models of sepsis and their clinical relevance. Shock 30, 53–9. doi:10.1097/SHK.0b013e318181a343

Ramirez, S.H., Haskó, J., Skuba, A., Fan, S., Dykstra, H., McCormick, R., Reichenbach, N., Krizbai, I., Mahadevan, A., Zhang, M., Tuma, R., Son, Y.-J., Persidsky, Y., 2012. Activation of cannabinoid receptor 2 attenuates leukocyte-endothelial cell interactions and blood-brain barrier dysfunction under inflammatory conditions. J. Neurosci. 32, 4004–16. doi:10.1523/JNEUROSCI.4628-11.2012

Remick, D.G., 2007. Pathophysiology of sepsis. Am. J. Pathol. 170, 1435–44. doi:10.2353/ajpath.2007.060872

Remick, D.G., Ward, P.A., 2005. Evaluation of endotoxin models for the study of sepsis. Shock 24 Suppl 1, 7–11.

Rempel, V., Volz, N., Gläser, F., 2013. Antagonists for the orphan G-protein-coupled receptor GPR55 based on a coumarin scaffold. J. Med. Chem. 56, 4798-810. doi: 10.1021/jm4005175.

Rice, T.W., 2006. Treatment of severe sepsis: where next? Current and future treatment approaches after the introduction of drotrecogin alfa. Vasc. Health Risk Manag. 2, 3–18.

Rockwell, C.E., Snider, N.T., Thompson, J.T., Vanden Heuvel, J.P., Kaminski, N.E., 2006. Interleukin-2 suppression by 2-arachidonyl glycerol is mediated through peroxisome proliferator-activated receptor gamma independently of cannabinoid receptors 1 and 2. Mol. Pharmacol. 70, 101–11. doi:10.1124/mol.105.019117

Rosenbaum, D.M., Rasmussen, S.G.F., Kobilka, B.K., 2009. The structure and function of G-protein-coupled receptors. Nature 459, 356–63. doi:10.1038/nature08144

Ross, R.A, 2011. L-α-lysophosphatidylinositol meets GPR55: a deadly relationship. Trends Pharmacol. Sci. 32, 265–9. doi:10.1016/j.tips.2011.01.005

Ryberg, E., Larsson, N., Sjögren, S., Hjorth, S., Hermansson, N.-O., Leonova, J., Elebring, T., Nilsson, K., Drmota, T., Greasley, P.J., 2007. The orphan receptor GPR55 is a novel cannabinoid receptor. Br. J. Pharmacol. 152, 1092–101. doi:10.1038/sj.bjp.0707460

Salomao, R., Brunialti, M.K.C., Rapozo, M.M., Baggio-Zappia, G.L., Galanos, C., Freudenberg, M., 2012. Bacterial sensing, cell signaling, and modulation of the immune response during sepsis. Shock 38, 227–42. doi:10.1097/SHK.0b013e318262c4b0

Sardinha, J., Kelly, M., Zhou, J., Lehmann, C., 2014. Experimental cannabinoid 2 receptor-mediated immune modulation in sepsis. Mediators Inflamm. 2014, 978678. doi:10.1155/2014/978678

Sawzdargo, M., Nguyen, T., Lee, D.K., Lynch, K.R., Cheng, R., Heng, H.H.Q., George, S.R., O'Dowd, B.F., 1999. Identification and cloning of three novel human G protein-coupled receptor genes GPR52, GPR53 and GPR55: GPR55 is extensively expressed in human brain. Mol. Brain Res. 64, 193–8. doi:10.1016/S0169-328X(98)00277-0

Schicho, R., Bashashati, M., Bawa, M., McHugh, D., Saur, D., Hu, H.M., Zimmer, A., Lutz, B., MacKie, K., Bradshaw, H.B., McCafferty, D.M., Sharkey, K.A., Storr, M., 2011. The atypical cannabinoid O-1602 protects against experimental colitis and inhibits neutrophil recruitment. Inflamm. Bowel Dis. 17, 1651–64. doi:10.1002/ibd.21538

Schicho, R., Storr, M., 2012. A potential role for GPR55 in gastrointestinal functions. Curr. Opin. Pharmacol. 12, 653–8. doi:10.1016/j.coph.2012.09.009

Schmidt, H., Secchi, A., Wellmann, R., Bach, A., Böhrer, H., Gebhard, M.M., Martin, E., 1996. Effect of endotoxemia on intestinal villus microcirculation in rats. J. Surg. Res. 61, 521–6. doi:10.1006/jsre.1996.0157

Seierstad, M., Breitenbucher, J.G., 2008. Discovery and development of fatty acid amide hydrolase (FAAH) inhibitors. J. Med. Chem. 51, 7327–43. doi:10.1021/jm800311k

Sharir, H., Abood, M.E., 2010. Pharmacological characterization of GPR55, a putative cannabinoid receptor. Pharmacol. Ther. 126, 301–13. doi:10.1016/j.pharmthera.2010.02.004

Sharir, H., Console-Bram, L., Mundy, C., Popoff, S.N., Kapur, A., Abood, M.E., 2012. The endocannabinoids anandamide and virodhamine modulate the activity of the candidate cannabinoid receptor GPR55. J. Neuroimmune Pharmacol. 7, 856–65. doi:10.1007/s11481-012-9351-6

Singer, M., Deutschman, C.S., Seymour, C.W., Shankar-Hari, M., Annane, D., Bauer, M., Bellomo, R., Bernard, G.R., Chiche, J.-D., Coopersmith, C.M., Hotchkiss, R.S., Levy, M.M., Marshall, J.C., Martin, G.S., Opal, S.M., Rubenfeld, G.D., van der Poll, T., Vincent, J.-L., Angus, D.C., 2016. The Third International Consensus Definitions for Sepsis and Septic Shock (Sepsis-3). JAMA 315, 801–10. doi:10.1001/jama.2016.0287

Soga, T., Ohishi, T., Matsui, T., Saito, T., Matsumoto, M., Takasaki, J., Matsumoto, S.-I., Kamohara, M., Hiyama, H., Yoshida, S., Momose, K., Ueda, Y., Matsushime, H., Kobori, M., Furuichi, K., 2005. Lysophosphatidylcholine enhances glucose-dependent insulin secretion via an orphan G-protein-coupled receptor. Biochem. Biophys. Res. Commun. 326, 744–51. doi:10.1016/j.bbrc.2004.11.120

Spronk, P.E., Zandstra, D.F., Ince, C., 2004. Bench-to-bedside review: sepsis is a disease of the microcirculation. Crit. Care 8, 462–8. doi:10.1186/cc2894

Stadnyk, A.W., 2002. Intestinal epithelial cells as a source of inflammatory cytokines and chemokines. Can. J. Gastroenterol. 16, 241–6.

Stančić, A., Jandl, K., Hasenöhrl, C., Reichmann, F., Marsche, G., Schuligoi, R., Heinemann, A., Storr, M., Schicho, R., 2015. The GPR55 antagonist CID16020046 protects against intestinal inflammation. Neurogastroenterol. Motil. 27, 1432–45. doi:10.1111/nmo.12639

Staton, P.C., Hatcher, J.P., Walker, D.J., Morrison, A.D., Shapland, E.M., Hughes, J.P., Chong, E., Mander, P.K., Green, P.J., Billinton, A., Fulleylove, M., Lancaster, H.C., Smith, J.C., Bailey, L.T., Wise, A., Brown, A.J., Richardson, J.C., Chessell, I.P., 2008. The putative cannabinoid receptor GPR55 plays a role in mechanical hyperalgesia associated with inflammatory and neuropathic pain. Pain 139, 225–36. doi:10.1016/j.pain.2008.04.006

Stearns-Kurosawa, D.J., Osuchowski, M.F., Valentine, C., Kurosawa, S., Remick, D.G., 2011. The pathogenesis of sepsis. Annu. Rev. Pathol. 6, 19–48. doi:10.1146/annurev-pathol-011110-130327

Sundd, P., Pospieszalska, M.K., Ley, K., 2013. Neutrophil rolling at high shear: Flattening, catch bond behavior, tethers and slings. Mol. Immunol. 55, 59–69. doi:10.1016/j.molimm.2012.10.025

Toguri, J.T., Lehmann, C., Laprairie, R.B., Szczesniak, A.M., Zhou, J., Denovan-Wright, E.M., Kelly, M.E.M., 2014. Anti-inflammatory effects of cannabinoid CB(2) receptor activation in endotoxin-induced uveitis. Br. J. Pharmacol. 171, 1448–61. doi:10.1111/bph.12545

Trzeciak, S., Cinel, I., Phillip Dellinger, R., Shapiro, N.I., Arnold, R.C., Parrillo, J.E., Hollenberg, S.M., 2008. Resuscitating the Microcirculation in Sepsis: The Central Role of Nitric Oxide, Emerging Concepts for Novel Therapies, and Challenges for Clinical Trials. Acad. Emerg. Med. 15, 399–413. doi:10.1111/j.1553-2712.2008.00109.x

Tsou, K., Brown, S., Sañudo-Peña, M.C., Mackie, K., Walker, J.M., 1998. Immunohistochemical distribution of cannabinoid CB1 receptors in the rat central nervous system. Neuroscience 83, 393–411. doi:10.1016/S0306-4522(97)00436-3

Tyagi, A., Sethi, A.K., Girotra, G., Mohta, M., 2009. The microcirculation in sepsis. Indian J. Anaesth. 53, 281–93.

van der Poll, T., Opal, S.M., 2008. Host–pathogen interactions in sepsis. Lancet Infect. Dis. 8, 32–43. doi:10.1016/S1473-3099(07)70265-7

Varga, K., Wagner, J.A., Bridgen, D.T., Kunos, G., 1998. Platelet- and macrophage-derived endogenous cannabinoids are involved in endotoxin-induced hypotension. FASEB J. 12, 1035–44.

Vincent, J.-L., Rello, J., Marshall, J., Silva, E., Anzueto, A., Martin, C.D., Moreno, R., Lipman, J., Gomersall, C., Sakr, Y., Reinhart, K., EPIC II Group of Investigators, 2009. International study of the prevalence and outcomes of infection in intensive care units. JAMA 302, 2323–9. doi:10.1001/jama.2009.1754

Vincent, J.-L., Sakr, Y., Sprung, C.L., Ranieri, V.M., Reinhart, K., Gerlach, H., Moreno, R., Carlet, J., Le Gall, J.-R., Payen, D., Sepsis Occurrence in Acutely Ill Patients Investigators, 2006. Sepsis in European intensive care units: results of the SOAP study. Crit. Care Med. 34, 344–53.

Wheeler, D.S., Zingarelli, B., Wheeler, W.J., Wong, H.R., 2009. Novel pharmacologic approaches to the management of sepsis: targeting the host inflammatory response. Recent Pat. Inflamm. Allergy Drug Discov. 3, 96–112.

Witkamp, R., Meijerink, J., 2014. The endocannabinoid system: an emerging key player in inflammation. Curr. Opin. Clin. Nutr. Metab. Care 17, 130–8. doi:10.1097/MCO.0000000000000027

Wittchen, E.S., 2009. Endothelial signaling in paracellular and transcellular leukocyte transmigration. Front. Biosci. (Landmark Ed.) 14, 2522–45.

Yang, H., Zhou, J., Lehmann, C., 2015. GPR55 - a putative “type 3” cannabinoid receptor in inflammation. J. Basic Clin. Physiol. Pharmacol. 27, 297-302. doi:10.1515/jbcpp-2015-0080

Yao, Y.-M., Luan, Y.-Y., Zhang, Q.-H., Sheng, Z.-Y., 2015. Pathophysiological aspects of sepsis: an overview. Methods Mol. Biol. 1237, 5–15. doi:10.1007/978-1-4939-1776-1_2

Zarbock, A., Ley, K., 2009. New insights into leukocyte recruitment by intravital microscopy. Curr. Top. Microbiol. Immunol. 334, 129–52. doi:10.1007/978-3-540-93864-4_6

Zeng, Y., Irvine, R., Hiley, C., 2015. Biased Signalling Might be the Answer to the Inconsistent Pharmacology of GPR55. FASEB J 29, 772.7.

Zhou, J., Schmidt, M., Johnston, B., Wilfart, F., Whynot, S., Hung, O., Murphy, M., Cerný, V., Pavlovic, D., Lehmann, C., 2011. Experimental endotoxemia induces leukocyte adherence and plasma extravasation within the rat pial microcirculation. Physiol. Res. 60, 853–9.

Zhou, X., Gao, X.-P., Fan, J., Liu, Q., Anwar, K.N., Frey, R.S., Malik, A.B., 2005. LPS activation of Toll-like receptor 4 signals CD11b/CD18 expression in neutrophils. Am. J. Physiol. Lung Cell. Mol. Physiol. 288, L655–62. doi:10.1152/ajplung.00327.2004